

**LATE QUATERNARY FLUCTUATIONS IN  
CARBONATE AND CARBONATE ION CONTENT IN  
THE NORTHERN INDIAN OCEAN**

Thesis submitted  
to



**Goa University**

for the award of degree of  
**DOCTOR OF PHILOSOPHY**

in  
**Marine Sciences**

by  
**Sushant Suresh Naik**



**National Institute of Oceanography**  
Dona Paula – 403 004, Goa, India

**2008**

578.77

NAI/Lat

T-394



DEDICATED TO MY PARENTS

## DECLARATION

*I hereby state that the present thesis entitled, "Late Quaternary Fluctuations in Carbonate and Carbonate Ion Content in the Northern Indian Ocean", is original contribution and the same has not been submitted on any previous occasions. To the best of my knowledge, the present study is first comprehensive work of its kind for the area mentioned. The literature related to the problem investigated has been cited. Due acknowledgements have been made wherever facilities and suggestions have been availed of.*



**Sushant Suresh Naik**



Dr. P. Divakar Naidu  
Scientist 'F'

June 21<sup>st</sup>, 2008

**CERTIFICATE**

*As required under the university ordinance OB-9.9, I certify that the thesis entitled "Late Quaternary Fluctuations in Carbonate and Carbonate Ion Content in the Northern Indian Ocean", submitted by Mr. Sushant Suresh Naik for the award of the Degree of Philosophy in Marine Sciences is based on original studies carried out by him under my supervision. The thesis or any part thereof has not been previously submitted for any other degree or diploma in any university or institution.*

*P. Divakar Naidu*

(P. Divakar Naidu)

Research Guide

*No corrections have been suggested*

*C. RAJSHANKAR*

(C. RAJSHANKAR)

*External Exam 26.6.08*



# CONTENTS

	<i>Page No.</i>
<b>Certificates</b>	
<b>Preface</b>	IX
<b>Acknowledgement</b>	XV
<b>CHAPTER I</b>	
<b>Introduction</b>	1-21
1.1 General Introduction	1
1.2 Seawater carbonate chemistry	3
1.3 Carbonate production in the ocean	5
1.4 Lysocline and the CCD	8
1.5 Importance of $\text{CO}_3^{=}$ in the oceanic $\text{CO}_2$ cycle	10
1.6 Study Area	12
1.6.1 Oceanographic settings	12
1.7 Previous Studies	17
1.7.1 Calcium carbonate fluctuations	17
1.7.2 Paleocarbonate ion Proxies	19
1. 8 Objectives	20
<b>CHAPTER II</b>	
<b>Materials and Methods</b>	22-34
2.1 Materials	22

2.1.1 Cores from Atlantic, Pacific and Indian Ocean	22
2.1.2 Core tops from the Indian Ocean	24
2.1.3 Cores from the Indian Ocean	25
2.2 Methods	26
2.2.1 Size fraction analysis	26
2.2.2 Calcium carbonate analysis of sediment	27
2.2.3 Calculation of Size Index parameter	28
2.2.4 Calculation of in-situ and pressure-normalized carbonate ion concentration	28
2.2.5 Shell weights	29
2.2.6 Calcite Crystallinity	30
2.2.7 Scanning Electron Micrographs	32
2.2.8 Chronology of the sediment cores	33
2.2.9 Mg/Ca	33

## **CHAPTER III**

### **Results** 35-54

3.1 CaCO <sub>3</sub> fluctuations in the equatorial region of the major world oceans	35
3.1.1 The Atlantic Ocean	35
3.1.2 The Pacific Ocean	37
3.1.3 The Indian Ocean	37
3.2 Changes of Carbonate ion concentrations in the Indian Ocean	40
3.2.1 Core top sediment samples	40
3.2.2 ODP Site 752 and 715	46

3.3.3 Cores AAS9/21 and SK218/A	49
---------------------------------	----

## **CHAPTER IV**

<b>Discussions</b>	55-93
4.1 Calcium Carbonate fluctuations from the world oceans	55
4.1.1 Dilution by non-calcareous material	56
4.1.2 Productivity	56
4.1.3 Dissolution	58
4.2 Validation and application of paleocarbonate ion proxies in the Indian Ocean	62
4.2.1 Understanding calcite dissolution mechanisms in the Indian Ocean	67
4.2.2 Constraints in using size index and shell weights to determine carbonate ion concentrations	70
4.3 Reconstruction of paleocarbonate ion in the northern Indian Ocean	74
4.3.1 Role of temperature and/or carbonate ion in determining initial shell weights	78
4.3.2 Carbonate ion change from Last Glacial Maximum to Holocene	81
4.3.3 Carbonate ion change during the Holocene	85
4.4 The Indian Ocean CCD change	89

## **CHAPTER V**

### **Summary and Conclusions**

94-102

### **References**

#### **Publications:**

1. **Naik, S. S.**, and Naidu, P. D. (2007), Calcite dissolution along a transect in the western tropical Indian Ocean: A multiproxy approach, *Geochemistry Geophysics Geosystems*, 8, Q08009, doi:10.1029/2007GC001615.
2. **Naik, S.S.**, and Naidu P.D. (2008), Possible factors that control the calcite dissolution in the Western Tropical Indian Ocean, *Current Science*, 95(1), 22-23.



## LIST OF FIGURES

<i>Figure No.</i>	<i>Title</i>	<i>Page No.</i>
<b>Fig. 1</b>	Mauna Loa Carbon Dioxide Record.	1
<b>Fig. 2</b>	Temperature and CO <sub>2</sub> concentration in atmosphere over the past 400,000 years.	2
<b>Fig. 3</b>	The global biogeochemical cycling of calcium carbonate.	3
<b>Fig. 4</b>	The concentrations of the dissolved carbonate species as a function of pH.	4
<b>Fig. 5</b>	Schematic of the ocean carbon biological pump.	6
<b>Fig. 6</b>	Surface circulation in the Indian Ocean during the peak period (August) of the SW monsoon.	13
<b>Fig. 7</b>	Surface circulation in the Indian Ocean during the peak period (August) of the NE monsoon.	14
<b>Fig. 8</b>	Map showing location of deep-sea cores in the equatorial Pacific, Atlantic and Indian Ocean.	23
<b>Fig. 9</b>	Core tops and cores from the northern Indian Ocean and GEOSECS stations.	25
<b>Fig. 10</b>	SEM images of a) <i>G. ruber</i> b) <i>G. sacculifer</i> c) <i>P. obliquiloculata</i> and d) <i>N. dutertrei</i> .	31
<b>Fig. 11</b>	CaCO <sub>3</sub> fluctuations during the Late Quaternary in the Atlantic Ocean cores.	36
<b>Fig. 12</b>	CaCO <sub>3</sub> fluctuations during the Late Quaternary in the Pacific Ocean.	38
<b>Fig. 13</b>	CaCO <sub>3</sub> fluctuations during the Late Quaternary in the Indian Ocean.	39
<b>Fig. 14</b>	<i>In-situ</i> CO <sub>3</sub> <sup>=</sup> concentrations (μmol/kg) calculated from GEOSECS stations with respect to depth (m)	

	at (a) stations 417, 420, and 425 for the western tropical Indian Ocean and (b) station 446, 448, 451, and 437 for the eastern tropical Indian Ocean.	41
<b>Fig. 15</b>	Size index values plotted as a function of depth in the tropical Indian Ocean.	42
<b>Fig. 16</b>	Size index versus $\text{CO}_3^{=*}$ concentration ( $\mu\text{mol/kg}$ ) plotted a reference line (Broecker and Clark, 1999) for the three major world oceans.	42
<b>Fig. 17.</b>	<i>Globigerinoides sacculifer</i> shell weights versus <i>Pulleniatina obliquiloculata</i> and <i>Neogloboquadrina dutertrei</i> shell weights show a linear trend, suggesting no measurement error or shell fill.	43
<b>Fig. 18.</b>	Shell weights of <i>Globigerinoides sacculifer</i> , <i>Pulleniatina obliquiloculata</i> , and <i>Neogloboquadrina dutertrei</i> versus bottom water $\text{CO}_3^{=*}$ concentrations.	
<b>Fig. 19.</b>	Calcite (104) FWHM ( $^{\circ}2\theta$ ) values plotted against pressure - normalized $\text{CO}_3^{=*}$ concentrations ( $\mu\text{mol/kg}$ ).	44
<b>Fig. 20.</b>	Comparison between the three proxies shows good linear regression. (a) Shell weight ( $\mu\text{g}$ ) versus size index % ( $R^2 = 0.7$ ), (b) calcite (104) FWHM ( $^{\circ}2\theta$ ) versus size index % ( $R^2 = 0.7$ ), and (c) calcite (104) FWHM ( $^{\circ}2\theta$ ) versus shell weight ( $\mu\text{g}$ ) ( $R^2 = 0.75$ ).	44
<b>Fig. 21.</b>	Fluctuations of total $\text{CaCO}_3$ and size index values at a) ODP Site 752 and b) ODP Site 715.	47
<b>Fig. 22.</b>	Fluctuations of $\text{CaCO}_3$ in $<63\mu\text{m}$ fraction at a) ODP Site 752 and b) ODP Site 715.	48
<b>Fig. 23.</b>	Fluctuations in <i>G. ruber</i> shell weights at ODP Site 715.	49
<b>Fig. 24.</b>	Fluctuations in $\text{CaCO}_3$ for the two cores a) AAS9/21 and b) SK218/A.	50
<b>Fig. 25.</b>	Fluctuations in size index for the two cores a) AAS9/21 and b) SK218/A.	51

<b>Fig. 26.</b>	Fluctuations in <i>G. sacculifer</i> shell weights for the two cores a) AAS9/21 and b) SK218/A.	52
<b>Fig. 27.</b>	Fluctuations in Mg/Ca for the two cores a) AAS9/21 and b) SK218/A.	53
<b>Fig. 28.</b>	The CaCO <sub>3</sub> % from core tops of the Atlantic, Pacific and Indian Ocean showing a linear variation with respect to pressure-normalised CO <sub>3</sub> <sup>=*</sup> calculated from GEOSECS stations (R <sup>2</sup> =0.7).	59
<b>Fig. 29.</b>	(a and b) SEM micrographs of <i>Globigerinoides sacculifer</i> from 3944 m water depth (SK199C/7) showing dissolution features. (c and d) Well-preserved tests of <i>Globigerinoides sacculifer</i> from 2250m water depth (SK199C/6).	65
<b>Fig. 30.</b>	Surface ocean CO <sub>3</sub> <sup>=</sup> concentrations (calculated from GEOSECS stations 417, 418, 419, 420, 421,424, and 425) and <i>Globigerinoides sacculifer</i> shell weights plotted as a function of latitude.	67
<b>Fig. 31.</b>	<i>G. sacculifer</i> shell weights from both the cores AAS9/21 and SK218/A at selective sections show a linear relation to Mg/Ca ratio at corresponding depths (R <sup>2</sup> =0.6).	80
<b>Fig. 32.</b>	CO <sub>3</sub> <sup>=</sup> concentrations calculated from <i>G. sacculifer</i> shell weights from the core AAS9/21 show a close relation to CO <sub>2</sub> measurements from an ice core (Taylor Dome, Antarctica).	85
<b>Fig. 33.</b>	CO <sub>3</sub> <sup>=</sup> concentrations water depth (m) for today's Indian Ocean and the glacial CO <sub>3</sub> <sup>=</sup> concentrations calculated from <i>G. sacculifer</i> shell weights from the cores AAS9/21 and SK218/A.	91

## LIST OF TABLES

<i>Table</i>	<i>Title</i>	<i>Page No.</i>
<b>Table 1.</b>	Cores recovered from the Atlantic, Pacific and Indian oceans at various locations and water depths.	22
<b>Table 2.</b>	Core tops from the Indian Ocean at various locations and water depths.	24
<b>Table 3.</b>	Cores from the Indian Ocean from various locations water depths. Also shown is the length of core recovered and used in the present study.	26
<b>Table 4.</b>	Various GEOSECS locations used in the present study from the Atlantic, Pacific and Indian Oceans.	29

## PREFACE

Carbon dioxide is one of the most important greenhouse gases responsible for global warming. The Oceans serve as major sinks and source of this gas through adjustments in its calcium carbonate reservoir. Investigation of this entity provides much of our knowledge of paleoclimatic change and is valuable in understanding the global carbon cycle (Farrell and Prell, 1989). The spatial and temporal accumulation patterns of calcium carbonate in the marine sediment records are thus a primary source of data about the carbonate chemistry, circulation of past oceans, global biogeochemical cycle of CO<sub>2</sub> (Peterson, 2001). Since the dissolution of calcium carbonates in the ocean sediments is primarily controlled by the degree of bottom water saturation with respect to the carbonate ion, the changes in carbonate ion concentrations during glacial and interglacials have attracted the attention of paleoceanographers (Broecker, 2004).

Three important paleocarbonate ion proxies find their application in understanding the depth of the calcite transition zone; the size index parameter (Broecker and Clark, 1999); shell weights of planktonic foraminifera (Lohmann, 1995) and; calcite crystallinity (Bassinot et al, 2004). Though these proxies have been largely applied to the Atlantic and Pacific, their application to the Indian Ocean is rare (Broecker and Clark, 1999; Broecker and Clark, 2001). The Indian Ocean remains to be a relatively lesser-studied region and more importantly so the northern Indian Ocean, with its unique monsoon circulation characteristics (Wyrki, 1973) is a genuine platform to evaluate the glacial to interglacial changes in CO<sub>2</sub> sequestration.

In this context, the proposed research is aimed to understand the Late Quaternary fluctuations in carbonate and carbonate ion content in the northern Indian Ocean with the following specific objectives:

- To identify suitable paleocarbonate ion proxy/proxies for understanding calcite dissolution in the Indian Ocean.
- To compare these proxies within themselves and use of these proxy/proxies in identifying calcite dissolution events and understanding the dissolution mechanisms on the seafloor.
- To understand the dependency of planktonic foraminiferal shell weights on initial growth conditions i.e. carbonate ion and/or temperature from tropical waters.
- To reconstruct the carbonate ion content for the northern Indian Ocean during the Late Quaternary.

This thesis consists of five chapters; contents of each chapter are listed below:

## **Chapter I**

This chapter deals with general introduction to carbon dioxide, its importance as a greenhouse gas, dissolution in seawater and its control over sedimentary calcite, the formation of carbonate ion and its significance. Also discussed here the circulation patterns of the Northern Indian Ocean during the Southwest (SW) and Northeast (NE) monsoons and whether Indian Ocean is a source or sink for CO<sub>2</sub>. An overview of available literature concerning the tackled problem is also put forth.

## Chapter II

This chapter deals with materials and methods. To achieve the proposed objectives, detailed work has been carried out on sediment core top samples from the western and eastern tropical Indian Ocean; SK199C/6, 7, 8, 9, 10, 11, SK218/A and Ocean Drilling Program Site (ODP) 752. Four sediment cores have been used; 1) Arabian Sea core AAS9/21, 2) Bay of Bengal core SK218/A, 3) ODP Site 715 from northern equatorial Indian Ocean on the eastern margin of Maldives Ridge and 4) ODP Site 752 from the eastern Indian Ocean near the crest of Broken Ridge. Data set for 10 cores from Atlantic, Pacific and Indian oceans were obtained from National Geophysical Data Centre (NGDC) of NOAA.

Core tops as well as sectioned core samples were subjected to size fraction analysis and calcium carbonate analysis, of  $>63\mu\text{m}$  and bulk sediment. The size index parameter was calculated from the  $>63\mu\text{m}$   $\text{CaCO}_3$  and bulk sediment  $\text{CaCO}_3$  data. Additionally, Carbonate analysis were carried out from  $<63\mu\text{m}$  fraction of sediment from ODP Sites 715 and 752. The ODP Site 752 core site is situated towards the southern Indian Ocean on a topographic high and has been used for a comparison. Carbonate ion concentration for the respective core sites was estimated from GEOSECS (GEOchemical SECTIONS Study) data. Shell weights (*Globigerinoides sacculifer*, *Neogloboquadrina dutetrei* and *Pulleniatina obliquiloculata*) were determined on selective coretop samples. *Globigerinoides sacculifer* shell weights were determined for the AAS9/21 and SK218/A cores. Shell weights for *Globigerinoides ruber* were determined for the ODP Site 715. Calcite crystallinity was measured on the species *Globigerinoides sacculifer* for the coretops. Scanning Electron Micrographs of *Globigerinoides sacculifer* shell were taken for specific

samples to show the impact of dissolution. Mg/Ca data from *Globigerinoides sacculifer* from the cores AAS9/21 and SK218/A was used as a proxy for temperature. Accelerator Mass Spectrometer radiocarbon dates were used to establish the chronology in AAS9/21 and SK218/A whereas for the ODP Sites 715 and ODP 752 available age control from nannofossil datum's were used (Duncan, 1990; Rea, 1990).

### **Chapter III**

This chapter gives a detailed account of the results obtained from the measurements stated above. The CaCO<sub>3</sub> variations patterns for the Atlantic, Pacific and Indian Oceans have been presented covering a time span of last 600kyr. Various carbonate ion proxies i.e. size index, shell weight and calcite crystallinity are compared within themselves using the core top samples. In-situ carbonate ion calculated from GEOSECS stations data have been used wherever comparison was required with respect to carbonate ion. The comparison shows significant relationships and suggests that all the three proxies can prove useful in the northern Indian Ocean to understand calcite dissolution and underlying mechanisms. A comparison has been made using the ODP Sites 715 and 752 and the CaCO<sub>3</sub> content of finer (<63 µm) and coarser fraction (>63 µm) to understand the temporal significance of size index proxy. ODP Site 752 shows high carbonate content throughout the 400kyr period, which is attributed to winnowing at shallow depths. Results show that carbonate content of the finer size fraction controls the bulk CaCO<sub>3</sub> variations in core ODP Site 715 as opposed to ODP Site 752. Shell weights from cores AAS9/21 and SK218/A are compared with the Mg/Ca data to understand the



effects of sea surface temperatures on shell weights. The core SK218/A is seen to be composed largely of broken foram shells for the last 10kyr as compared to core AAS9/21 which displays a continuous well preserved record and heavier shells.

## **Chapter IV**

This chapter consists of discussions on four important issues; 1) An overview of  $\text{CaCO}_3$  fluctuations during glacial and interglacials in equatorial regions of Pacific, Atlantic and Indian Oceans. A positive correlation has been found between carbonate content and bottom water carbonate ion concentration at respective depths for all the three major oceans which suggests a carbonate ion control over dissolution in the equatorial regions; 2) Using core top sediment samples from a western tropical Indian Ocean transect,  $\text{CaCO}_3$  size index, shell weights and calcite crystallinity have been successfully utilized to understand calcite dissolution and it is found that calcite dissolution starts from as shallow as 2500m and becomes intense from 3900m onwards in the equatorial Indian Ocean. This is because of bottom water undersaturation with respect to carbonate ion and not due to acidification of pore waters. It has also been shown that shell weights are dependant on growth conditions i.e. surface water carbonate ion in the tropical Indian Ocean. (3) The contradictory variations between size index and  $<63 \mu\text{m}$   $\text{CaCO}_3$  content in ODP Site 715 as compared to ODP Site 752 suggest that at ODP Site 715, the finer fractions mainly composed of coccoliths, controls the  $\text{CaCO}_3$  content of the sediment. This presents a severe drawback for application of the size index to understand the temporal carbonate ion variations; 4) Absence of sufficient number of planktonic foraminifera shells during the Holocene from core SK218/A suggest the corrosive nature of Bay of Bengal waters at 3000m during the Late Holocene compared to the Last Glacial

Maximum (LGM) when the carbonate ion gradient was steeper. Results from AAS9/21 show that the 90ppmV change in atmospheric CO<sub>2</sub> from LGM to the present interglacial has produced a 45- $\mu$ mol/kg change in surface water carbonate ion causing CO<sub>2</sub> sequestration.

## **Chapter V**

Deals with summary and conclusions on the use of proxies in understanding the glacial-interglacial carbonate ion changes in the Northern Indian Ocean.



## Acknowledgement

Foremost, I am greatly indebted to **Dr. P. Divakar Naidu**, my thesis guide who has encouraged me throughout. At the time of my PhD registration I got an opportunity to be a part of the National Centre for Antarctic and Ocean Research, and had to juggle between two diverse research fields. My research guide has been very patient in this regard in seeing me complete my thesis work. Needless to say this thesis would not have been possible without his guidance.

I thank **Prof. G. N. Nayak**, Head, Department of Marine Sciences, and my thesis co-guide, **Dr. S. Upadhay**, Reader, Department of Marine Sciences, Goa University for their kind support.

I wish to thank the National Institute of Oceanography for providing me an opportunity to work for this thesis. The Ex-Director of NIO, **Dr. Ehrlich Desa** set the course and direction for this work. His enthusiasm has always been contagious and he has forever encouraged me in this venture. Thereafter I am thankful to Director NIO, **Dr. S. R. Shetye** for allowing me to continue my thesis work and providing me the permission to work at the laboratories during on and off days.

I owe a favor to **Shri. Rasik Ravindra**, Director NCAOR, who has encouraged me in my job and shown the confidence in me to entrust some important tasks. He has been liberal in providing his much required support in completing this thesis.

I express my sincere thanks to the Founder Director of NCAOR, **Prof. P. C. Pandey** whose positive attitude has provided me the much needed boost in my work. I also thank **Dr. M. Sudhakar**, Scientist G, NCAOR, for his support and encouragement during various stages of this work.

I thank all the members of the 'Faculty Research Committee', **Prof. P. V. Dessai**, Dean, Faculty of Life Sciences and Environment, Goa University, **Prof. G. N. Nayak**, **Prof. D. J. Bhat**, Former Dean and **Dr. R. Nigam**, Vice-Chancellors nominee, who have encouraged me, shown me my shortcomings and steered this research work in the right direction.

I also thank senior scientists at NIO, **Drs. A.C. Anil**, **V. Banakar**, **J. Pattan**, **V. Ramaswamy**, **B. Nagendranath**, **M. Dileep Kumar**, **D. V. Borole**, **M. Tapaswi**, **G. Parthiban**, **K. Srinivas**, **P. V. Shirodkar** and **V. V. Gopalakrishna** who have helped during various stages of this work. Thanks are due to **Shri. V. Khedekar** for the SEM pictures and **Shri. G. Prabhu** from NIO for the XRD analysis.

I specially thank **Dr. Thamban Meloth**, Scientist and Lab in-charge, NCAOR, for providing his much needed encouragement and support. **Dr. Rahul Mohan**, Scientist, NCAOR, has helped with the microscopes and the SEM. He has also been a constant source of encouragement for me.

I also wish to thank the senior scientists at NCAOR, **Drs. Rajan** and **Shivaji** for their support and **Shri. Javed Beg**, Scientist, NCAOR for extending his help during my compilation work. I appreciate the encouragement and well-wishes of my colleagues **Dr. Witty**, **Laluraj**, **Prashant**, **Ashish**, **Anand**, **Kalindi** and **Sunaina**. Thanks are also due to **Dr. P. Govil** for his help with the core samples and **Dr. S. K. Chaturvedi** for the core top samples.

I thank **Shri. Mukesh** from NCAOR and **Shri. Mahale** and **Uchil** from NIO for help with the figures. **Shri. P. Shetkar**, **Lalit**, **Nixon** and **Gupfetry** have helped with the computers. I express thanks to **Shri. Nagoji Rao** from NCAOR for his support during difficult times. I also thank **Shri. Keshav Naik** for his assistance during initial stages of this work.

Special thanks to **Shri. S. N, Jakhi** from NIO, who has devoted his precious time in final arrangement of this thesis.

**Prof. Wally Broecker** and **Dr. Taro Takahashi** from **LDEO, Columbia** helped me with the calculations required in the thesis. Discussion with **Prof. Henry Elderfield**, University of Cambridge, UK, and **Dr. Frank Bassinot**, Senior Scientist, IPSL/LSCE, France, proved fruitful.

Thanks are due to my teachers at the Marine Sciences Department of Goa University, **Drs. Upadhay, Matta, Menon** and **Rivonkar**. Thanks are also due to the Marine Sciences Department's office staff, **Sanjana, Narayan, Serrao** and **Ulhas**.

My acknowledgements are incomplete without mention of my friends at the Micropaleontology laboratory, NIO, **Rajani, Sujata, Lea, Sanjay** and **Shanmukha** who were ever ready to help during odd hours. I am also in particular grateful to my friends whom I may have unknowingly missed out from this list.

Finally, I thank my parents for their unending love and support throughout. I also thank little **Suhani**, my daughter who has helped me in shuffling and re-shuffling many of the reprints used in this thesis.

# CHAPTER I

## INTRODUCTION

### 1.1 General Introduction:

The greenhouse effect is one of Earth's natural processes which helps to regulate the temperature of our planet and hence is essential for life on Earth. It is the result of heat absorption by certain gases in the atmosphere known as 'the greenhouse gases' because they effectively 'trap' heat in the lower atmosphere and re-radiate some of the heat downwards. Without a natural greenhouse effect, the temperature of the Earth would be about 0°F (-18°C) instead of its present 57°F (14°C). Water vapor is the most abundant greenhouse gas, followed by carbon dioxide and other trace gases. The foremost among these and of growing concern is carbon dioxide emitted from combustion of coal oil and gas. Human activity has been increasing the concentration of greenhouse gases in the atmosphere. The present values of this gas in the atmosphere have exceeded 380 ppmv (Fig. 1).

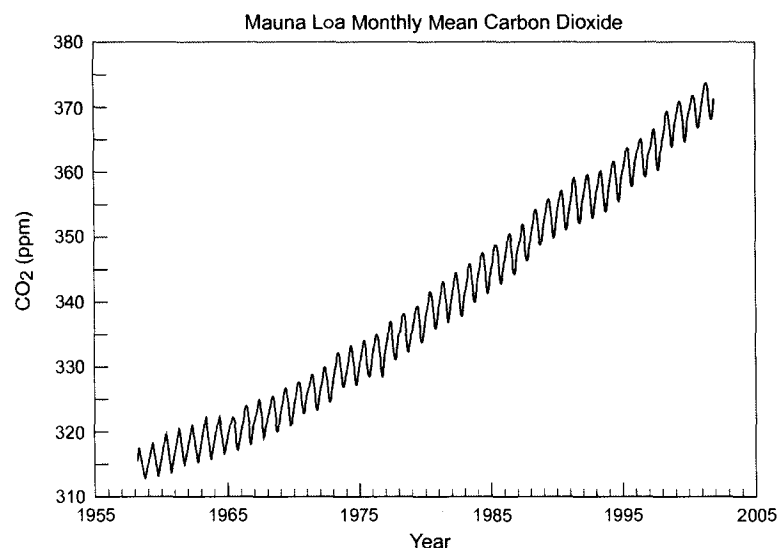


**Fig. 1. Mauna Loa Carbon Dioxide Record documents a 0.53% or two parts million per year increase in atmospheric carbon dioxide since 1958. This gas alone is responsible for 63% of the warming attributable to all greenhouse gases according to NOAA's Earth System Research Lab (source: National Oceanographic and Atmospheric Administration)**

The direct evidence for natural variations in atmospheric CO<sub>2</sub> comes from the air that is trapped in Antarctic glacial ice. Records from Antarctic ice cores indicate that the concentration of CO<sub>2</sub> in the atmosphere has varied in step with the waxing and waning of ice ages (Barnola *et al.*, 1987; Petit *et al.*, 1999) (Fig. 2). The concentration of CO<sub>2</sub> in our atmosphere today is the highest, not been exceeded in the last 420,000 years, and likely not in the last 20 million years (Petit *et al.*, 1999). At the end of the last ice age 18 thousand years ago (18ka), CO<sub>2</sub> rose from a glacial minimum of 189 ppm to 265 ppm at the beginning of the Holocene.

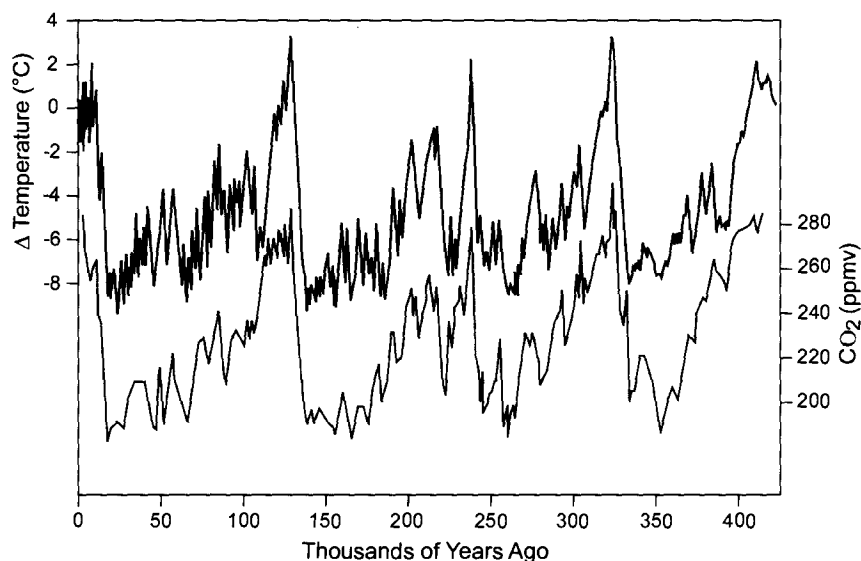


**Fig. 2. Temperature and CO<sub>2</sub> concentrations in atmosphere over the past 400,000 years (from Petit *et al.*, 1999).**

This concentration of CO<sub>2</sub> in the atmosphere is set by the separation of carbon between the various reservoirs of the ‘surficial’ system and ‘geological’ reservoirs (Berner and Caldeira, 1997). The former includes atmosphere, oceans, biosphere, soils and exchangeable sediments in the marine environment (Fig. 3a and b) while the

latter include crustal rocks and deeply buried sediments in addition to the underlying mantle.

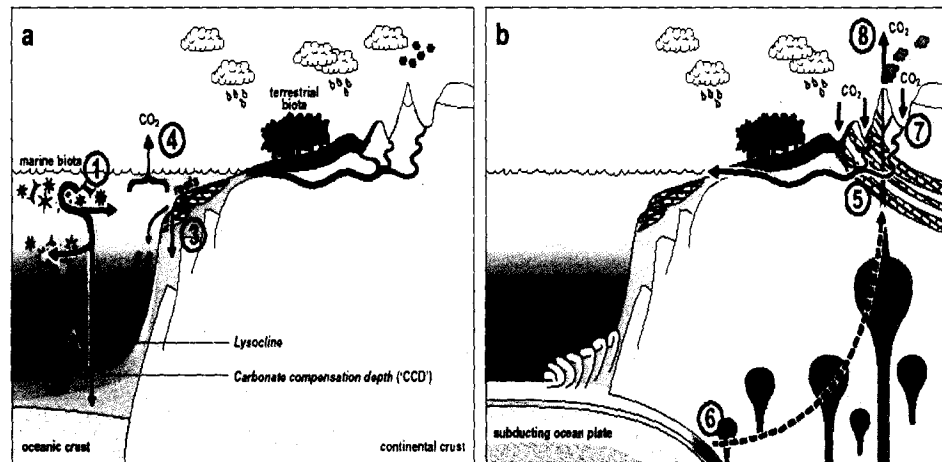


**Fig. 3.** The global biogeochemical cycling of calcium carbonate. (a) Modes of CaCO<sub>3</sub> transformation and recycling within the surficial system and loss to the geological reservoir (labeled '1' through '4'). 1) Precipitation of calcite by coccolithophores and foraminifera in the open ocean, 2) Carbonate reaching deep-sea sediments and subsequent dissolution if the bottom water is under-saturated and/or the organic matter flux to the sediments is sufficiently high, 3) Precipitation of CaCO<sub>3</sub> by corals and shelly animals. Because modern surface waters are over-saturated relatively little of this carbonate dissolves *in-situ*, and instead contributes to the formation of reefal structures or is exported to the adjoining continental slopes, 4) Precipitation of CaCO<sub>3</sub> resulting in higher pCO<sub>2</sub> at the surface, driving a net transfer of CO<sub>2</sub> from the ocean to the atmosphere. (b) Modes of CaCO<sub>3</sub> transformation and recycling within the geologic reservoirs and return to the surficial system (labeled '5' through '8'). 5) CaCO<sub>3</sub> laid down in shallow seas as platform and reef carbonates and chalks can be uplifted and exposed to erosion through rifting and mountain-building episodes. CaCO<sub>3</sub> can then be directly recycled, 6) Thermal breakdown of carbonates subducted into the mantle, resulting in release of CO<sub>2</sub>, 7) Weathering of silicate rocks, 8) Emission to the atmosphere of CO<sub>2</sub> produced through decarbonation. This closes the carbon cycle on the very longest time-scales (from Ridgwell and Zeebe, 2005)

## 1.2 Seawater carbonate chemistry:

In seawater, carbon occurs as several species: CO<sub>2</sub> gas, H<sub>2</sub>CO<sub>3</sub>, HCO<sub>3</sub><sup>-</sup> and CO<sub>3</sub><sup>=</sup> as well as carbon combined in organic molecules. HCO<sub>3</sub><sup>-</sup> and CO<sub>3</sub><sup>=</sup> are the most important of these. Precipitation of CaCO<sub>3</sub> from seawater may be described by the following reaction:





Under typical marine conditions, carbon dioxide will largely hydrate to form a proton ( $\text{H}^+$ ) and a bicarbonate ion ( $\text{HCO}_3^-$ );  $\text{H}_2\text{O} + \text{CO}_2(\text{aq}) \rightarrow \text{H}^+ + \text{HCO}_3^-$ , while true carbonic acid ( $\text{H}_2\text{CO}_3$ ) is only present in very small concentrations. A fraction of  $\text{HCO}_3^-$  dissociates to form a carbonate ion ( $\text{CO}_3^{2-}$ );  $\text{HCO}_3^- \rightarrow \text{H}^+ + \text{CO}_3^{2-}$ . The sum total;  $\text{CO}_2(\text{aq}) + \text{H}_2\text{CO}_3 + \text{HCO}_3^- + \text{CO}_3^{2-}$  is collectively termed dissolved inorganic carbon (DIC) (Fig. 4).

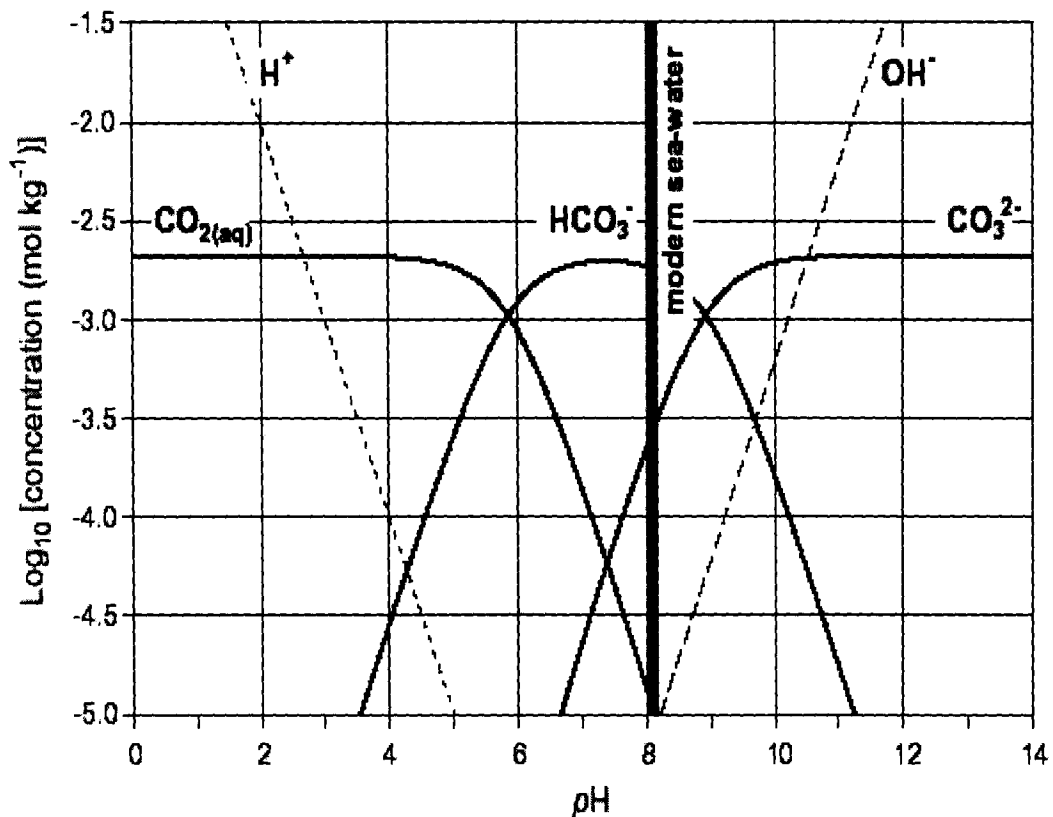


**Fig. 4.** The concentrations of the dissolved carbonate species as a function of pH : Dissolved carbon dioxide ( $\text{CO}_{2(\text{aq})}$ ), bicarbonate ( $\text{HCO}_3^-$ ), carbonate ion ( $\text{CO}_3^{2-}$ ), hydrogen ion ( $\text{H}^+$ ), and hydroxyl ion ( $\text{OH}^-$ ). At modern seawater pH, most of the dissolved inorganic carbon is in the form of bicarbonate. Note that in seawater, the relative proportions of  $\text{CO}_2$ ,  $\text{HCO}_3^-$ , and  $\text{CO}_3^{2-}$  control the pH and not vice versa. (from Ridgwell and Zeebe, 2005).

The climatic importance of the  $\text{CaCO}_3$  precipitation reaction arises because although the sum total of dissolved carbon species (DIC) is reduced, the remaining carbon is re-partitioned in favor of  $\text{CO}_2(\text{aq})$ , resulting in a higher partial pressure of  $\text{CO}_2$  ( $p\text{CO}_2$ ) in the surface ocean. Precipitation of carbonate carbon drives an increase

in ocean  $p\text{CO}_2$ , and with it, an increase in atmospheric  $\text{CO}_2$  concentration. Conversely, dissolution of  $\text{CaCO}_3$  drives a  $p\text{CO}_2$  (and atmospheric  $\text{CO}_2$ ) decrease. Whether  $\text{CaCO}_3$  precipitates or dissolves depends on the relative stability of its crystal structure. This can be directly related to the ambient concentrations (strictly, activities) of  $\text{Ca}^{2+}$  and  $\text{CO}_3^{=}$  by the saturation state (also known as the solubility ratio)  $\Omega$  of the solution, defined;  $\Omega = [\text{Ca}^{2+}] * [\text{CO}_3^{=}] / K_{sp}$ , where  $K_{sp}$  is a solubility constant (Zeebe and Gladrow, 2001). The precipitation of calcium carbonate from seawater is thermodynamically favorable when  $\Omega$  is greater than unity and occurs at a rate taking the form of a proportionality with  $(\Omega - 1)^n$  (Zhong and Mucci, 1993), where 'n' is a measure of how strongly the precipitation rate responds to a change in  $\text{CO}_3^{=}$ . Conversely,  $\text{CaCO}_3$  will tend to dissolve at  $\Omega < 1.0$ , and at a rate proportional to  $(1 - \Omega)^n$  (Walter and Morse, 1985). As well as the concentrations of  $\text{Ca}^{2+}$  and  $\text{CO}_3^{=}$ , depth in the ocean is also important because  $K_{sp}$  scales with increasing pressure. Since  $K_{sp}$  and  $\Omega$  are inversely related, the greater the depth in the ocean the more likely the ambient environment is to be under-saturated (i.e.,  $\Omega < 1.0$ ).

### 1.3 Carbonate production in the ocean:

Biological productivity in the ocean plays a central role in the sequestration of atmospheric carbon dioxide, which is referred to as the “biological pump” (Fig. 5). The biological pump extracts carbon from the “surface skin” of the ocean that interacts with the atmosphere, presenting a lower partial pressure of carbon dioxide to the atmosphere and thus lowering its  $\text{CO}_2$  content (Sigman and Haug, 2003). The ocean receives a continual input of calcium from riverine and groundwater sources and from the hydrothermal alteration of oceanic crust at mid-ocean ridge spreading centers. Balancing this input is the biological precipitation of calcium carbonate

(CaCO<sub>3</sub>) by shell and skeletal-building organisms in both shallow marine and open-ocean environments.

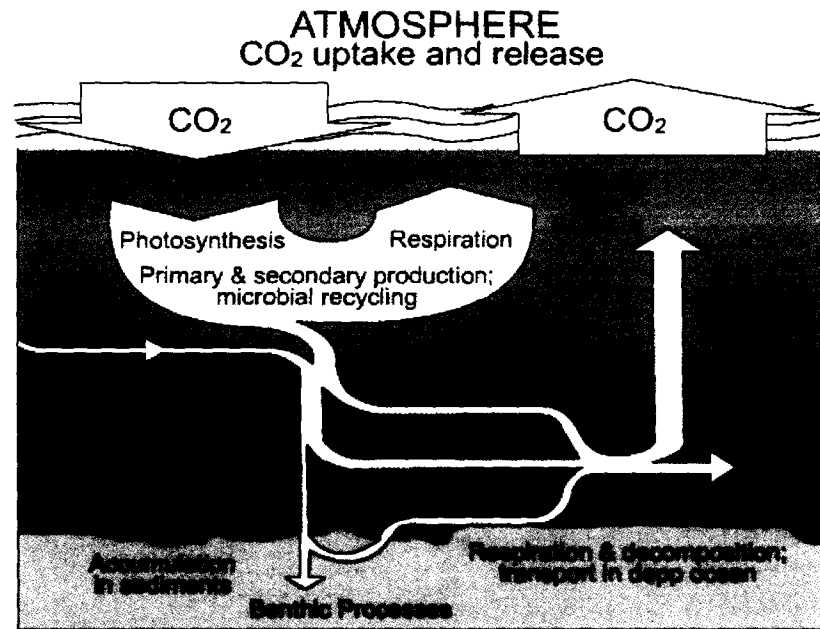


**Fig. 5. Schematic of the ocean carbon biological pump.** Transfer of CO<sub>2</sub> from the surface oceans to the deep water is brought about by photosynthesis. Marine algae are responsible for nearly one third of the global gross photosynthetic production. The important fraction of this cycling is the amount of carbon that is lost from the surface layer to the deeper ocean (the export production) compared to the carbon that is simply recycled in, or near, the euphotic zone (up to the top 50 metres). The sequestration of carbon in the ocean interior by the growth of phytoplankton in the sunlit surface ocean, the downward rain of organic matter back to carbon dioxide (CO<sub>2</sub>). The nutrients and CO<sub>2</sub> are reintroduced to the surface ocean by mixing and upwelling. The biological pump lowers the CO<sub>2</sub> content of the atmosphere by extracting it from the surface ocean (which exchanges CO<sub>2</sub> with the atmosphere) and sequestering it in the isolated waters of the ocean interior. In most of the lower and mid-latitude ocean, the surface is isolated from the deep-sea by a temperature-driven density gradient, or “thermocline” (Houghton et al., 1996).

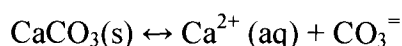
In the deep sea, the primary contributors to the carbonate budget of open-ocean sediments are the skeletal remains of calcareous plankton that have settled down from the surface after death. Calcareous skeletal material is made of either calcite or aragonite, both of which have the same chemical formula, CaCO<sub>3</sub>, but different crystalline structure. Foraminifera are amongst the important carbonate

producers in the open ocean along with coccolithophorids, unicellular phytoplankton and zooplankton. Foraminifera produce a calcareous shell or 'test', a few hundred microns in size that sinks after death or reproduction to the seafloor. They construct their skeletal elements out of mineral calcite, the more stable polymorph of  $\text{CaCO}_3$ . Seafloor sediments consisting of more than 30% by weight calcium carbonate are traditionally referred to as calcareous or carbonate ooze. Such oozes accumulate at the rate of 1-4cm per 1000yrs and cover roughly half of the ocean bottom. Carbonate oozes are the most widespread biogenous sediments in the ocean.

While the biological production of calcium carbonate in oversaturated surface waters determines the input of carbonate to the deep sea, it is the dissolution of carbonate in undersaturated deep waters that has the dominant control on calcium carbonate accumulation in the open ocean. Since carbonate production rates in the surface ocean today greatly exceed the rate of supply of calcium, this 'compensation' through dissolution must occur in order to keep the system in steady state. Increased dissolution at depth is largely a function of the effect of increasing hydrostatic pressure on the solubility of carbonate. However superimposed on this bathymetric effect are regional preservation patterns related to differences in carbonate input and the carbonate chemistry of deep water masses. Carbonate oozes in the deep-sea serve as a major reservoir of calcium and carbon dioxide on the earth's surface. Their spatial and temporal accumulation patterns in the marine stratigraphic record are thus a primary source of data about the carbonate chemistry and circulation of past oceans as well as of the global biogeochemical cycle of  $\text{CO}_2$ .

## 1.4 Lysocline and the CCD:

The distribution of carbonate sediments in the ocean basins is far from uniform. Although surface productivity and dilution by non-carbonate sediment sources can locally influence the concentration of carbonate in the deep-sea sediments, the clear-cut relationship between calcium carbonate content and water depth indicates that carbonate dissolution plays a major role in governing carbonate dissolution patterns (Peterson, 2001). To a first approximation, the dissolution of carbonate on the sea floor is a function of the corrosiveness or saturation state of the overlying bottom waters.



At equilibrium, the rate of carbonate dissolution is equal to the rate of its precipitation and the seawater is said to be saturated with respect to the carbonate phase. In the deep sea, the degree of calcium carbonate saturation (D) can be expressed as:

$$D = \frac{[\text{Ca}^{2+}]_{\text{seawater}} \times [\text{CO}_3^{2-}]_{\text{seawater}}}{[\text{Ca}^{2+}]_{\text{saturation}} \times [\text{CO}_3^{2-}]_{\text{saturation}}}$$

Where  $[\text{Ca}^{2+}]_{\text{seawater}}$  and  $[\text{CO}_3^{2-}]_{\text{seawater}}$  are the *in situ* concentrations in the water mass of interest and  $[\text{Ca}^{2+}]_{\text{saturation}}$  and  $[\text{CO}_3^{2-}]_{\text{saturation}}$  are the concentrations of these ions at equilibrium or saturation at the same conditions of pressure and temperature (Peterson, 2001). Since shell formation and dissolution cause the concentration of  $\text{Ca}^{2+}$  to vary less than 1% in the ocean, the degree of calcium carbonate saturation (D) can be simplified and expressed in terms of the concentration of the carbonate ions only:

$$D = \frac{[\text{CO}_3^{2-}]_{\text{seawater}}}{[\text{CO}_3^{2-}]_{\text{saturation}}}$$

D is thus a measure to the degree to which a seawater sample is saturated with respect to calcite. Values of  $D > 1$  indicates oversaturation while values of  $D < 1$  indicate undersaturation and a tendency for calcium carbonate to dissolve. Since the saturation carbonate ion concentration increases with increasing pressure and decreasing temperature, calcium carbonate is more soluble in deep sea than at the surface. At the depth in the water column where  $D = 1$ , the transition from oversaturated to undersaturated conditions is reached. This depth is known as the saturation horizon.

The carbonate used by many planktonic organisms to form their hard parts redissolves when the organisms die and sink into deep water, releasing calcium and carbonate ions back into solution. The depth at which the dissolution of calcareous skeletal material begins (i.e. the depth where the water has become significantly undersaturated) is called the **lysocline**. The depth at which all the carbonate has dissolved is called the Calcite Compensation Depth (**CCD**). The aragonite structure is thermodynamically less stable than that of calcite, so aragonite dissolves more readily than calcite. Therefore the lysocline and CCD are shallower for aragonite than for calcite, because skeletal material is much more commonly formed of calcite than aragonite. It is rare to find aragonite remains in sediments below 1-2km and sediments below 4km seldom contain significant amount of calcite debris.

Variations in depth of the lysocline are controlled by the chemistry of the water column (carbonate equilibria and pH). Variations in the CCD are controlled partly by chemistry and partly by the supply of calcareous material sinking from the

surface. Because it is not easy to determine how much material has been dissolved, both lysocline and CCD are depth zones rather than precisely defined levels. High biological production results in large populations of organisms and a high rate of supply of calcareous skeletal material to deep water when the organisms die. A heavy 'rain' of carbonate debris will reach greater depths before it all dissolves than would a meager supply of calcareous material sinking from a region of low biological production. So the CCD tends to be depressed beneath areas of high biological production. Cullen and Prell, (1984), made an extensive study using surface sediment samples from the northern Indian Ocean to determine how abundance of planktonic foraminifera species are affected by dissolution. Variations in abundance of dissolution resistant planktonic foraminifera species with water depth reveal the foraminiferal lysocline (FL) to be at 3800m in the equatorial Indian Ocean, 3300m in the Arabian Sea and 2600 to 2000m in the Bay of Bengal. Lower to these depths whole foraminiferal tests are absent, below 4600m in eastern equatorial region, below 5000m in western equatorial region and below 3000m in the Bay of Bengal (Cullen and Prell, 1984). This depth is the Foraminiferal Compensation Depth which is similar to the CCD.

### **1.5 Importance of $\text{CO}_3^{=}$ in the oceanic $\text{CO}_2$ cycle:**

In today's ocean, marine organisms secrete calcitic hard parts at a rate several times faster than  $\text{CO}_2$  is being added to the ocean-atmosphere system (via planetary outgassing and weathering of continental rocks) (Broecker, 2003). While the state of saturation in the ocean is set by the product of the  $\text{Ca}^{2+}$  and  $\text{CO}_3^{=}$  concentrations, calcium has such a long residence ( $10^6$  yr) that, at least on the timescale of a single glacial cycle ( $\sim 10^5$  yr), its concentration can be assumed to have remained unchanged

(Broecker, 2003). In contrast, the dissolved inorganic carbon in the ocean is replaced on a timescale roughly equal to that of the major glacial to interglacial cycle ( $10^5$  yr). But, since in the deep sea  $\text{CO}_3^{=}$  ion makes up only  $\sim 5\%$  of the total dissolved inorganic carbon, its adjustment time turns out to be only about one-twentieth that for dissolved inorganic carbon  $\sim 5,000$  yr (Broecker, 2003). Hence, the concentration of  $\text{CO}_3^{=}$  has gradients within the sea and likely has undergone climate-induced changes. These changes involve both the carbonate ion concentration averaged over the entire deep ocean and its distribution with respect to water depth and geographical location. It is the global average carbonate ion concentration in the deep sea that adjusts in order to assure the burial of  $\text{CaCO}_3$  in the sediments matches the input of  $\text{CO}_2$  to the ocean atmosphere system. As part of the Geochemical Section Studies (GEOSECS), Transient Tracers in the Ocean program (TTO), South Atlantic Ventilation Experiment (SAVE) and World Ocean Circulation Experiment (WOCE) ocean surveys,  $\Sigma \text{CO}_2$  and alkalinity measurements were made on water samples at various depths from the world oceans. Given the depth, temperature, salinity and phosphate it is possible to compute *in situ* carbonate ion concentrations. Taro Takahashi from Lamont Doherty Earth Observatory has played a key role in these measurements and conversion to *in situ* carbonate ion concentrations. A complete picture of the  $\text{CO}_3^{=}$  ion concentrations in the deep sea is now available. Below 1,500m in the world ocean, the distribution of carbonate ion concentration is remarkably simple. For the most part, waters in the Pacific, Indian and Southern Oceans have concentrations confined to the range  $83 \pm 8 \mu\text{mol kg}^{-1}$  (Takahashi, 2001). The exception is the northern Pacific, where the values drop to as low as  $60 \mu\text{mol kg}^{-1}$ . In contrast much of the deep water in the Atlantic has concentrations in the range  $112 \pm 5 \mu\text{mol kg}^{-1}$  (Takahashi, 2001).



Attention is therefore now focused on distribution of  $\text{CO}_3^{=}$  concentration in the deep sea for it alone sets the depth of the transition zone.

Dissolution of calcite proceeds probably by three different mechanisms: The first of these is termed water column dissolution. As foraminifera shells fall quite rapidly and as they encounter calcite-undersaturated water only at great depth, it might be concluded that dissolution during fall is unimportant. But it has been suggested that organisms feeding on falling debris ingest and partially dissolve calcite entities (Milliman *et al.*, 1999). The two other processes involve dissolution of calcite after it reaches the seafloor. A distinction is made between dissolution that occurs before burial (i.e. interface dissolution) and dissolution that take place after burial (i.e. pore water dissolution). The former presumably occurs only at water depth greater than that of the saturation horizon. But the later has been documented to occur above the calcite saturation horizon. It is driven by respiration  $\text{CO}_2$  released to the pore waters.

## **1.6 Study Area:**

### **1.6.1 Oceanographic settings:**

The Indian Ocean ranks third in size amongst the major oceans of the world. It covers an area of 73million square kilometers. It has a triangular and asymmetric shape with width exceeding 10,000kms between the Cape of Good Hope and Western Australia and decreases sharply on moving northwards to India. The Indian Ocean is unique in that it is limited in the north by the Asian continent and lies well below  $30^\circ\text{N}$ , cut off from the cold waters of polar origin.

The most unique characteristics of the northern Indian Ocean are the semi-annually reversing monsoon winds (Wyrтки, 1973). The influence of the monsoons on the Indian Ocean is seen in the reversal of the surface circulation and in the hydrographical conditions of the surface waters down to 10-20°S. During the South West (SW) monsoon (May through October) the surface low level of southeasterly trade winds of the Southern Hemisphere extend across the equator to become southerly or southwesterly in the Northern Hemisphere which drive the Somali Current (SC), South Equatorial Current (SEC) and the Monsoon Current (MC) (Fig. 6). The northward flowing Somali Current invokes intense upwelling along the coast of Somalia (Bruce, 1974; Schott, 1983). During the SW monsoon period the strong winds blow parallel to the Oman coast and develop another centre of intense upwelling. The volume and nutrient enrichment caused by the upwelling along the Oman Margin is stronger compared to the volume and enrichment resulting from upwelling along the Somali Margin (Wyrтки, 1973; Bruce, 1974; Shallow; 1984). Along the west coast of India weak upwelling centres develop under favourable conditions during this period (Wyrтки, 1973).

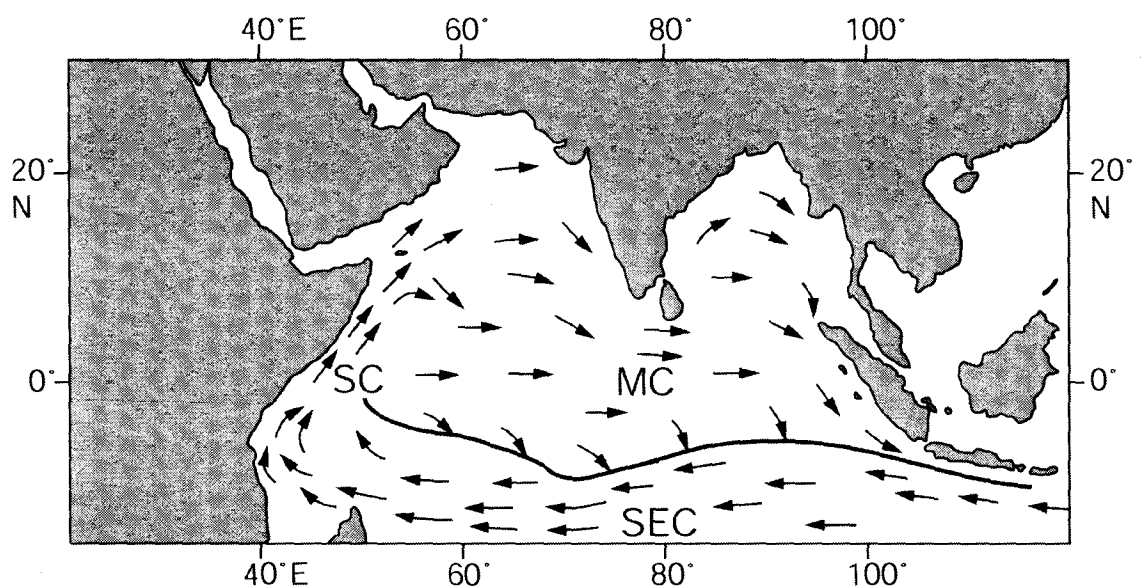


**Fig. 6. Surface circulation in the Indian Ocean during the peak period (August) of the SW monsoon (from Wyrтки, 1973)**

Oceanic circulation during the NE monsoon is relatively weak and characterized by the North Equatorial Current (NEC), an eastward flowing Equatorial Counter Current (ECC), and a moderately developed anticyclonic gyre (Fig.7).

Two surface-water masses form in the northern Indian Ocean (Wyrтки, 1973). A high-salinity water mass is formed in the Arabian Sea due to excess evaporation and the subsurface flow of Persian Gulf and Red Sea water. A low-salinity water mass is formed in the Bay of Bengal by excess precipitation and abundant river runoff. Thus a great salinity gradient exists in the northern Indian Ocean. The low-salinity water mass of the Bay of Bengal flows to the south of Ceylon; one branch continues westward along latitude of 5°N and another branch extends northwestwardly along the coast of India during the North East (NE) monsoon.

In contrast to the salinity patterns in the northern Indian Ocean, variation in sea-surface temperature (SST) is minor.

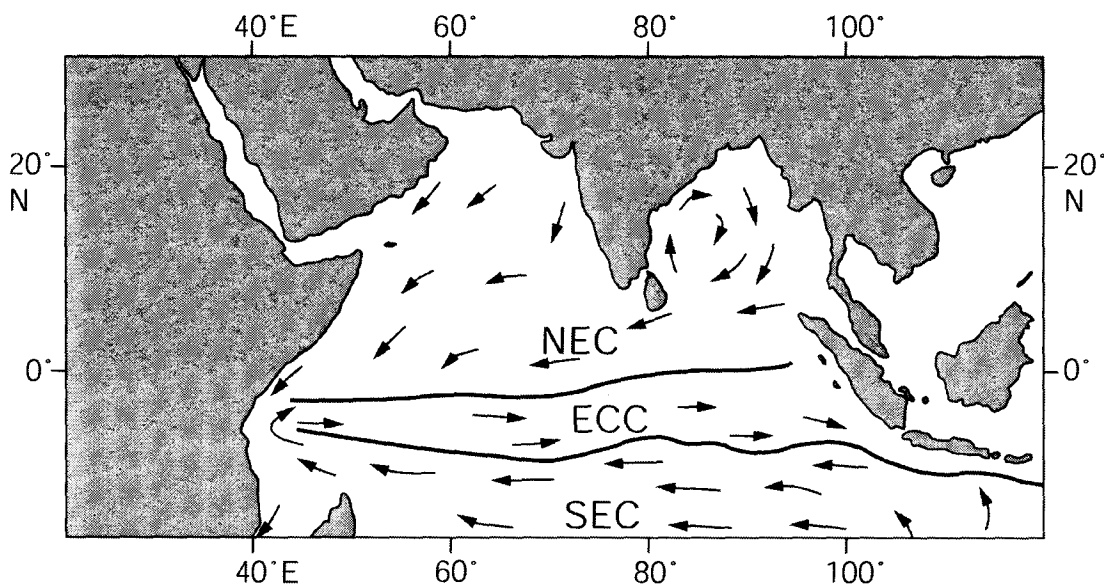


**Fig. 7. Surface circulation in the Indian Ocean during the peak period (February) of the NE monsoon (from Wyrтки, 1973)**

Much of the regional temperature variation is due to upwelling of cooler subsurface waters in the western Arabian Sea during the SW monsoon. This creates an east-west temperature gradient in the region. During the NE monsoon, equatorial surface waters remain between 28°C and 28.5°C. A weak north-south temperature gradient is observed in the Bay of Bengal, and a weak NW- SE gradient occurs in the Arabian Sea. However, equatorial upwelling does not occur in the Indian Ocean as in the Pacific and Atlantic, because in those oceans, upwelling occurs as a result of the southeast trade winds blowing across the equator and causing surface divergence, which are not present in the Indian Ocean. The Indian Ocean, north of the Hydrochemical Front (a strong discontinuity in hydrochemical structure at 10°S), has been believed to serve as a source of CO<sub>2</sub> to the atmosphere for quite some time (George *et al.*, 1994; Takahashi, 1989). Due to the very high partial pressure of CO<sub>2</sub> (pCO<sub>2</sub>) in subsurface waters (>1000 l atm), upwelling and vertical mixing were expected to favor outgassing of CO<sub>2</sub> from the surface layer in the northwestern Indian Ocean (George *et al.*, 1994). This effect would be aided by the biological precipitation of CaCO<sub>3</sub> (calcification), which raises pCO<sub>2</sub> of surface waters (pCO<sub>2</sub><sup>sw</sup>), but opposed by the high rate of photosynthetic production, which lowers pCO<sub>2</sub><sup>sw</sup>, sustained by copious nutrients in the mixed-layer. The results of the Joint Global Ocean Flux Study (JGOFS) undertaken between 1993 and 1997 have conclusively established that the Arabian Sea serves as a source of CO<sub>2</sub> for the atmosphere at almost all places and during all seasons (Naqvi *et al.*, 2005). An earlier study by George *et al.* (1994), had led to an estimate of 79 Tg C for the annual CO<sub>2</sub> emission from the Arabian Sea (area 6.2 x 10<sup>6</sup> km<sup>2</sup>). Thus, while the unique physical forcing results in extremely pronounced changes in the flux of CO<sub>2</sub> both in space and time with the SW Monsoon accounting for the bulk of the emissions, the overall contribution of the Arabian Sea

to the global air–sea CO<sub>2</sub> exchange is not very significant due to its small area. The northwestern Indian Ocean, which receives outflows from the Persian Gulf and the Red Sea, appears to hold more anthropogenic CO<sub>2</sub> than the equatorial Indian Ocean. The total inventory of anthropogenic CO<sub>2</sub> in the Indian Ocean north of 35°S has been estimated to be 13.6 Pg C (1 Pg = 10<sup>15</sup> g). Also, unlike the Pacific and the Atlantic Oceans the equatorial Indian Ocean appears to be a relatively small source of atmospheric CO<sub>2</sub> (Sabine *et al.*, 2000). The net annual flux of CO<sub>2</sub> for the region lying north of 36°S was 150 Tg C, and it was directed from the atmosphere to the ocean. The Indian Ocean as a whole (north of 36°S) oscillates between a weak net source (22 Tg) during January– March to a net sink (87 Tg) during July–September (Sabine *et al.*, 2000). Interestingly the period of maximal net absorption is the same as that of maximal SW Monsoon-forced emissions from the Arabian Sea, reflecting the dominance of removal by CO<sub>2</sub>-undersaturated waters in determining the CO<sub>2</sub> uptake/emission balance in the region.

Comparison for the three major world oceans shows that the Atlantic Ocean is the largest net sink for atmospheric CO<sub>2</sub> (39%) followed by Southern Ocean (26%), the Indian Ocean (24%) and the Pacific Ocean (11%) (Takahashi *et al.*, 1997; Takahashi, 2001). The behavior of the Atlantic Ocean as a strong sink of CO<sub>2</sub> is due to the fact that the North Atlantic contain low CO<sub>2</sub> concentrations, which are in turn caused primarily by the short residence time (~80y) of the North Atlantic Deep Waters (Takahashi, 2001). The Pacific Ocean behaves as a weak sink due to its balance as a CO<sub>2</sub> source during El Niño and non sink during El Niño periods whereas cold temperatures and moderate photosynthesis is responsible for the large CO<sub>2</sub> uptake by the Southern Ocean (Takahashi, 2001).

## 1.7 Previous Studies:

### 1.7.1 Calcium carbonate fluctuations:

The existence of interglacial/glacial  $\text{CaCO}_3$  cycles in the equatorial Pacific Ocean was first observed during the Swedish Deep Sea Expedition (1947-1948) (Arrhenius, 1952). Since then many studies have been devoted to unraveling  $\text{CaCO}_3$  cyclicity in the Pacific and Atlantic oceans and a few in the Indian Ocean. There has been a debate whether productivity of  $\text{CaCO}_3$  secreting organisms or dissolution of  $\text{CaCO}_3$  essentially control the  $\text{CaCO}_3$  cycles. Arrhenius (1952, 1988) Olausson (1965, 1985), Emerson and Bender (1981) and Archer (1991) argued that productivity has the most important influence on  $\text{CaCO}_3$  content in the deep-sea sediments, whereas Gardner (1975), Berger (1973,1992), Farrell and Prell (1989) were of the opinion that it is mainly controlled by dissolution.

In the Pacific Ocean, it is widely accepted that  $\text{CaCO}_3$  content is higher during glacial and lower during interglacials (Volat *et al.*, 1980). This pattern has been termed as the 'Pacific pattern'. In contrast, in the Atlantic Ocean,  $\text{CaCO}_3$  content is generally higher during interglacials and lower during glacial (Volat *et al.*, 1980), which is termed as the 'Atlantic pattern'. However, the typical Pacific pattern of  $\text{CaCO}_3$  variation has only a limited geographical extent in the Pacific (Snoeckx and Rea, 1994), and thus the entire Pacific Ocean is not marked by the same pattern of  $\text{CaCO}_3$  changes in the Quaternary. The Quaternary  $\text{CaCO}_3$  patterns in the Indian Ocean have not been analyzed in such detail as in the Pacific and Atlantic Oceans. In the Indian Ocean some sites exhibit a Pacific pattern (Olausson, 1967, 1969, 1971; Oba, 1969; Naidu, 1991, 1994; Berger, 1992), whereas others show both Pacific and Atlantic patterns (Peterson and Prell, 1985; Naidu *et al.*, 1993).

A few studies with regard to calcium carbonate fluctuations have been carried out in the Indian Ocean. Peterson and Prell (1985b) have used a foraminifera-based Composite Dissolution Index (CDI) to identify the present level of the lysocline to be at a water depth of 3800m. Cores from the Ninetyeast Ridge at 6°S from the same study, suggest that the dissolution of carbonate is out of phase with glacial-interglacial  $\delta^{18}\text{O}$  cycles.

Naidu (1991), have shown using two cores from the western continental margin in the Arabian Sea that  $\text{CaCO}_3$  variations depend on the productivity of the overlying waters and that the productivity was higher during the glacials and vice versa. Also the riverine material from the Indus River in the eastern Arabian Sea influences the glacial-interglacial  $\text{CaCO}_3$  variations. Such terrigenous dilution, caused by variations in the terrigenous lithogenic flux derived from the Arabian and Somalian Peninsulas has been studied by Murray and Prell (1992). By using the Berger Dissolution Index (BDI) on three cores (SDSE 144, 147 and 154) from the western equatorial Indian Ocean, Naidu *et al.*, (1994), have demonstrated that there is a good agreement between carbonate maxima and less dissolution as well as carbonate minima and more dissolution. This suggests that the dissolution of  $\text{CaCO}_3$  controls the Quaternary  $\text{CaCO}_3$  cycles in the equatorial Indian Ocean. Dissolution indices data show that the CCD depth has shown cyclic variations in the Late Pleistocene. Another study by Naidu and Malmgren (1999) shows that in the western equatorial Indian Ocean, productivity changes are very significant for the last 1370kyr.

### 1.7.2 Paleocarbonate ion Proxies:

Calcite dissolution in marine sediments is driven by saturation state of the overlying waters and/or responds to sedimentary organic matter respiration and the acidification of pore waters that results from that (Emerson and Bender, 1981; Archer and Maier-Reimer, 1994). Specifically, differences in the carbonate ion concentrations of bottom water are believed to be responsible for the first-order variations in the depth of the lysocline between and within oceans (Peterson and Prell, 1985).

Attempts to reconstruct the carbonate ion history from sediments of the world oceans amongst others have yielded two important proxies; the size index (Broecker and Clark, 1999) and the shell weight method (Lohmann, 1995). Both these proxies have been applied largely to the Atlantic Ocean (Broecker and Clark, 1999; Broecker *et al.*, 1999; Broecker and Sutherland, 2000; Broecker and Clark, 2001a; Broecker and Clark, 2001b; Broecker and Clark, 2001c; Broecker and Clark, 2001d; Broecker *et al.*, 2001b; Broecker and Clark, 2002a; Broecker and Clark, 2003a; Broecker and Clark, 2003b; Broecker and Clark, 2003c; Broecker and Clark, 2003d) the Pacific Ocean (Broecker and Clark, 1999; Broecker and Sutherland, 2000; Broecker *et al.*, 2001a; Broecker *et al.*, 2001b; Broecker and Clark, 2001a; Broecker and Clark, 2001c; Broecker and Clark, 2001d; Broecker and Clark, 2003a; Broecker and Clark, 2003b; Broecker and Clark, 2003c; Broecker and Clark, 2003d) the Indian Ocean (Broecker and Clark, 1999; Broecker and Clark, 2001a) and the Caribbean Sea (Broecker and Clark, 2002b, Broecker *et al.*, 2003). Largely, in the above studies the shell weights of selected planktonic foraminifer species has been successfully utilized



in understanding the carbonate ion variations during the Holocene and the Last glacial maxima (LGM).

The size index and planktonic foraminifera shell weight have also been employed to discuss calcite dissolution above the lysocline in the Atlantic, Pacific and Indian oceans (de Villiers, 2005; Schulte and Bard, 2003). Though these studies could quantify the  $\text{CO}_3^{=}$  concentrations to some extent, they could certainly identify the calcite dissolution and preservation events (Broecker *et al.*, 2003). Another parameter, calcite crystallinity, was also used as a proxy of carbonate ion in the Atlantic and Pacific Oceans (Bassinot *et al.*, 2004; Gehlen *et al.*, 2005). Recently, shell weights have been used to understand the CCD variations and hence carbonate ion over the course of the Cenozoic (Broecker, 2008). However, the paleocarbonate ion studies in the Indian Ocean are very sparse compared to more rigorously studied Atlantic and Pacific oceans.

### 1.8 Objectives:

The primary objectives of this study are:

1. To identify suitable paleocarbonate ion proxy/proxies for understanding calcite dissolution in the Indian Ocean.
2. To compare these proxies within themselves and use of these proxy/proxies in identifying calcite dissolution events and understanding the dissolution mechanisms on the seafloor.
3. To understand the dependency of planktonic foraminiferal shell weights on initial growth conditions i.e. carbonate ion and/or temperature from tropical waters.



4. To reconstruct the carbonate ion content for the northern Indian Ocean during the Late Quaternary.

## CHAPTER II

### MATERIALS AND METHODS

#### 2.1 Materials:

##### 2.1.1 Cores from Atlantic, Pacific and Indian Ocean:

Ten cores were chosen from the equatorial regions of Atlantic, Pacific and Indian Ocean. Core locations and water depths of these cores are shown in Table 1, Fig. 8.

**Table 1. Cores recovered from the Atlantic, Pacific and Indian oceans at various locations and water depths.**

OCEAN	Core	Latitude	Longitude	Water Depth (m)
Atlantic	RC24-16	05.04°S	10.19°W	3559
	V30-40	00.20°S	23.15°W	3706
	V25-59	01.37°N	33.48°W	3824
Pacific	DSDP-572	01.43°N	113.85°W	3903
	SDSE 59	03.05°N	133.10°W	4370
	RC11-210	01.82°N	140.05°W	4420
	V28-179	04.62°N	139.60°W	4509
	SDSE 60	01.58°N	134.95°W	4540
Indian	ODP 709A	03.91°S	60.56°E	3038
	SDSE 154	01.00°S	54.00°E	4860

The equatorial region of the world ocean is known to be a strong CO<sub>2</sub> source to the atmosphere (Takahashi *et al.*, 1997). The core locations are chosen such that they are situated far off from the continental landmass so that the effect of terrigenous dilution is minimal. Such a selection is used to focus attention on carbonate variations

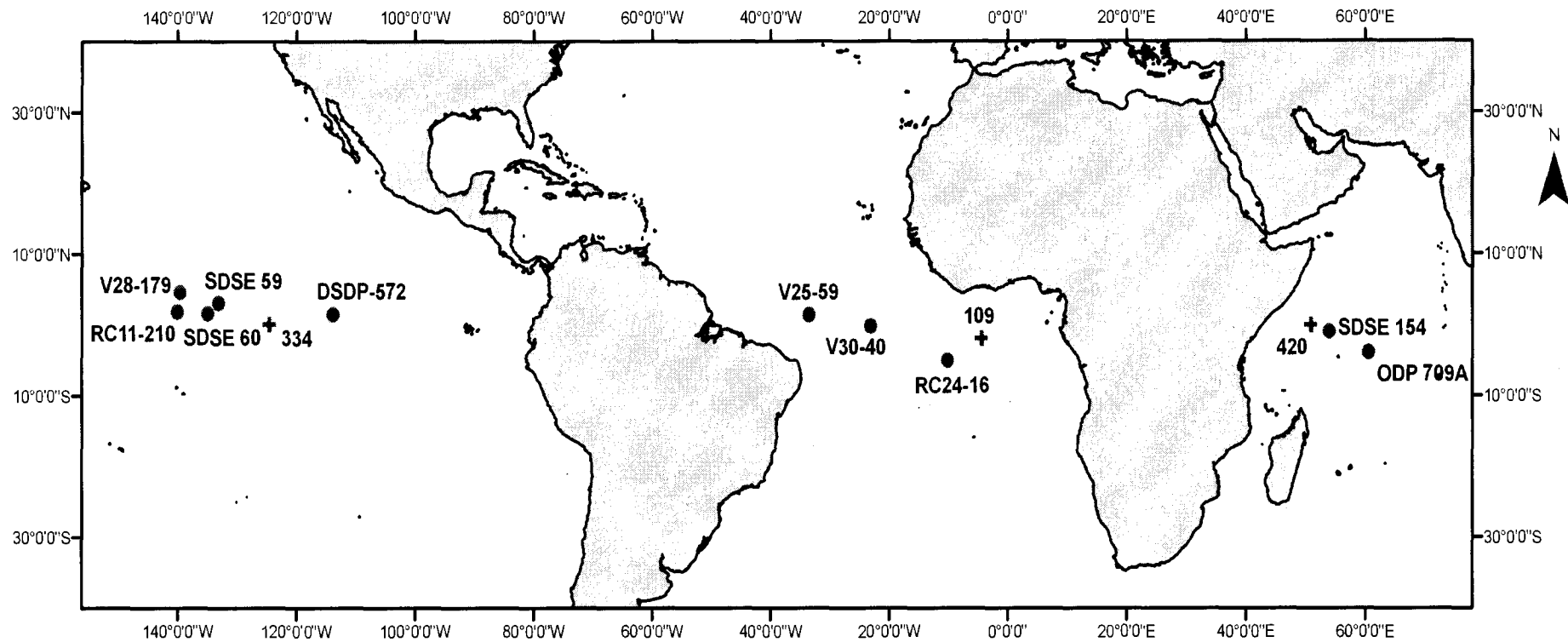


**Fig. 8. Map showing location of deep-sea cores in the equatorial Pacific, Atlantic and Indian Ocean, shown by dots. Plus signs indicate the GEOSECS stations.**

due to dissolution. The cores having a continuous sediment record have been preferred. The CaCO<sub>3</sub> data set for the ten cores used is obtained from National Geophysical Data Centre (NGDC) of NOAA. This data set was contributed by Dr. William Ruddiman of the Lamont-Doherty Geological Observatory, and by Dr. John Farrell of Brown University. J. Imbrie and A. Duffy of Brown University compiled ages for the cores for the SPECMAP project. The cores cover a time span of 0.6Ma, which clearly covers six major glacial-interglacial cycles.

### 2.1.2 Core tops from the Indian Ocean:

The paleocarbonate ion proxies have been tested using several core top samples from the western and eastern tropical Indian Ocean. These core tops were collected during the SK199 cruise in December 2003 and core tops of ODP Sites 711, 718 and 752 were obtained from the Ocean Drilling Programme repository (Table 2, Fig. 9).

**Table 2. Core tops from the Indian Ocean at various locations and water depths.**

Station.	Water Depth (m)	Latitude	Longitude
SK199C/6	2250	08.13°N	73.56°E
SK199C/10	3305	07.36°S	67.17°E
SK199C/9	3320	04.86°S	67.09°E
SK199C/14	3368	15.27°S	66.01°E
SK199C/11	3373	09.17°S	65.95°E
SK199C/7	3944	05.51°N	69.34°E
ODP 711	4430	02.74°S	61.16°E
ODP 718	4730	00.92°S	81.39°E

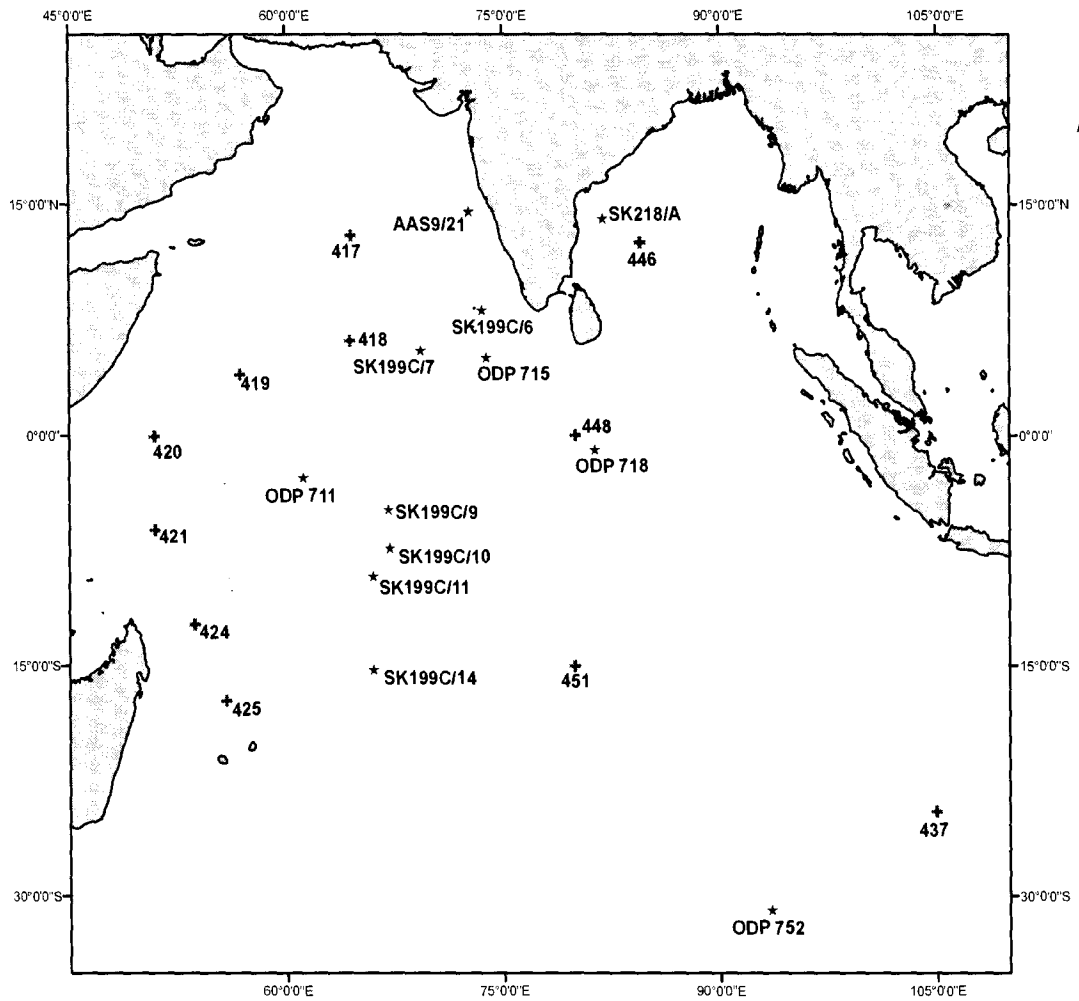


**Fig. 9.** Core tops and cores from the northern Indian Ocean indicated by stars, and GEOSECS stations indicated by crosses.

### 2.1.3 Cores from the Indian Ocean:

Four sediment cores have been selected from the Indian Ocean (Table 3, Fig. 9), ODP Site 752 was recovered from the eastern Indian Ocean near the crest of Broken Ridge which lies on a topographic high, whereas ODP Site 715 was recovered from the northern equatorial Indian Ocean on the eastern margin of Maldives Ridge. ODP Sites

752 and 715 are used to examine the suitability of size index and planktonic foraminifera shell weights applied to understand temporal carbonate ion variations. Cores AAS9/21 and SK218/A were recovered from the Arabian Sea and Bay of Bengal (Fig. 9).

**Table 3. Cores from the Indian Ocean from various locations water depths. Also shown is the length of core recovered and used in the present study.**

Station.	Water Depth (m)	Latitude	Longitude	Core length (m)	Length of core used (m)
ODP 752	1086	30.89°S	93.58°E	217.3	1.01
ODP 715	2266	05.08°N	73.83°E	137.6	1.89
AAS 9/21	1807	14.51°N	72.65°E	4.4	2.16
SK 218/A	3307	14.04°N	82.00°E	8.26	4.40

These cores were chosen to study the relationship between carbonate ion concentration and temperature.

## 2.2 Methods:

### 2.2.1 Size fraction analysis:

All the samples were oven dried at 50°C; a portion of the sample was weighed and disaggregated by soaking in distilled water to remove the lumps of clay and organic matter, 10ml of 10% Sodium Hexa-Meta-Phosphate and 5ml of Hydrogen Peroxide was added, respectively and kept overnight. The samples were then wet sieved through a 63µm sieve, taking care to see that no shells were broken or material lost. Both the size fractions, >63µm and <63µm were collected carefully. The >63µm fraction was dried again in an oven at 50°C. The <63µm fraction, which contained a copious amount of washing water was left for settling. Later it was decanted by discarding the supernatant

clear solution and the residue was then dried in an oven at 50°C. The material, coarse and fine fractions were then weighed separately following the procedure described by Broecker and Clark, (1999). The content of CaCO<sub>3</sub> in the sediment sample as a whole, < 63µm and in the >63µm fractions were determined using coulometric titration method as described hereafter.

### 2.2.2 Calcium carbonate analysis of sediment:

An automated carbon dioxide coulometric titrator was used in this work. Carbon dioxide was evolved from the sample by addition of 4ml 2M-Hydrochloric acid. A small portion of the acid was added initially with mixing to ensure complete wetting of the sample. Carrier gas of Potassium Hydroxide-scrubbed air was passed through the heated sample slurry at a flow rate of 100 cm/min. The CO<sub>2</sub> laden carrier gas was passed through two gas scrubbers, which contained 3% H<sub>2</sub>O<sub>2</sub> and saturated with AgSO<sub>4</sub> at pH 3 for removal of chlorine and sulphur. After removal of interferences the CO<sub>2</sub> was adsorbed in the coulometric titration cell. The cell contained a platinum cathode, silver anode and a proprietary solution containing monoethanolamine and thymolphthalein indicator (Coulometrics®). Carbon dioxide was converted to hydroxyethylcarbamic acid, which was automatically titrated with a coulometrically generated base to a coulometric endpoint by means of a photometric detector set at 612 nm (Engleman *et al.*, 1985). A normal sample analysis required seven to ten minutes. The coulometer was calibrated with synthetic (commercially available CaCO<sub>3</sub>) as well as geological standard contained from U.S. Geological Survey (MAG-1). The precision obtained is ± 0.7% (n=10).



### 2.2.3. Calculation of Size Index parameter:

The CaCO<sub>3</sub> content of all the three fractions, < 63µm, >63µm and total sediment were converted to weights in 'g'. The size index is calculated as the ratio of coarse calcite to total calcite [ $(>63\mu\text{m CaCO}_3/\text{Total CaCO}_3) \times 100$ ]. It has been shown by Broecker and Clark (1999) that in today's tropical ocean the percentage of CaCO<sub>3</sub> contained in grains >63µm in size is closely tied to the pressure-normalized carbonate ion of water bathing the sea floor. The idea being that, since the >63µm fraction is dominated by foraminifera shells and the lesser fraction contains coccoliths, juvenile foraminifera and foraminiferal fragments, this size index actually is the ratio of CaCO<sub>3</sub> contained in whole foraminifera shells to CaCO<sub>3</sub> contained in total sediments.

### 2.2.4 Calculation of in-situ and pressure-normalized carbonate ion concentration:

Carbonate ion concentrations were calculated using a programme in visual basic designed by Dr. Taro Takahashi of Lamont Doherty Earth Observatory. The following parameters were the inputs for the programme: Depth (dB), Temperature (°C), Salinity (‰), Alkalinity (µEq/kg), Total CO<sub>2</sub> (µmol/kg), Silicate (µmol/kg) and Phosphate (µmol/kg). Data from the GEOSECS stations in the Indian, Atlantic and Pacific Oceans was used for this purpose (Table 4, Fig. 8 & 9). It is necessary to take into account the increase in calcite solubility with pressure and hence water depth. Following the method of Broecker and Clark, (1999), The CO<sub>3</sub><sup>=</sup> concentrations were normalized to a depth of 4km as follows:

$$\text{CO}_3^{=*} = \text{CO}_3^{=} + 20(4-h) \mu\text{mol/kg}$$

Where  $h$  is the water depth in km at the core site and  $20\mu\text{mol/kg}$  is the increase with water depth of the solubility of calcite.  $\text{CO}_3^{=}$  is used to avoid the necessity of selecting a value for the solubility of calcite.

**Table 4. Various GEOSECS locations used in the present study from the Atlantic, Pacific and Indian Oceans.**

Station	Latitude	Longitude
ATLANTIC OCEAN		
109	04.50°W	02.00°S
PACIFIC OCEAN		
334	124.57°W	00.06°N
INDIAN OCEAN		
419	03.95°N	56.80°E
420	00.05°S	50.93°E
421	06.15°S	50.91°E
424	12.30°S	53.69°E
425	17.30°S	55.85°E
446	12.52°N	84.51°E
448	00.02°N	80.05°E
451	14.98°S	79.96°E
437	104.93°E	24.48°S

### 2.2.5 Shell weights:

Shell weight measurements were done following the procedure of Lohman (1995). A portion of the coarse fraction ( $>63\mu\text{m}$ ) separated previously was cleaned and sonicated in methanol at 40hz for 8secs in order to remove fines that could fill the last chambers. The material was then dried in an oven at 50°C and then passed through sieves in order to isolate the 300-350 $\mu\text{m}$  and 350-420  $\mu\text{m}$  size fractions. About 50 whole shells of

*Globigerinoides ruber* from the 300-350 $\mu$ m fraction and *Globigerinoides sacculifer*, *Pulleniatina obliquiloculata* and *Neogloboquadrina dutertrei* from the 350-420 $\mu$ m size fractions were picked by using Sterio Binocular Microscope and weighed on a microbalance, which has the least count of 1 $\mu$ g (Fig. 10). Precision obtained is  $\pm 2\mu$ g. Planktonic foraminifera species were identified by following the taxonomy of Bé (1967) and Hemleben *et al.*, (1983).

### 2.2.6 Calcite Crystallinity:

The crystallinity, measured by X-Ray Diffraction (XRD), is related to the degree of perfection of a given crystal lattice [e.g., Lipson and Steeple, 1970]. The full width at half maximum (FWHM) of the (104) calcite X-ray diffraction peak (given in  $^{\circ}2\theta$ ) was used which is as an indication of the degree of crystallinity of foraminifera shells (Bassinot *et al.*, 2004). Shells showing a narrow (104) calcite peak on XRD powder diagrams are interpreted as being better crystallized than those showing a broader diffraction peak. Ultimately, XRD peak broadening depends on two main parameters at the lattice level: (1) it can be related to strain within the crystal structure, or (2) it can reflect the granulometry of the perfectly crystallized subdomains (hereafter referred to as “crystallites”) that constitute the whole crystal. In the later case, peak broadening results from the slight misalignment of crystallites with respect to each other (“mosaic” structure of the crystal lattice); the smaller the average size of these crystallites, the broader the diffraction peaks (e.g., Lipson and Steeple, 1970). *Globigerinoides sacculifer* which was hand picked from the 350– 420 $\mu$ m size fraction was soaked in methanol and ultrasonically cleaned in order to remove fines that could fill the chambers. The purpose

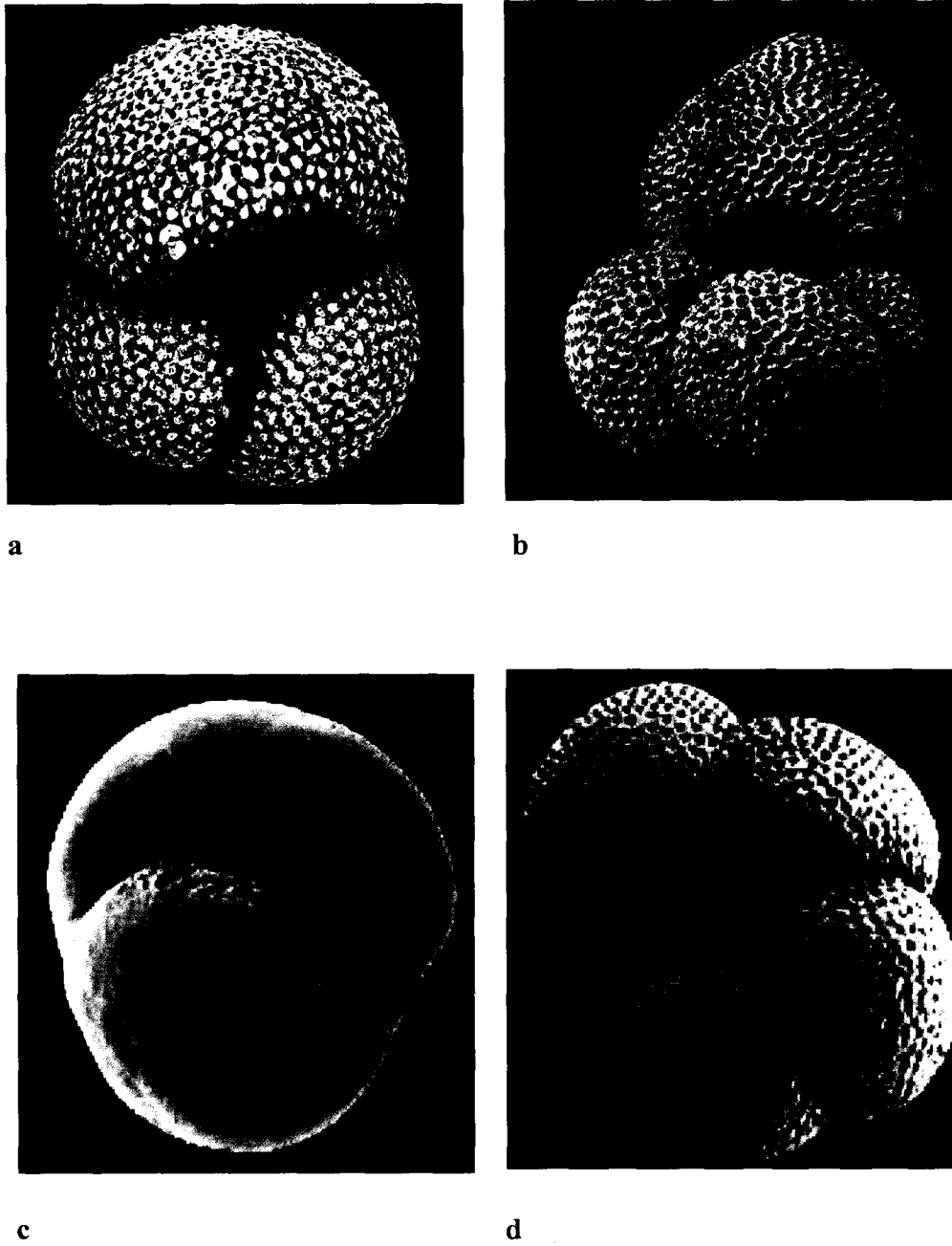


Fig. 10. SEM images of a) *G. ruber* b) *G. sacculifer* c) *P. obliquiloculata* and d) *N. dutertrei*.

of such a cleaning procedure is to reduce the contribution of coccolith calcite to the XRD crystallinity results. Because the broadening of foraminiferal calcite X-ray diffraction peak is likely related to the size of the perfectly crystallized sub domains that constitute the calcite, it is crucial that the sample preparation does not introduce a granulometry bias. Shells were gently crushed with a glass slide, directly in the sample holder following the method from Barthelemy-Bonneau (1978). This is too coarse a granulometry to introduce a bias in the width of calcite XRD peak since apparent grain size of crystallite affecting XRD peak broadening is smaller than a few tenth of micrometers. Thus, this sample preparation technique ensures that no peak-broadening bias is introduced and that data genuinely reflect calcite crystallinity from the foraminifera shells. Each sample was run three times. Average value of calcite (104) FWHM and the related standard deviation were calculated from those three. The internal standard deviation thus obtained is  $\pm 0.003^{\circ}2\theta$  ( $1\sigma$ ). The system is a Philips PW1840-XRD (Cu-K $\alpha$ , 40 KV, 20mA). The following manual adjustments were possible within the instrument: Counting aperture; 0.2mm and goniometer rotation speed; 1.2  $^{\circ}2\theta$ /min.

### **2.2.7 Scanning Electron Micrographs:**

Scanning Electron Micrographs were obtained in order to visually examine any changes in shell structure as an evidence of dissolution following the procedure of Dittert and Henrich, (2000). Individual foraminifera shells were placed on a sticky SEM stub and gold-palladium coated for 30–40 s in a JEOL JFC-100 auto fine sputter coater. The stubs were then imaged using a JEOL instrument. The SEM was tuned to get a resolution

of 150X and then a higher resolution for observing the dissolution feature at 2500X. The JEOL JSM –6360LV microscope was used with a voltage setting at 10 kV.

### 2.2.8 Chronology of the sediment cores:

The chronology of the cores from Atlantic, Pacific and the Indian Ocean was based on oxygen isotope stage boundaries, compiled by J. Imbrie and A. Duffy at Brown University for the SPECMAP project. Chronology of the Sites 715 and 752 was based on calcareous nanofossil datum's (Duncan *et al.*, 1990; Rea, 1990). Carbon-14 dates obtained by Accelerator Mass Spectrometer (AMS) at Kiel University, Germany were used to establish the chronology of AAS9/21 and SK218/A. About 10 mg of planktonic foraminifera, consisting of diverse species in the size range of 250-350µm, were used for AMS carbon dates. <sup>14</sup>C dates were calculated to calendar years by using the calibration program online CalPal version quickcal 2005 ver 1.4 (Weninger *et al.*, 2006).

### 2.2.9 Mg/Ca:

Mg/Ca analyses were carried out at Bremen University, Germany. In calcareous skeletons of foraminifera made up of CaCO<sub>3</sub>; some of the Ca atoms are replaced by other bivalent cations such as Mg atoms. As incorporating atoms of abnormal size in a crystal lattice requires additional energy, this occurs in warm environments due to sufficient availability of thermal energy. Therefore, ratio of Mg to Ca in a calcite shell serves as a measure of past sea water temperature. For determination of Mg/Ca, for each sample 30 to 40 individuals of *Globigerinoides ruber* (white variety) from a size range of 250 to 350µm were picked. The picked specimens were then cleaned using the elemental analysis technique (Barker *et al.*, 2003). Splits of the cleaned sample were then analyzed

for 'Mg' and 'Ca' by inductively coupled plasma atomic mass spectrometry (ICP-MS) by the method described by Barker *et al.*, (2003). Study shows that the reproducibility of the method, for *G. ruber* in a core-top sample from the Arabian Sea was  $\pm 1.8\%$  for Mg/Ca (Barker, 2003). During the present study 40 replicate *G. ruber* samples were measured from site SK218/A. However, the repeatability for Mg/Ca was routinely better than 0.1mmol/mol. The analytical error for the Mg and Ca concentrations was better than 0.7% relative standard deviation (RSD).

## CHAPTER III

### RESULTS

#### **3.1 CaCO<sub>3</sub> fluctuations in the equatorial region of the major world oceans:**

CaCO<sub>3</sub> content data of ten cores collected from the equatorial region over the world oceans are used to reconstruct bathymetric patterns of CaCO<sub>3</sub> preservation spanning the past 0.6 Ma (Table 1, Fig. 8), which clearly cover the major glacial/interglacial intervals of the Late Quaternary period. The exceptions to these are cores from the Atlantic Ocean, which cover a maximum time span of 0.42 Ma. CaCO<sub>3</sub> fluctuations from the equatorial regions of Atlantic, Pacific and Indian Ocean are discussed individually.

##### **3.1.1 The Atlantic Ocean:**

Three cores have been selected to discuss the CaCO<sub>3</sub> fluctuations in the Atlantic Ocean (Fig. 11). All the cores are from above the lysocline depth. The total length of the Core RC24-16 spans back to 0.42 Ma, Core V30-40 covers the past 0.26 Ma and Core V25-59 covers 0.17 Ma. The CaCO<sub>3</sub> content ranges from 82 to 92% in Core RC24-16, 58 to 91% in Core V30-40 and 44 to 84% in V25-59. In general, interglacials show high CaCO<sub>3</sub> content whereas glacials show low CaCO<sub>3</sub> content (Fig. 11). Marine Isotopic Stage (MIS) 1 which is the interglacial shows a calcium carbonate peak in all the three cores. The %CaCO<sub>3</sub> maximum of MIS 1 is very prominent in Core V25-59. CaCO<sub>3</sub> content in MIS 2, representing the late Wisconsin glacial maximum shows a dissolution pattern for the three cores whereas in MIS 3,



preservation is noticed. The transition from interglacial to glacial maximum shows a sharp depletion. In Core V25-59 this depletion in  $\text{CaCO}_3$  is from 84 to 56% and in Core V30-40 it ranges from 91 to 65%. Core RC24-16 does not show a very distinguished peak in this respect. MIS 4 shows %  $\text{CaCO}_3$  minima in all the three

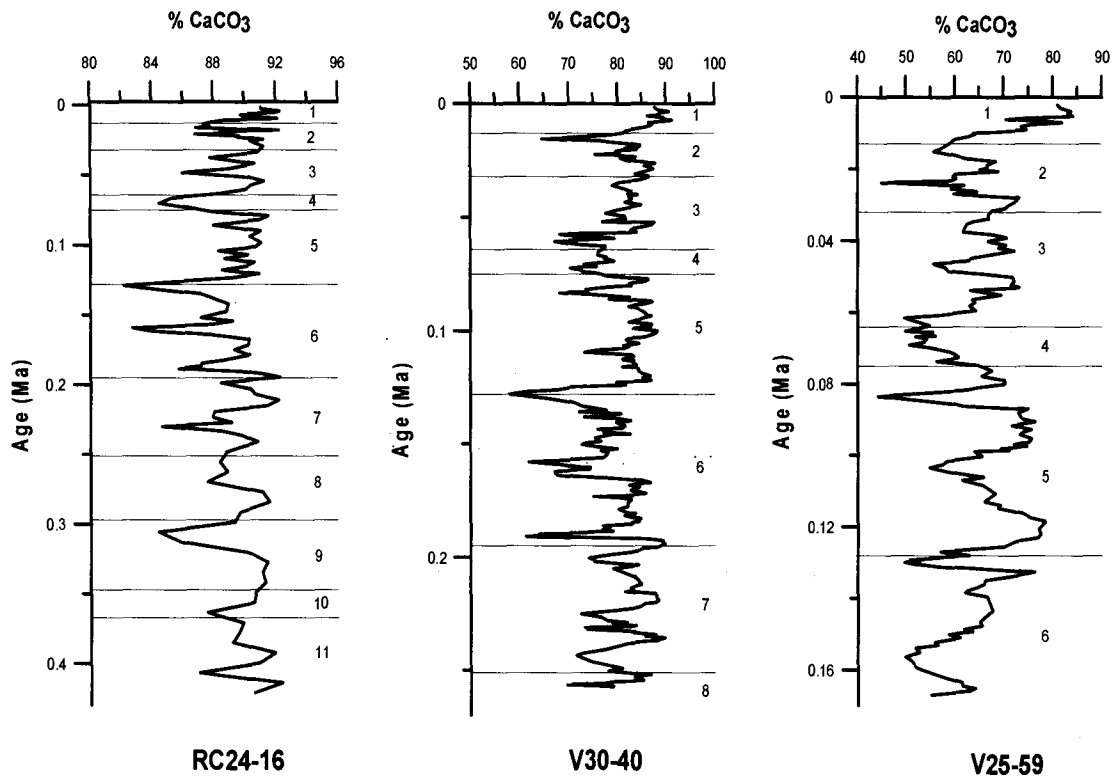


**Fig. 11.  $\text{CaCO}_3$  fluctuations during the Late Quaternary in the Atlantic Ocean cores. Marine Isotope Stages boundaries are marked with horizontal lines and MIS stage numbers are labeled.**

cores, whereas MIS 5 i.e. last interglacial coincides with a preservation event and is a common feature in all the cores. MIS 6, which is the glacial maxima, shows relative depletion in all the three cores. Core V25-59 that is retrieved from the mid-Atlantic ridge shows high fluctuations in % $\text{CaCO}_3$  content unlike other 2 cores.

In general the observed pattern shows maximum values during interglacials and minimum values during glacials, which has already been termed as the ‘Atlantic

pattern'. The maxima and minima values for  $\text{CaCO}_3$  may not be the same for any of the cores as they lie in different sedimentary regimes. Therefore, there will be diverse contributions from each factor controlling total carbonate (dilution, dissolution and productivity). But, the factors vary in such a way that their combined nature and timing produces the observed classic patterns.

### 3.1.2 The Pacific Ocean:

Five cores covering a time span of 0.6Ma were chosen from the equatorial Pacific region (Fig. 12). The cores were collected from a water depth range of 3900 to 4500m. All these cores are from below the lysocline but lie above the present day CCD (Farell and Prell, 1989).  $\text{CaCO}_3$  content ranges from 59 to 91% in DSDP Site 572, from 38 to 90% in Core SDSE 59, from 47 to 95% in Core RC11-210, from 26 to 84% in Core V28-179 and 24 to 91% in Core SDSE 60. All peaks and troughs in  $\text{CaCO}_3$  content are correlative from core to core. Interglacials show low  $\text{CaCO}_3$  values and glacials show high  $\text{CaCO}_3$  values in all these cores (Fig. 12). Such a  $\text{CaCO}_3$  fluctuation pattern has been termed the 'Pacific pattern' showing better preservation during glacials. As seen in Fig. 12, most of the preservation maximas lie towards the latter half of the glacial stages. A gradual increase in the amplitude of  $\text{CaCO}_3$  variations is noticed with increase in water depth. Core SDSE 60 shows the greatest variations in % $\text{CaCO}_3$  and Core DSDP-572 the least variation. Both these cores demonstrate the effect of carbonate dissolution with increasing water depth.

### 3.1.3 The Indian Ocean:

The ODP Site 709A and core SDSE 154 were chosen to document the  $\text{CaCO}_3$  fluctuations in the Indian Ocean (Fig. 13). ODP Site 709A was drilled at a water

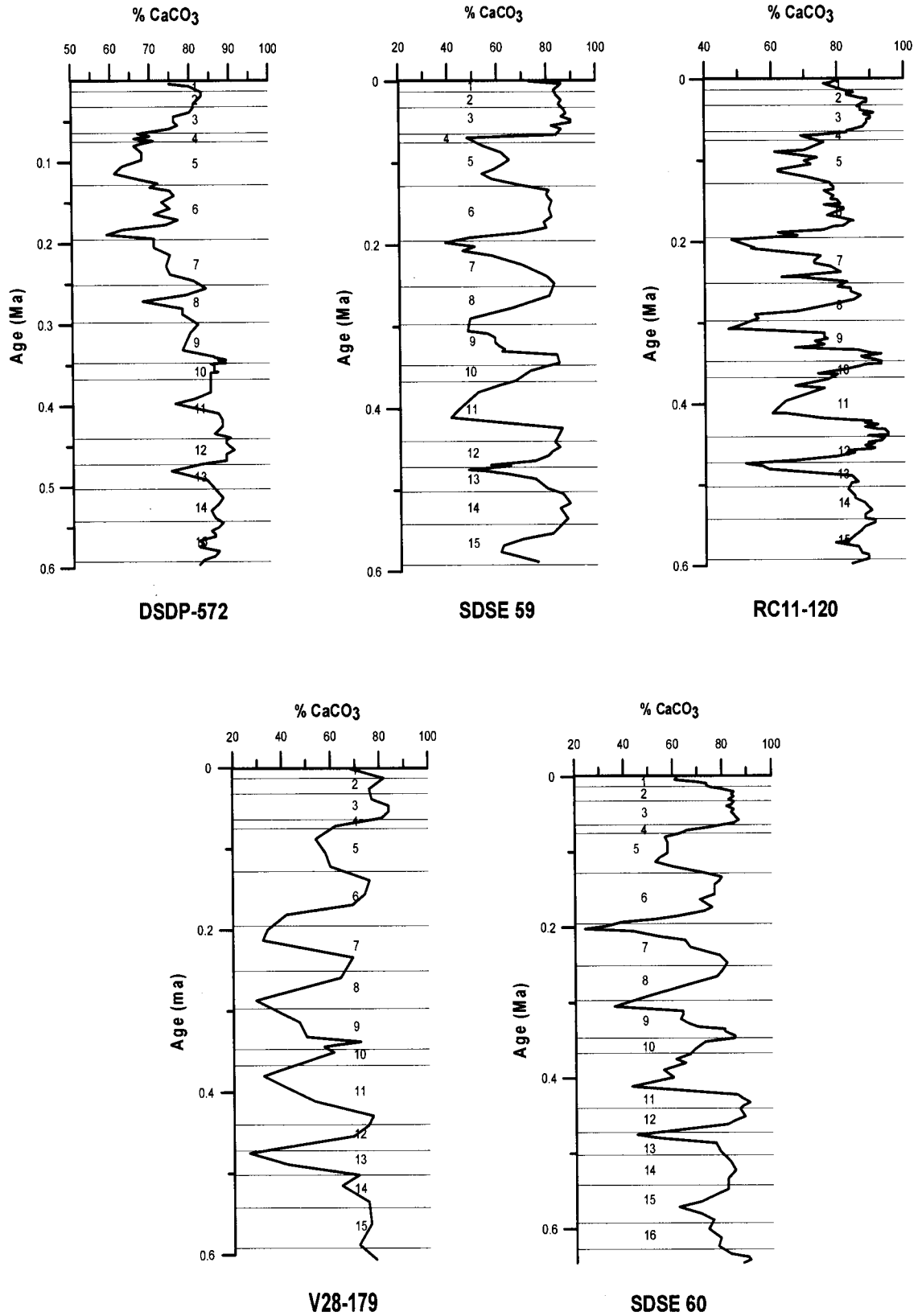
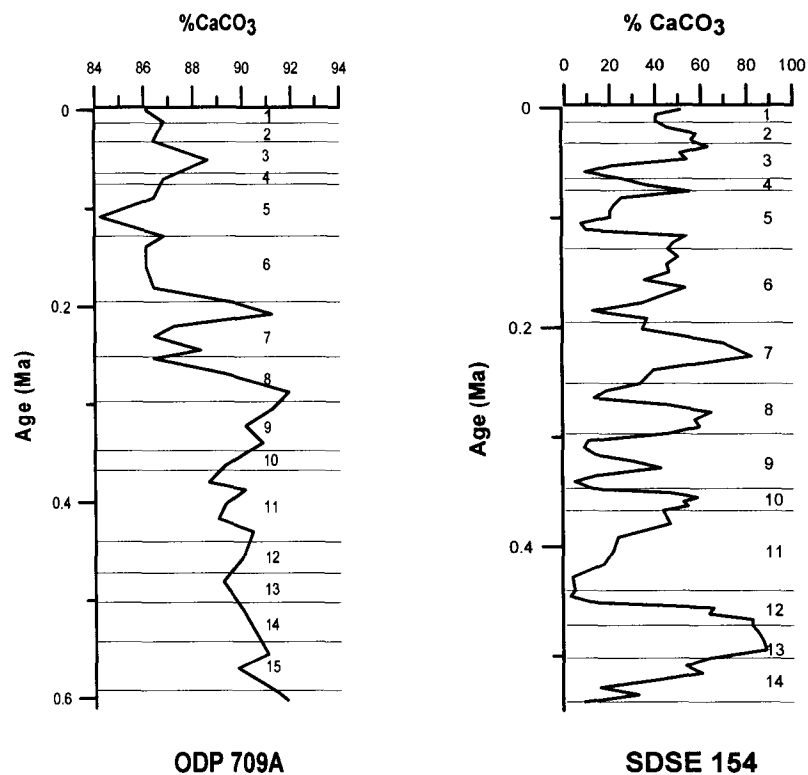


Fig. 12. CaCO<sub>3</sub> fluctuations during the Late Quaternary in the Pacific Ocean.

depth of 3800m which lies above the regional calcite lysocline depth. The  $\text{CaCO}_3$  content in this core varies from 84.2% to around 92% for the last 0.6Ma.  $\text{CaCO}_3$  variations do not exhibit any specific type of variations throughout the glacial-interglacial stages, which indicates that the  $\text{CaCO}_3$  content in the total sediment is



**Fig. 13.  $\text{CaCO}_3$  fluctuations for the past 0.6Ma in the Indian Ocean.**

apparently not related to the glacial and interglacial  $\delta^{18}\text{O}$  cycles (Naidu and Malmgren, 1999). The high concentrations of  $\text{CaCO}_3$  at the ODP Site 709A probably rules out a significant influence from dilution by non-carbonate and terrigenous material. Therefore  $\text{CaCO}_3$  fluctuations could reflect either the surface water carbonate productivity or dissolution effects.

Core SDSE 154 was collected from the western equatorial Indian Ocean (Somali basin) at a water depth of 4860m, which lies below the regional lysocline and covers a time period of 0.55Ma. Higher percentages of CaCO<sub>3</sub> occur during glacial and lower during interglacial isotope stages. Interglacial MIS 7 and 13 display exceptionally high percentages of CaCO<sub>3</sub>. This core shows a 'Pacific type' dissolution pattern caused owing to dissolution due to organic matter degradation (Naidu *et al.*, 1993).

Comparison of CaCO<sub>3</sub> fluctuations during Late Quaternary from the three major oceans reveal that the Indian and Pacific Ocean show higher CaCO<sub>3</sub> content in the glacial and/or at glacial/interglacial transitions. By contrast in the Atlantic Ocean, higher CaCO<sub>3</sub> content during interglacials and lower CaCO<sub>3</sub> content during glacial were noticed. The CaCO<sub>3</sub> cycles observed in the Atlantic and Indo-Pacific Oceans show a correspondence with the CO<sub>2</sub> variations and ice volume observed in the Vostok ice cores with an increase in the CO<sub>2</sub> concentrations during the interglacials and a decrease during glacial (Petit *et al.*, 1999).

## **3.2 Changes of Carbonate ion concentrations in the Indian Ocean:**

### **3.2.1 Core top sediment samples:**

The *in-situ* carbonate ion concentrations [CO<sub>3</sub><sup>=</sup>] of the water bathing the core tops, were computed from different GEOSECS stations for the Western and Eastern Indian Ocean separately (Table 2,3 & 4, Fig. 9 &14). GEOSECS Station Nos. 417,420 and 425 which lie along a transect in the western Indian Ocean and in proximity to the coretop locations were selected. For the western Indian Ocean GEOSECS stations 446, 448, 451 and 437 were selected for similar reasons. The CO<sub>3</sub><sup>=</sup> concentration with respect to water depth show good similarity for the western

and eastern Indian Ocean. Below a depth of 1000m the concentrations are known to be remarkably similar in the Atlantic, Pacific and Indian Oceans (Broecker, 2003). Therefore, these concentrations can be confidently extrapolated to our core top

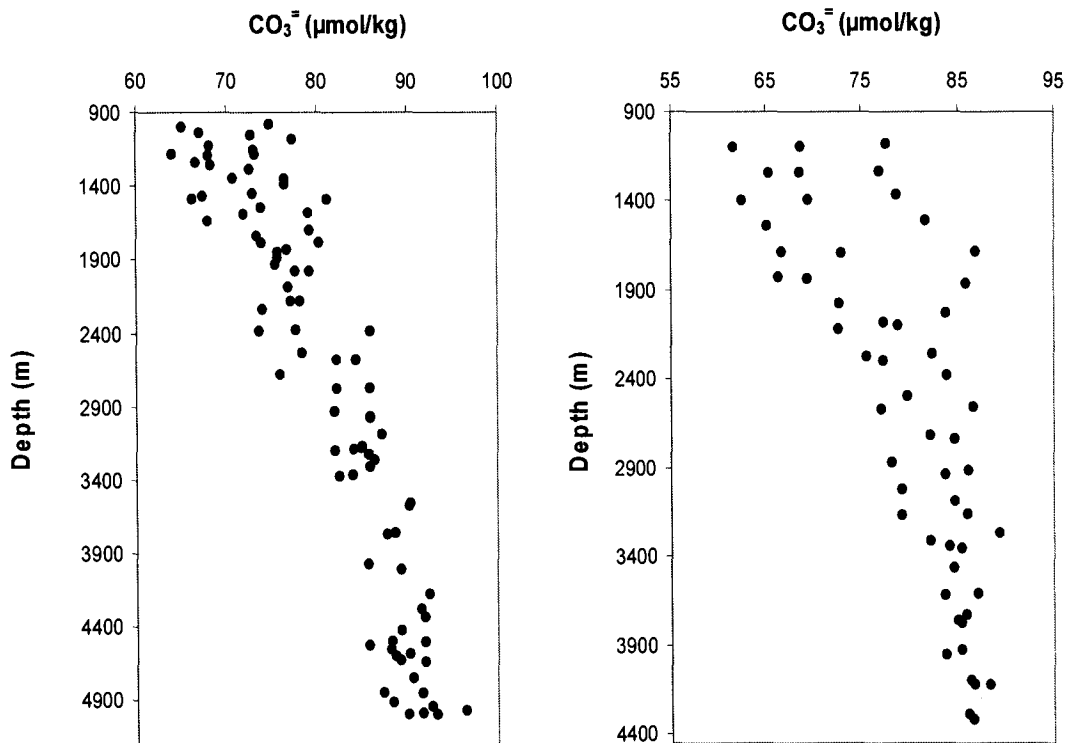


**Fig. 14. In-situ  $\text{CO}_3^{2-}$  concentrations ( $\mu\text{mol/kg}$ ) calculated from GEOSECS stations with respect to depth(m) at (a) stations 417, 420, and 425 for the western tropical Indian Ocean and (b) station 446, 448, 451, and 437 for the eastern tropical Indian Ocean.**

locations. Plots show that  $\text{CO}_3^{2-}$  concentrations decrease from a range of 60 to 80  $\mu\text{mol/kg}$  at 900m to a much tighter range of 85 to 90  $\mu\text{mol/kg}$  at the deeper depths. The reason for computing  $\text{CO}_3^{2-}$  concentrations for depths below 900m is that the core tops have been recovered from lower water depths.

Size index of coarse calcite to total calcite shows high values for core tops from above 3307m water depths (Table 2 and Fig. 15). Values for depths above 3307m are as high as 95%. Strikingly, a significant change of size index varying from

8 to 95% is noticed in the water depth range of 1000 to 4700m. A gradual decrease in size index values is noticed from 2250m water depth onwards. In the present study

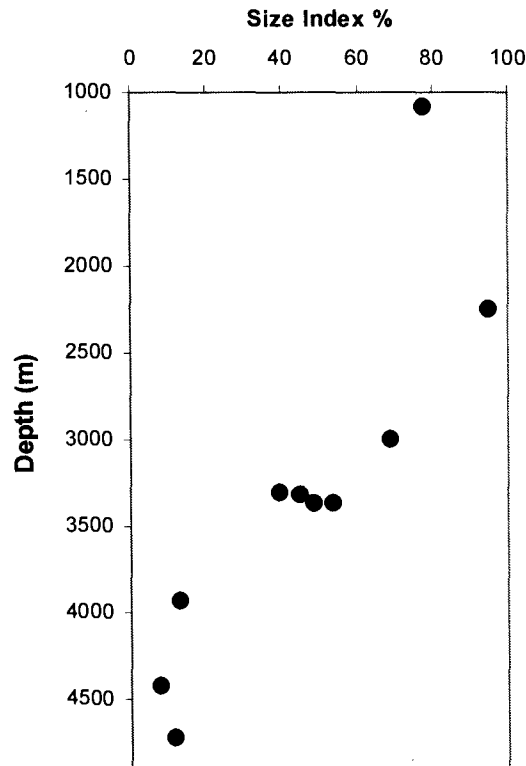


**Fig. 15.** Size index values plotted as a function of depth in the tropical Indian Ocean. A gradual decrease in the size index values from 2250 m onward and a drastic decrease from 3900 m water depth are noticed.

a linear decline in the ratio of  $\text{CaCO}_3$  in the  $>63\mu\text{m}$  fraction to the total  $\text{CaCO}_3$  in bulk sample occurs in the  $\text{CO}_3^{=}$  concentration range of 126 to  $70\mu\text{mol/kg}$ , (Fig. 16).

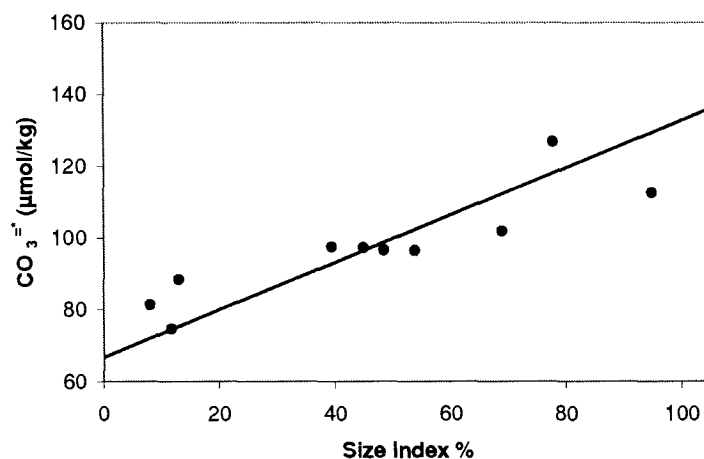


**Fig. 16.** Size index versus  $\text{CO}_3^{=}$  concentration ( $\mu\text{mol/kg}$ ) plotted on a reference line (Broecker and Clark, 1999) for the three major world's oceans.

Shell weight measurements were performed on planktonic foraminifera, *G. sacculifer*, which is a species sensitive to dissolution and eventually on two other species *N. dutertrei* and *P. obliquiloculata*. Shell weights of *G. sacculifer* range from 26.77 to 35.3 $\mu\text{g}$ , *P. obliquiloculata* shell weights range from 26 to 35.1 $\mu\text{g}$  whereas that for *N. dutertrei* ranges from 27 to 34.5 $\mu\text{g}$ . All the three foraminifera species exhibit more or less similar shell weights. A good correlation is seen between *G. sacculifer* shell weights and *N. dutertrei* and *P. obliquiloculata* shell weights, which confirm that there is no measurement error or shell fill (Fig. 17).

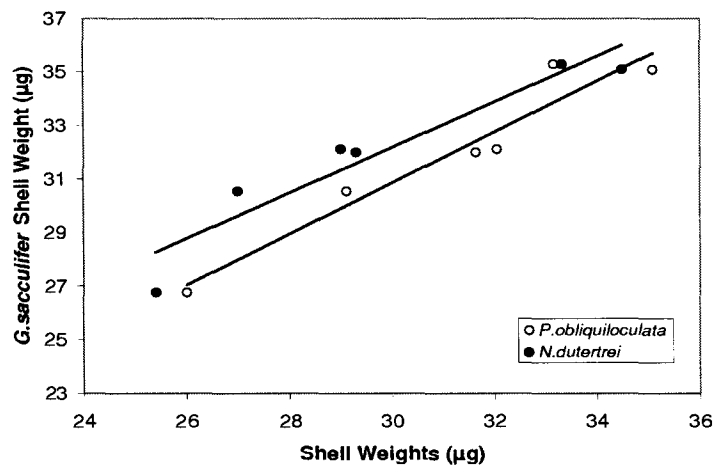


**Fig. 17.** *Globigerinoides sacculifer* shell weights versus *Pulleniatina obliquiloculata* and *Neogloboquadrina dutertrei* shell weights show a linear trend, suggesting no measurement error or shell fill.

A linear decrease in shell weight is observed in the pressure-normalized carbonate ion ( $\text{CO}_3^{=*}$ ) range from 90 to 125 $\mu\text{mol kg}^{-1}$  in the tropical region of the world oceans with a weight loss of  $0.30 \pm 0.05\mu\text{g } \mu\text{mol}^{-1}\text{kg}^{-1}$  (Broecker and Clark, 2001d). Bottom water  $\text{CO}_3^{=*}$  concentration bathing the core tops are in the range of 88 to 113  $\mu\text{molkg}^{-1}$ , lying in the shell weight decrease zone documented by Broecker and Clark (2001d). It is found that in the present study foraminifera shell weights show marginally higher values than those in the eastern Indian Ocean documented by Broecker and Clark, (2001d). A large variability in shell weights corresponding to



$\text{CO}_3^{=}$  concentration of around  $97\mu\text{mol kg}^{-1}$  is found, which lie at a depth of 3300 to 3400m ( Fig. 18).

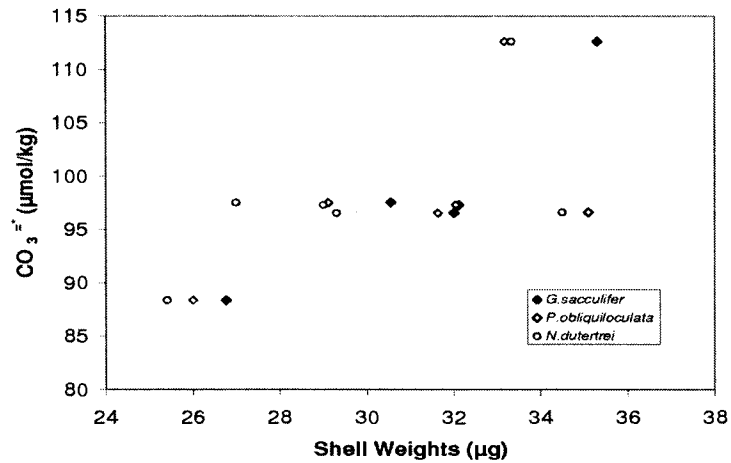


**Fig. 18.** Shell weights of *Globigerinoides sacculifer*, *Pulleniatina obliquiloculata*, and *Neogloboquadrina dutertrei* versus bottom water  $\text{CO}_3^{=}$  concentrations. A large variability is seen at pressure-normalized carbonate ion concentrations of  $97\mu\text{mol/kg}$ .

Calcite crystallinity measurements have been carried out on *G. sacculifer*, which is a dissolution sensitive species. Sites SK199C/6, 9, 10, 11 and 14 show similar crystallinity ranging from  $0.275$  to  $0.265^{\circ}2\theta$  values over a range of bottom water  $[\text{CO}_3^{=}]$  (Fig. 19) which indicate that dissolution affects more or less evenly in the water depths ranging from 3300 to 3400m.

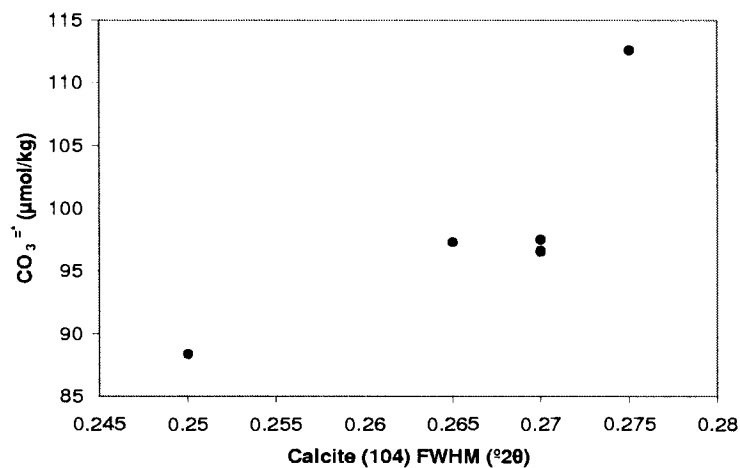


**Fig. 19.** Calcite (104) FWHM ( $^{\circ}2\theta$ ) values plotted against pressure-normalized  $\text{CO}_3^{=}$  concentrations ( $\mu\text{mol/kg}$ ). The lowest value of calcite (104) FWHM is seen at a  $\text{CO}_3^{=}$  concentration of  $88\mu\text{mol kg}^{-1}$ .

Comparatively, Site SK199C/7 shows lower calcite (104) FWHM (Full Width at Half Maximum) value of 0.25 suggesting intense dissolution at this water depth (3900m). All the three proxies, size index, shell weights and calcite crystallinity, applied to a set of core top samples in the western Indian Ocean show a linear regression which varies from 0.7 to 0.75 between them (Fig. 20).

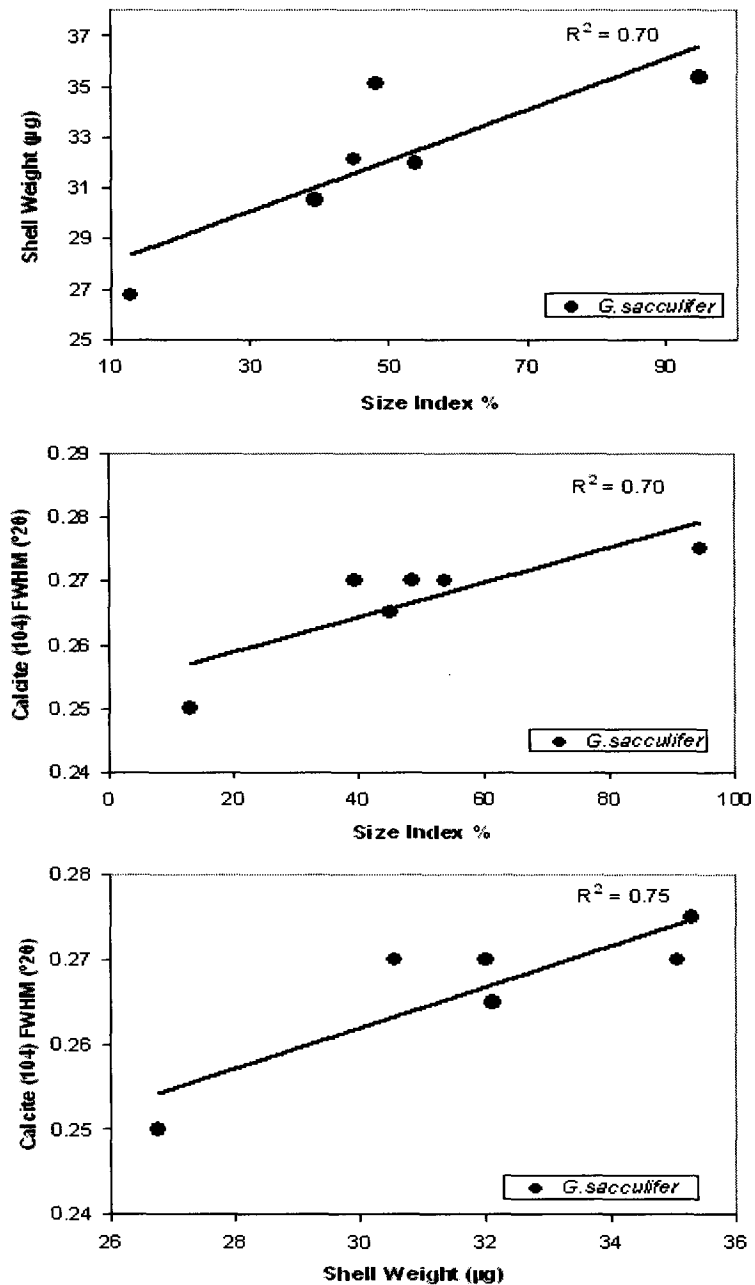
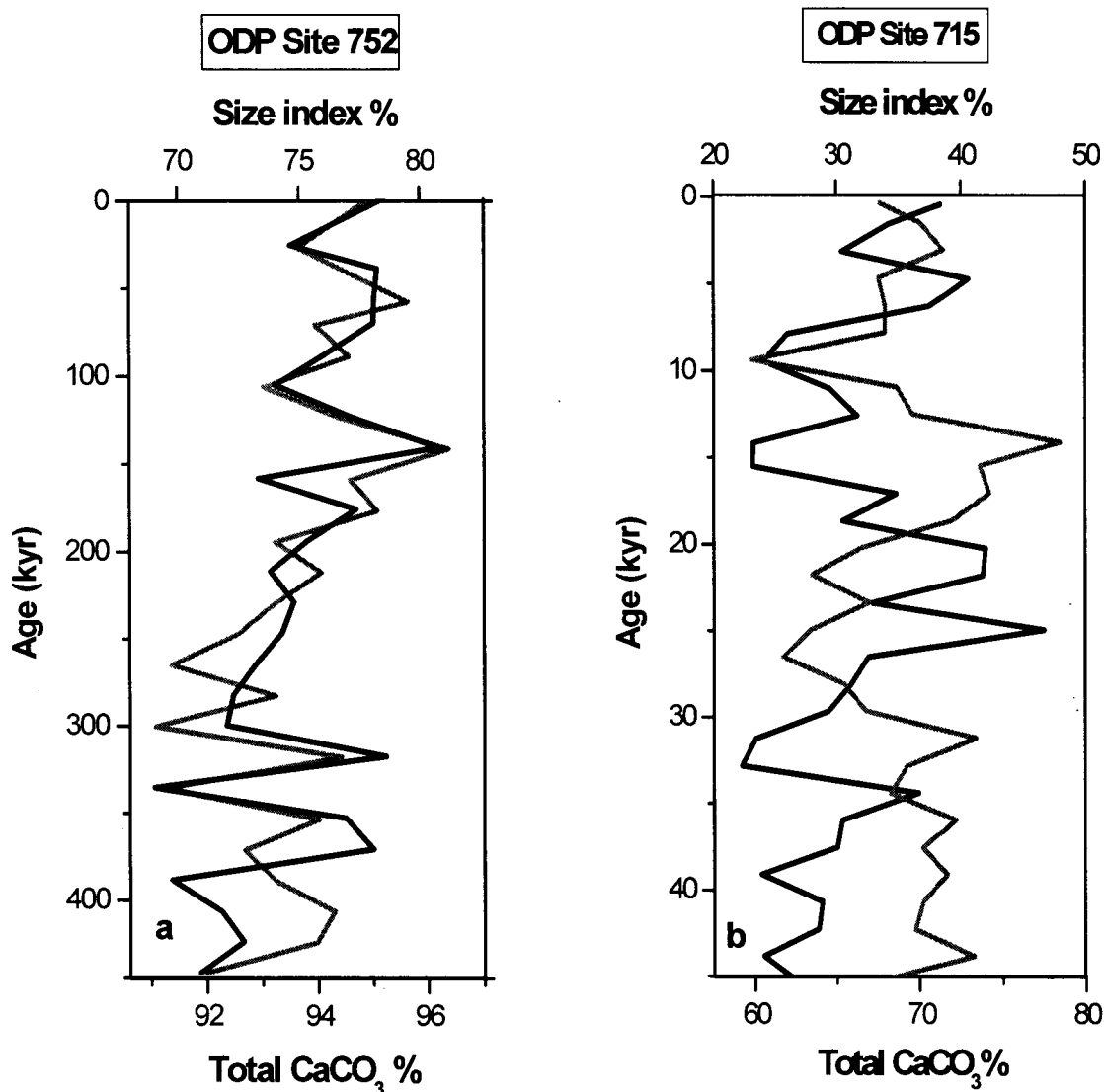


Fig. 20. Comparison between the three proxies shows good linear regression. (a) Shell weight (µg) versus size index % ( $R^2 = 0.7$ ), (b) calcite (104) FWHM (°2θ) versus size index % ( $R^2 = 0.7$ ), and (c) calcite (104) FWHM (°2θ) versus shell weight (µg) ( $R^2 = 0.75$ ).

### 3.2.2 ODP Site 752 and 715:

Two cores, ODP Sites 752 and 715 were drilled at shallow water depths from the (Table 3, Fig. 9). Top 1m of ODP Site 752, which covers a time span of 442kyr was analyzed for  $\text{CaCO}_3$ . Since this core has been recovered from a very shallow depth of 1086m, from a topographic high, it is used in the present study to make a comparison with another deep core as well as to understand supralysoclineal dissolution if any. At this site, total  $\text{CaCO}_3$  content varies from 91 to 96% over the last 442 kyr (Fig. 21a). There is no specific variation pattern in carbonate content noticed throughout the core. Very high  $\text{CaCO}_3$  content and minor changes of  $\text{CaCO}_3$  variation at Site 752 suggests that dilution plays a very insignificant role here. Furthermore, this site is situated relatively far away from landmass and therefore, dilution by terrigenous material is not significant. Since this site lies very much above the lysocline, dissolution does not seem to affect this core. Basically the minor variations observed in the carbonate content at ODP Site 752 may be due to changes in productivity of the overlying waters. At ODP Site 715, total  $\text{CaCO}_3$  content varies from 59 to 77% over last 45kyr (Fig. 21b). During the Holocene  $\text{CaCO}_3$  content is comparatively lower than during 13 to 24kyr, which corresponds to MIS 2 and documents high  $\text{CaCO}_3$  content. Thereafter,  $\text{CaCO}_3$  content remains low. Overall, this core does not seem to be display any specific pattern of  $\text{CaCO}_3$  fluctuations. Larger variations in  $\text{CaCO}_3$  content at Site 715 are possibly attributed to its proximity to the Indian sub-continent and hence influence by terrigenous material derived from the landmass.

The size index shows variation from 69 to 81% with a core top value of 78% at Site 752 (Fig. 21a). There has been a significant variation in the size index for this



**Fig. 21.** Fluctuations of total CaCO<sub>3</sub> and size index values at a) ODP Site 752 and b) ODP Site 715.

core. The high size index values obtained for ODP Site 752 confirms the finding that dissolution does not affect the sediments from this region. The size index values for ODP Site 715 vary from 23 to 41% with core top value of 34% (Fig. 21b). Again there is a large variation in size index for this core. Lower size index values obtained from ODP Site 715 cannot be attributed only to dissolution and further reasons need to be determined. Further, the CaCO<sub>3</sub> content of the finer fraction has been determined for both the cores. The <63 $\mu$ m fraction CaCO<sub>3</sub> for Site 752 remains high throughout

and varies from 82 to 96% (Fig. 22a). For Site 715 the  $<63\mu\text{m}$  fraction  $\text{CaCO}_3$  shows large variations ranging from 50 to 77% (Fig. 22b). There is a striking resemblance of  $<63\mu\text{m}$  fraction  $\text{CaCO}_3$  with the total  $\text{CaCO}_3$  content for Site 715. This feature is not seen for the  $<63\mu\text{m}$  fraction  $\text{CaCO}_3$  of Site 752.

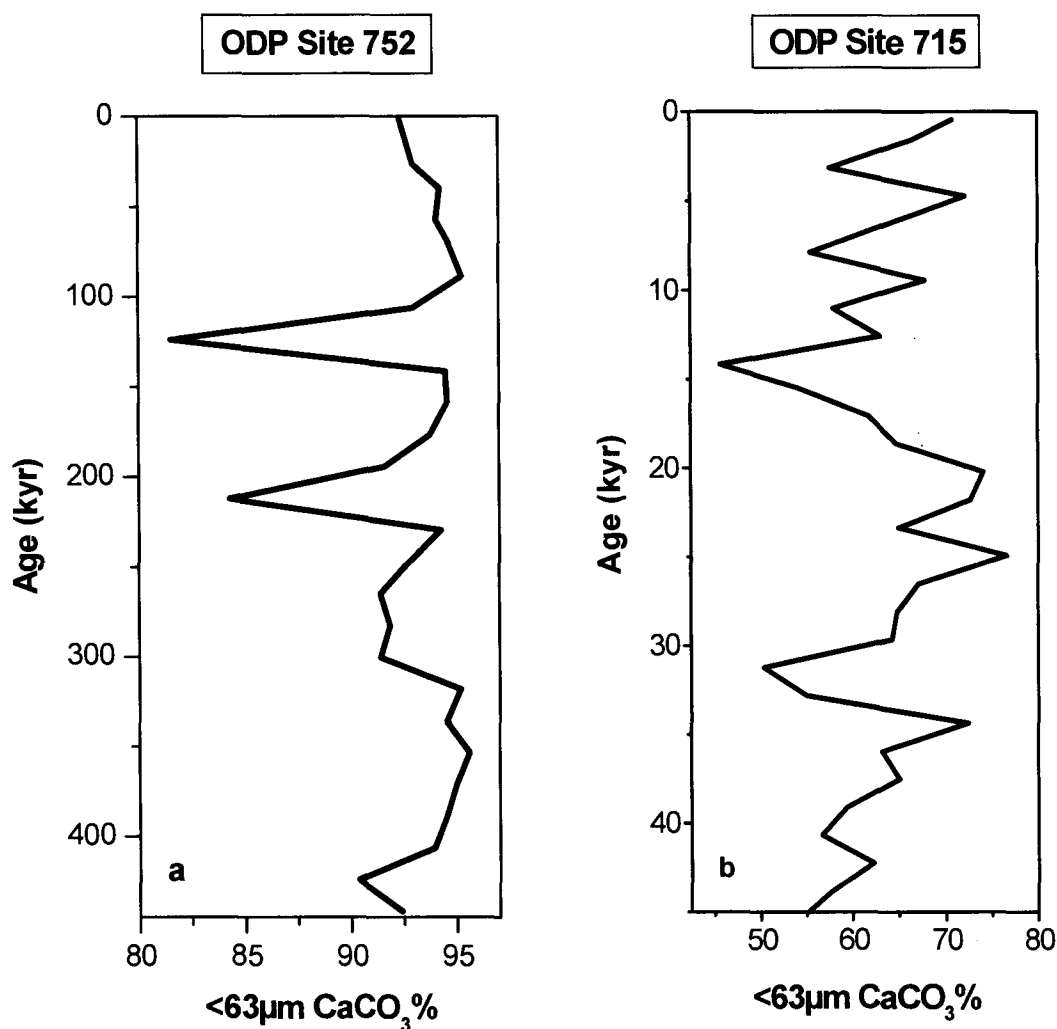


Fig. 22. Fluctuations of  $\text{CaCO}_3$  in  $<63\mu\text{m}$  fraction at a) ODP Site 752 and b) ODP Site 715.

Another, paleocarbonate ion proxy, planktonic foraminifera shell weight has been applied to the ODP Site 715. In order to get a better picture of the processes controlling the  $\text{CaCO}_3$  variations in this core, shell weight measurements were performed on *G. ruber* for the entire core. Shell weights show variability from 16 to

20.26 $\mu$ g throughout the core (Fig. 23). *G. ruber* shells do not show a typically expected glacial-interglacial difference in weight. Overall the shell weight trend is anomalous throughout the core thus obscuring the topic of concern.

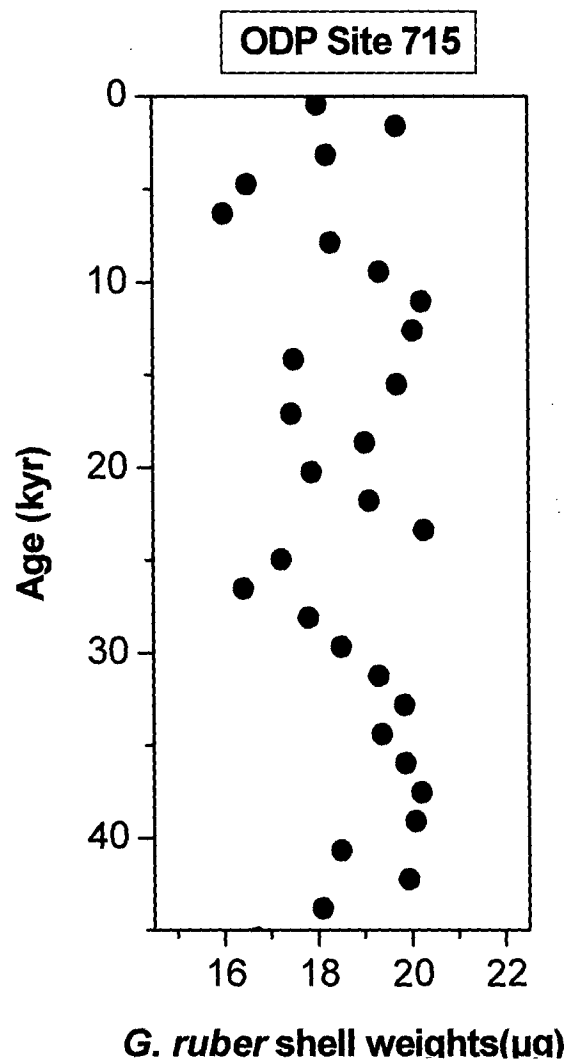


Fig. 23. Fluctuations in *G. ruber* shell weights at ODP Site 715.

### 3.2.3 Cores AAS9/21 and SK218/A:

Core AAS9/21 was recovered from the Arabian Sea, and core SK218/A, was recovered from the Bay of Bengal (Table 3, Fig. 9). Both cores lie in two unique environments but along a similar latitudinal transect. Both cores cover a time span of 25kyr, which covers the Last Glacial Maximum (LGM). Core AAS9/21 from the

Arabian Sea lies at a depth of 1807m.  $\text{CaCO}_3$  content in this core ranges from 18 to 45% (Fig. 24a). Low  $\text{CaCO}_3$  values were noticed from 0 to 10kyr and relatively high  $\text{CaCO}_3$  values were noticed from 10 to 20kyr. At around 18kyr highest  $\text{CaCO}_3$  values are recorded. In core SK218/A,  $\text{CaCO}_3$  values ranges from 1 to 12.5 % throughout the core (Fig. 24b). The  $\text{CaCO}_3$  content remains comparatively lower up to 10kyr i.e.

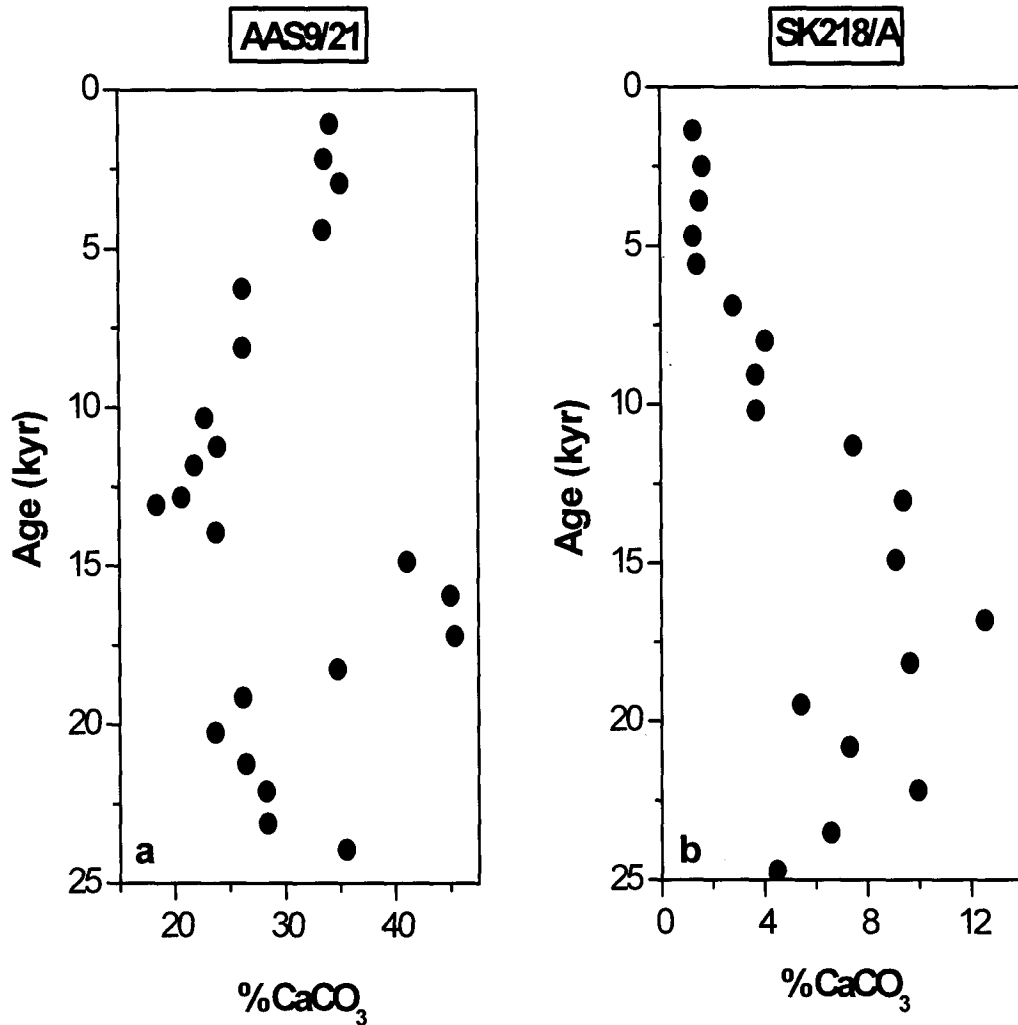


Fig. 24. Fluctuations in  $\text{CaCO}_3$  for the two cores a) AAS9/21 and b) SK218/A.

during the Holocene. During this period the  $\text{CaCO}_3$  content ranges from 1 to 4% below which a steep increase is noticed. The peak point in  $\text{CaCO}_3\%$  occurs at around 17kyr, which is of 12.5%. This corresponds to Late Glacial Maximum (LGM). Such a

CaCO<sub>3</sub> variation is indicative of the ‘Pacific pattern’. Size index values in core AAS9/21 show a gradual increase from glacial to the Holocene and then a marginal increase during the course of the Holocene. The range of size index values is from 10 to 40% (Fig. 25a). Holocene values range from 10% to 24%. A maximum in size index value of 40% is noted at around 19kyr. Size index in core SK218/A ranges from 10 to 46%. Size index remains comparatively lower during the Holocene, with values ranging from 10% to 20% (Fig. 25b). From 10kyr downwards there is a increase in

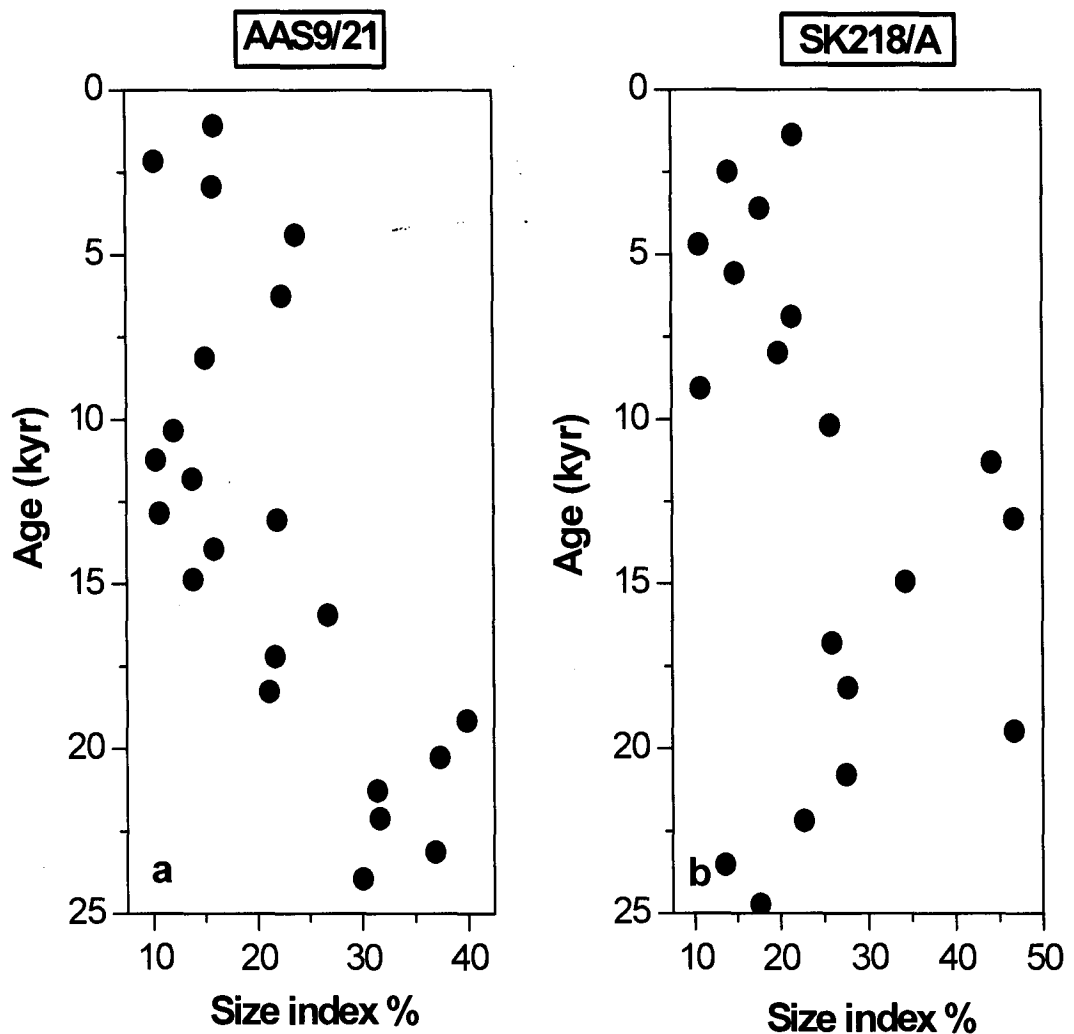


Fig. 25. Fluctuations in size index for the two cores a) AAS9/21 and b) SK218/A .



size index values with maximum value of 46% at around 19kyr, which corresponds to the LGM. The coretop size index value observed is 21%, which shoots up to 44% during the last glacial period. The size index values are indicative of dissolution, but reasons cannot be ascertained based on this lone indicator. In general the  $\text{CaCO}_3$  content and size index for both the cores, AAS9/21 and SK218/A show lower values during the interglacial and higher values during the glacial, indicative of a Pacific pattern of carbonate content fluctuation.

*G. sacculifer* shell weights from AAS9/21 show an increase from 31 to 41 $\mu\text{g}$  for the entire core (Fig. 26a). The steep increase in shell weights is encountered only

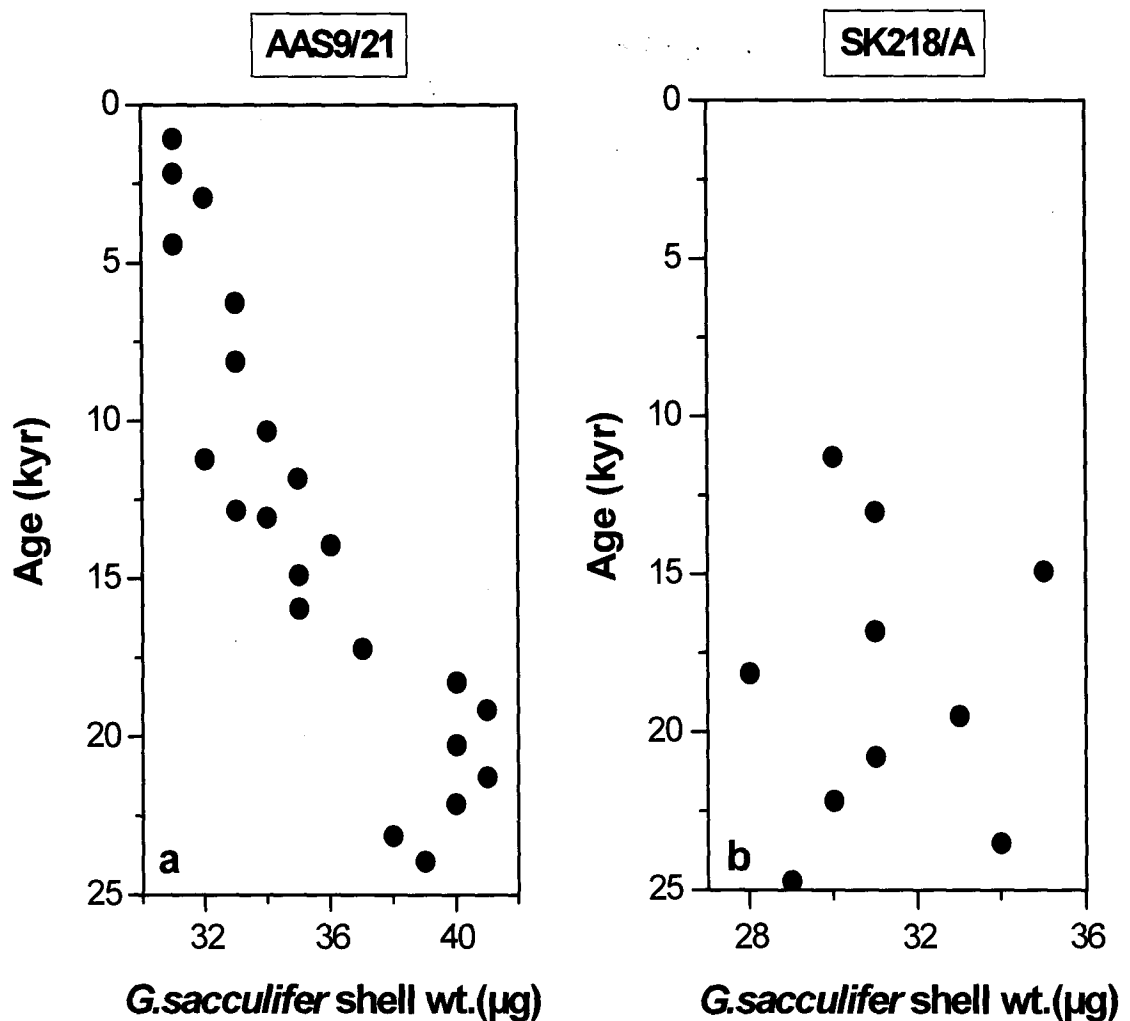


Fig. 26. Fluctuations in *G. sacculifer* shell weights for the two cores a) AAS9/21 and b) SK218/A.

after the Holocene as observed in  $\text{CaCO}_3$  content and size index. Maximum shell weight of  $41\mu\text{g}$  is observed at 19kyr. In the Core SK218/A, shell weights of *G. sacculifer* range from 28 to  $35\mu\text{g}$  (Fig. 26b). For the Holocene period broken *G. sacculifer* shells are encountered and therefore no shell weights can be derived for this interval. Below 10kyr, shell weights do not show any noticeable increase during the LGM as encountered in  $\text{CaCO}_3$  content and size index.

Mg/Ca ratios of foraminifera have been determined for the two cores AAS9/21 and SK218/A (Fig. 27a and b). Mg/Ca ratios of foraminifera are a well

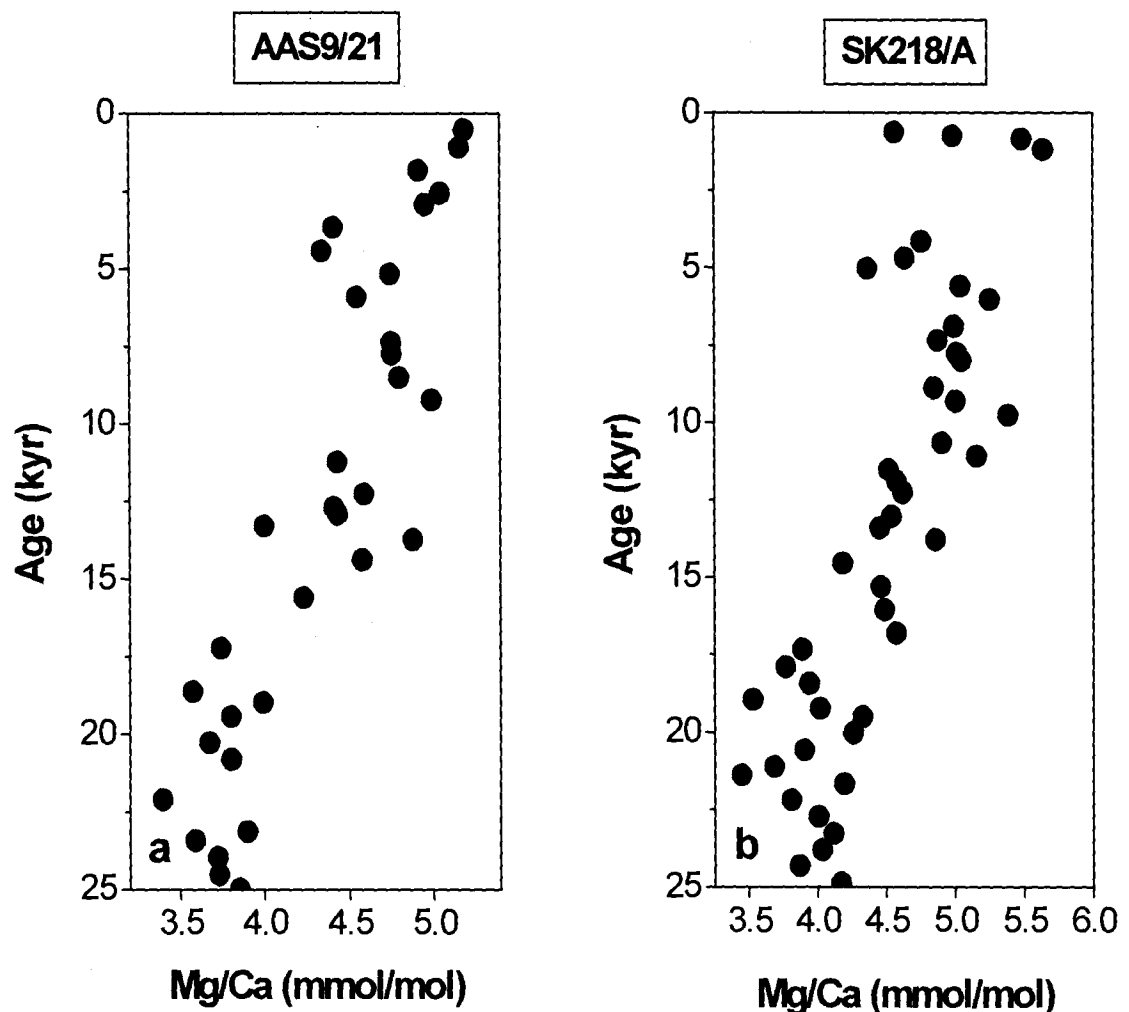


Fig. 27. Fluctuations in Mg/Ca for the two cores a) AAS9/21 and b) SK218/A.

established proxy for Sea Surface Temperature (Nürnberg *et al.*, 1996).  $Mg^{2+}$  is one of several divalent cations which may substitute for  $Ca^{2+}$  during the formation of biogenic calcium carbonate. Its incorporation into foraminiferal calcite is influenced by the temperature of the surrounding seawater during growth such that foraminiferal Mg/Ca ratios increase with increasing temperature (Barker *et al.*, 2005). Mg/Ca results from both the cores AAS9/21 and SK218/A show a downcore decrease which is an indicator of the temperature increase since the past 25kyr. In AAS9/21, Mg/Ca values range from 3.4 to 5.2mmol/mol (Fig. 27a). During the Holocene, Mg/Ca values show a decreasing trend with values in the range of 5.2 to 4.3mmol/mol. Thereafter, a steep decrease is seen from 4.9 to 3.4 mmol/mol during the last glacial. The lowest value is encountered at ~22kyr which is around the LGM. Mg/Ca values in Core SK218/A range from 3.4 to 5.6mmol/mol (Fig. 27b). Holocene values in this core also show a decreasing trend in the range of 5.6 to 4.4mmol/mol. Mg/Ca values started to decline from 13kyr onwards and minimum values were noticed during the LGM.

## CHAPTER IV

### DISCUSSIONS

#### 4.1 Calcium Carbonate fluctuations from the world oceans:

The CaCO<sub>3</sub> patterns over the equatorial sector of the Atlantic, Pacific and Indian oceans, covering a time span of last 0.6Ma are assessed to address the basic differences amongst the three oceans. CaCO<sub>3</sub> fluctuations over the last 0.6Ma covers the major glacial/interglacial intervals of the Late Quaternary Period and thus provides an overview about the relationships between climate and CaCO<sub>3</sub>. This exercise shall give a synoptic view of the world's ocean CaCO<sub>3</sub> cycle and a better understanding of the past CO<sub>2</sub> variations.

The total carbonate content at any given location may fluctuate due to three major factors: 1) productivity of carbonate secreting organisms, 2) dilution by non-calcareous material and; 3) dissolution of calcareous tests during and after deposition (Damuth, 1975). In the Pacific Ocean, it is widely accepted that CaCO<sub>3</sub> content was higher during glacials and lower during interglacials. This pattern has been termed as the 'Pacific pattern'. In contrast, in the Atlantic Ocean, CaCO<sub>3</sub> content is generally higher during interglacials and lower during glacials, which is termed as the 'Atlantic pattern'. The Quaternary CaCO<sub>3</sub> patterns in the Indian Ocean have not been analyzed in such detail as in the Pacific and Atlantic Oceans. In the Indian Ocean some sites are known to exhibit a Pacific pattern (Olausson, 1965; Oba, 1969; Naidu, 1991; Naidu et al., 1993), whereas other cores show both Pacific and Atlantic patterns (Peterson and Prell, 1985). Swedish Deep Sea Expedition core 154 (Volat *et al.*, 1980), generally exhibits a Pacific type of dissolution pattern in major portion of the records whereas

studies from above the lysocline depth eg., core ODP709A, do not show either a Pacific or an Atlantic type pattern (Naidu and Malmgren, 1999).

It has been discussed here, which factor is the most important in shaping the calcium carbonate patterns from the equatorial region of the world oceans.

#### **4.1.1 Dilution by non-calcareous material:**

The principal source of dilution by non-calcareous material is terrigenous input, the other source being siliceous productivity. Olausson (1969) states that the continental surface drained to the Atlantic Ocean is almost twice that drained to both the Pacific and Indian oceans. This is due to the major rivers, which drain into the Atlantic (Amazon, Mississippi, Niger, Congo etc). Therefore dilution could be an important factor controlling the  $\text{CaCO}_3$  variations in the Atlantic Ocean. But the scenario in the Indian and Pacific oceans is different. A detailed study of the  $\text{CaCO}_3$  distribution in surficial sediments indicate that the dilution effects are very insignificant in the equatorial Indian Ocean (Kolla *et al.*, 1976), whereas the central Pacific Ocean is relatively unaffected by dilution from terrestrial sediment sources (Adelseck and Anderson, 1978).

#### **4.1.2 Productivity:**

High surface productivity leads to high accumulation of  $\text{CaCO}_3$  due to enhanced supply of biogenic material. Olausson (1985) suggested that accumulation of  $\text{CaCO}_3$  increased during glacials in the Indo-Pacific Ocean due to intensified sink water formation in the northernmost Atlantic Ocean and intensified upwelling in the Indo-Pacific Ocean. This hypothesis would explain the difference in dissolution patterns between Atlantic and Pacific oceans (Olausson, 1985). One would expect a

Pacific type of carbonate pattern in Indian Ocean cores raised from above the lysocline depth if simultaneous upwelling takes place in Indo-Pacific oceans. Instead as seen in Site 709A (Fig. 13), where variations in  $\text{CaCO}_3$  are suggested to be due to productivity changes, does not show either a clear Pacific pattern of  $\text{CaCO}_3$  fluctuation or any relationship with glacial/interglacial cycles. This points to a lack of coeval upwelling in the equatorial Pacific and Indian Oceans (Naidu and Malmgren, 1999). Therefore, the  $\text{CaCO}_3$  patterns differ between the Indian and Pacific Oceans at shallow depth sites.

Surface water productivity changes are of secondary importance in the central Pacific Ocean (Adelseck and Anderson, 1978). Arrhenius (1952) and other workers in the Atlantic are of the opinion that productivity increased during glacials. Wiseman (1956), (1965); Kellog (1975), (1976); Ruddiman and McIntyre (1976) agree with the correspondence between high productivity and interglacials in the Atlantic. Berger (1992) states that productivity increased during glacials in the Indian Ocean. Increased plankton productivity leads to a high vertical flux of organic carbon to the sea floor, and consequently more carbon dioxide is released into the bottom water by decay of organic matter, lowering the pH and increasing carbonate dissolution. On a larger scale high productivity means stronger extraction of carbonate from water, which then becomes under saturated (Berger, 1977). The rain rates of calcite and organic carbon to the sediments depend on the surface water productivity (Olausson, 1971, 1985; Arrhenius 1952, 1988; Archer, 1991). Thus, low productivity may induce good general preservation of tests. The core SDSE 154, is an example of enhanced dissolution of  $\text{CaCO}_3$  during interglacials due to high productivity (Naidu *et al.*, 1993).

### 4.1.3 Dissolution:

Dissolution of  $\text{CaCO}_3$  in marine sediments is controlled by two factors, the understauration of calcite or aragonite in bottom waters and the undersaturation in pore waters due to production of  $\text{CO}_2$  by oxic respiration. Kuenen (1950), states that by far the greatest amount of dissolution takes place on the sea floor and not during settling. The  $\text{CO}_2$  content increases progressively in bottom water when flowing, owing to benthic organism's respiration and oxidation process, so that bottom water and dissolution are not directly correlated; "old" bottom water enhances dissolution much more than recently produced water (Volat *et al.*, 1980). Berger, (1977) stated that carbonate cycles during glacial and interglacial periods in the Pacific Ocean are largely a function of dissolution cycles. Broecker and Takahashi (1978) showed that the state of preservation does correspond to saturation on a global scale, at least in the vicinity of the lysocline and away from continental margins. A comparison of calcium carbonate preservation records of the Indian Ocean (Peterson and Prell, 1985a) with the calculated carbonate ion saturation in the water (Gröstch *et al.*, 1991) indicated that the preservation state is tied to saturation levels with respect to carbonate ion. The Indian and Pacific Oceans correspond in a similar way to changing deep-water circulation.

To better document the effect of  $\text{CO}_3^{=}$  undersaturation on the calcite preservation patterns from the three major world oceans, the dependency of  $\text{CaCO}_3$  content on  $\text{CO}_3^{=}$  was considered. For this purpose, GEOSECS stations were chosen from Atlantic, Pacific and Indian Ocean. The  $\text{CO}_3^{=}$  concentration profiles were calculated from Station Nos. 109, 334 and 420 from the Atlantic, Pacific and Indian oceans respectively. The selection of single stations for the three oceans is justified, as mentioned earlier, below 1500m  $\text{CO}_3^{=}$  concentrations are nearly constant. The

pressure-normalized carbonate ion concentration was then computed for respective depths and plotted versus the coretop  $\text{CaCO}_3$  content for all the ten cores. A linear fit is observed with significant correlation between the two ( $R^2=0.7$ ) (Fig. 28). This suggests that the  $\text{CaCO}_3$  patterns over the world oceans are closely tied to bottom water saturation with respect to carbonate ion and hence amongst other factors affecting regionally, calcite dissolution is the most important factor in shaping the

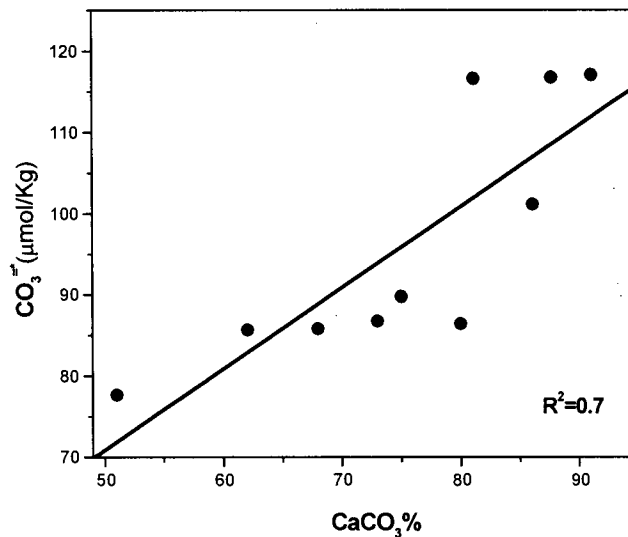


**Fig. 28.** The  $\text{CaCO}_3$  % from core tops of the Atlantic, Pacific and Indian Ocean showing a linear variation with respect to pressure-normalised  $\text{CO}_3^{2-}$  calculated from GEOSECS stations ( $R^2=0.7$ ).

$\text{CaCO}_3$  patterns.

Considering dissolution as the most important criteria in shaping the  $\text{CaCO}_3$  profiles, Van Andel (1975) suggested the criteria that the CCD is the depth wherein the  $\text{CaCO}_3$  content decreases to 20%. Ever since, various workers have made an attempt to calculate the depth of the CCD in different oceans. Peterson and Backman (1990) provide a CCD history for the western equatorial Indian Ocean, which suggests that from 22 to 2 million years it ranged from 3.8 to 4.5km. Then, during the last 2 million years, it deepened to 5km. Broecker and Peng (1982) include a summary of core top  $\text{CaCO}_3$  content versus water-depth plots for eight areas of the



ocean. On the basis of the 20% criteria, these plots suggest that in the Indian and Pacific oceans, the CCD currently resides at  $4.6 \pm 0.2$  km depth and in the northern Atlantic it resides at  $5.1 \pm 0.4$  km. Peterson and Prell (1985a) made a detailed study of the state of  $\text{CaCO}_3$  preservation on Ewing core tops from the 90°E Ridge in the Indian Ocean. They found a steady increase in the extent of fragmentation of whole foraminifera shells between 2.0 and 4.5 km. However, below this depth, the abundance of fragile shells (i.e., *G. ruber* and *G. sacculifer*) dropped precipitously while that of robust shells (i.e., *G. menardii*) decreased far more slowly.

Since, the importance of bottom water carbonate ion has been revealed; the criteria of Van Andel, (1975) can be applied to the cores in the present study. It was found that all the cores from the Atlantic Ocean are from above the CCD; those from the Pacific are immediately at or above the CCD; while those from the Indian Ocean include one from above the CCD and another, Core SDSE 154 from below the CCD. All the ten cores form classical examples of  $\text{CaCO}_3$  patterns from different oceans and illustrate the changing bottom water circulation and hence carbonate ion changes amongst oceans.

De Menocal *et al.* (1997) proposed that glacial-interglacial changes in deep Atlantic circulation were primarily responsible for the observed timing and spatial distributions of Pliocene–Pleistocene global carbonate burial cycles. Glacial reductions in NADW production allowed corrosive (low  $[\text{CO}_3^{=}]$ ) AABW to advance into the carbonate-rich sediments of the tropical and North Atlantic. Extensive and instantaneous Atlantic carbonate dissolution resulted from the associated rise in Atlantic calcite lysocline levels. Glacial mean ocean alkalinity levels increased in response to this dissolution, and the global ocean net carbonate burial (the amount of calcite which must be buried to balance the continental weathering supply of

alkalinity to the ocean) must have increased in the Pacific and Indian Oceans to balance decreases in Atlantic burial fluxes. This was achieved by a deepening of the calcite lysocline in the Pacific and Indian basins in response to increased mean ocean alkalinity levels, which thereby increase oceanic  $[\text{CO}_3^{=}]$  levels (using  $[\text{CO}_3^{=}] = [\text{Alk}] - [\Sigma\text{CO}_2]$ ; Broecker and Peng, 1982). However, this process of restoring the equilibrium global calcite burial is not instantaneous, but rather, is constrained by the mean response time of the oceans. Today, well ventilated (and hence high  $\text{CO}_3^{=}$ ) NADW water the Atlantic ocean is more preserving to calcite than the rest of the worlds oceans. NADW accumulates  $\text{CO}_2$  oxidized from falling debris on its “grand journey” to the Pacific and Indian oceans and becomes more corrosive to carbonate than the NADW (Broecker and Peng, 1982). During the last glacial NADW either formed more slowly or was less ventilated than it is today (Boyle and Keigwin, 1982; Shackleton *et al.*, 1983; Curry and Lohmann, 1983; Mix and Fairbanks, 1985). The production of NADW was diminished therefore less  $\text{CO}_2$  was pushed into deep Pacific by NADW (Boyle and Keigwin, 1985). Thus the distribution pattern was reversed. It is still an open discussion as to whether the good glacial Pacific carbonate preservation can be attributed to a source of well-ventilated deep water in the Pacific (Moore *et al.*, 1978; Keigwin, 1987; Curry *et al.*, 1988).

$\text{CaCO}_3$  in marine sediments as a function of water depth in today’s ocean or at any specific time in the most is a useful index of the extent of dissolution (Broecker, 2003). This relationship is highly non-linear. Deep water formed in the northern Atlantic has a higher  $\text{CO}_3^{=}$  concentration than that produced in Southern Ocean. The difference in  $\text{CO}_3^{=}$  concentration between NADW and the rest of the deep ocean is related to the difference in  $\text{PO}_4$  concentration. NADW has half the concentration of  $\text{PO}_4$  then the other water. The high phosphate content waters upwelling in the

southern ocean lose part of their excess  $\text{CO}_2$  to the atmosphere. This results in an increase in their  $\text{CO}_3^{=}$  ion content. In contrast low  $\text{PO}_4$  content water reaching in the northern Atlantic has  $\text{CO}_2$  partial pressures well below that in the atmosphere and hence they absorb  $\text{CO}_2$ . This reduces their  $\text{CO}_3^{=}$  concentration. In Pacific and Indian Oceans much of the floor lies below the transition zone. Hence most of the  $\text{CaCO}_3$  falling into the Deep Pacific and Indian Ocean dissolves. In the South Pacific Ocean and South Indian Ocean the  $\text{CO}_3^{=}$  ion concentration remains largely unchanged. Only in the northern reaches of these oceans does the release of metabolic  $\text{CO}_2$  overwhelm the supply of  $\text{CaCO}_3$  allowing the  $\text{CO}_3^{=}$  concentration to drop (Broecker, 2003).

Again, certain preservation and dissolution events of the Indo-Pacific and Atlantic Oceans are known to be in phase (Crowley, 1983). From the results put forth here it is interpreted that the Indian Ocean carbonate records do not exhibit a straightforward relationship with glacial-interglacial cycles. However, additional high-resolution studies are necessary from different physiographic regions of the Indian Ocean to enhance our understanding of the carbonate fluctuations during the Quaternary Period. To understand the glacial-interglacial changes in  $\text{CaCO}_3$  and hence  $\text{CO}_2$  better, it is necessary to be aware of the  $\text{CO}_3^{=}$  fluctuations during the glacial-interglacial changes in ocean operation. Three important paleocarbonate proxies are used in this attempt. But prior to any direct application of these proxies to the Indian Ocean sediments, they require to be validated.

## **4.2 Validation and application of paleocarbonate ion proxies in the Indian Ocean:**

Ten core top samples, providing a good spatial coverage in the tropical Indian Ocean, have been used in order to validate three important paleocarbonate ion proxies

for the northern Indian Ocean (Fig. 9). The chosen GEOSECS locations are expected to provide a complete picture of the  $\text{CO}_3^{=}$  concentration for required locations and water depth. In the Indian Ocean high values of size index have been reported above the lysocline depth (Peterson, 1984; Broecker and Clark, 1999). Peterson (1984) has reported size index values of 60 to 80% for water depth ranging from 2000 to 3000m in the tropical Indian Ocean, whereas above 4000m water depth the index is found to be nearly constant at a value of  $52 \pm 2\%$  (Broecker and Clark, 1999). In the present study size index value of 95% at a water depth of 1000m is noticed which seems to be very high as compared to the earlier reports from the Indian Ocean (Fig. 15). This could be due to winnowing at these shallow depths, which enriches the sediments in the larger entities. The values of size index in the Indian Ocean also are quite contrary to those obtained by Broecker and Clark, (1999) for the Atlantic and Pacific Oceans. From 2250m water depth onwards a gradual decrease in size index values is observed. The linear decline suggests that dissolution could be affecting shallowest samples from the depth of 1000m onwards. In the present study pressure-normalized carbonate ion concentrations [ $\text{CO}_3^{=*}$ ] have been computed for the coretop samples. Broecker and Clark (1999) have shown that for pressure-normalized carbonate ion concentrations below  $105\mu\text{mol/kg}$ , a linear decline in size index occurs for samples from all the three major oceans. Finally the index results were plotted against  $\text{CO}_3^{=*}$  and the offset was assessed between regions and scatter of results within a given region. To do this a best fit reference line for the Pacific and Indian Oceans was established. The slope of this line estimated by them was  $6.6\mu\text{mol/kg}$  per 10% change in the index.

Size index values were superimposed on the reference line of Broecker and Clark, (1999), show a considerable close fit with an average offset of  $-0.33$  from the

reference line (Fig. 16). This translates to a very negligible shift of 150m in saturation horizon of  $\text{CO}_3^{=}$  in the Indian Ocean. Large variation size index values (14%) within a change of  $1\mu\text{mol/kg}$  in  $\text{CO}_3^{=*}$  concentration (from 96 to  $97\mu\text{mol/kg}$ ) within a water depth range of 100m (3300 to 3400m) is noticed, which is significant in the Indian Ocean (Fig. 16). To better document the dissolution processes at these depth, the shell weight method of Lohmann (1995) was applied to selected core tops.

The shell weight method is also known to give a better picture of the dissolution intensity as it specifically targets at cleaned shells that are from a narrow size range nullifying the ill-effects caused by finer entities (Broecker and Clark, 2001c). *P. obliquiloculata* shells from the Indian Ocean weigh on the average  $\sim 10\mu\text{g}$  less than those from the Pacific Ocean and *N. dutertrei* shells from the Atlantic Ocean appear to be heavier than their Indian and Pacific Ocean counterparts (Broecker and Clark, 2001d). In the present study, it is found that *G. sacculifer* shell weights show marginally high values than those in the eastern Indian Ocean as documented by Broecker and Clark, (2001d). The large variability documented in the size index in the water depth range of 3300 to 3400m is manifested in the shell weights also (Fig. 18). To further shed light on the problem, calcite crystallinity was measured on the respective samples.

Shells that show a narrow (104) calcite peak on XRD powder diagrams are interpreted as being better crystallized than those showing a broader diffraction peak and dissolution improves shell crystallinity (Bassinot *et al.*, 2004). Therefore the calcite crystallinity could be used as a dissolution index that could be tied to a carbonate ion change in the deep sea (Bassinot *et al.*, 2004). Crystallinity measurements on *G. sacculifer* show similar crystallinity values over a range of bottom water [ $\text{CO}_3^{=*}$ ] (Fig. 19), which indicate that dissolution affects more or less

evenly in the water depths ranging from 3300 to 3400m whereas Site SK199C/7 shows lower values suggesting intense dissolution at this water depth (3900m).

In addition, we have compared the SEM micrographs of *G. sacculifer* from deeper depth (3944m) Site SK199C/7 and shallower depth (2250m) Site SK199C/6. Apparently, *G. sacculifer* from deeper depth site show dissolution features (Fig. 29 a and b), whereas, shallow depth site show well preserved *G. sacculifer* shells (Fig. 29 c and d). This observation as well as less abundance of *G. sacculifer* and *G. ruber*

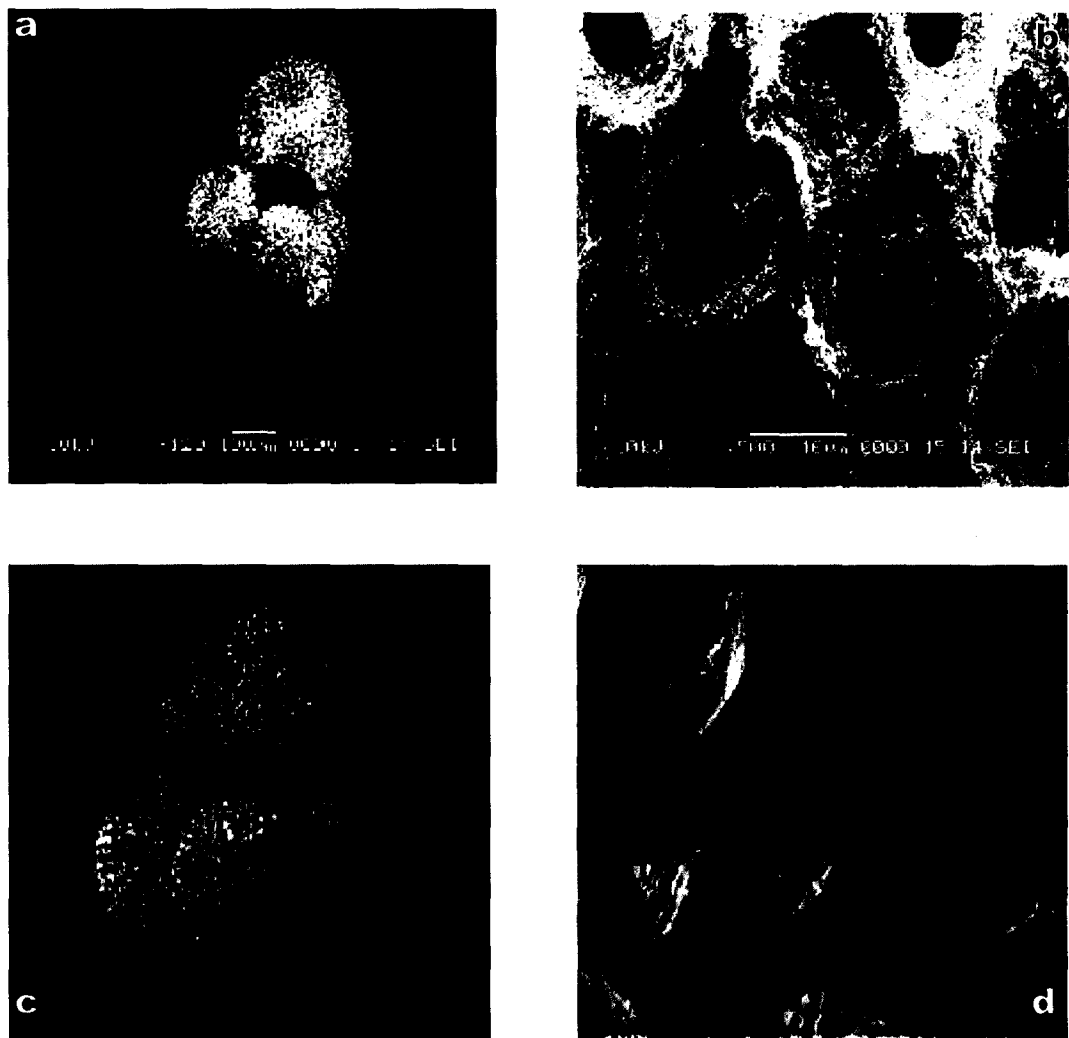


**Fig. 29. (a and b) SEM micrographs of *Globigerinoides sacculifer* from 3944 m water depth (SK199C/7) showing dissolution features. (c and d) Well-preserved tests of *Globigerinoides sacculifer* from 2250m water depth (SK199C/6).**

(P.D. Naidu unpublished data) from the sediments beyond 3900m water depth endorses that intense calcite dissolution occurs from 3900m depth in the Indian Ocean.

All three proxies reveal that dissolution affects planktonic foraminifera from 2250m and that intense dissolution occurs from 3900m onwards. However, a large variation in size index, shell weight and calcite crystallinity is noticed within a narrow range of 100m (3300 to 3400m) water depth. Foraminiferal shell weights from surface sediments not only depend on bottom water  $\text{CO}_3^{=}$ \* concentrations but also by the carbonate ion concentrations in the waters wherein they calcify (Barker and Elderfield, 2002). Thus, shell weight of several species of planktonic foraminifera from core top sediments vary systematically as a function of latitude in the North Atlantic Ocean (Barker and Elderfield, 2002). *G. sacculifer* is a surface dwelling species and calcifies at shallower depths as compared to *N. dutertrei* and *P. obliquiloculata* (Fairbanks et al, 1982) and therefore *G. sacculifer* shell weight should be affected by the carbonate ion concentrations of the surface waters. To understand relationship between shell weights and surface water carbonate ion concentration, shell weights variability of *G. sacculifer* from sites SK199C/6, 7, 9, 10, 11 and 14 has been compared to surface water carbonate ion concentrations for these sites in the western Indian Ocean (Fig. 30). Though there could possibly be marginal difference in the present surface carbonate ion concentrations and those at which the shells must have calcified, shell weights at sites SK199C/6, 9, 10, 11 and 14 shows a reasonably good correspondence with surface water  $\text{CO}_3^{=}$  concentrations. Surface waters are supersaturated with respect to  $\text{CO}_3^{=}$  concentrations, therefore, higher calcification rates in surface waters produce thicker shells without any change in shell size which is

reflected in the shell weights of planktonic foraminifera (Barker and Elderfield, 2002). It is observed here that foraminiferal calcite from sediment bathed by similar  $\text{CO}_3^{=}$  concentration from depths shallower than 3900, trace the surface ocean  $\text{CO}_3^{=}$  concentrations.

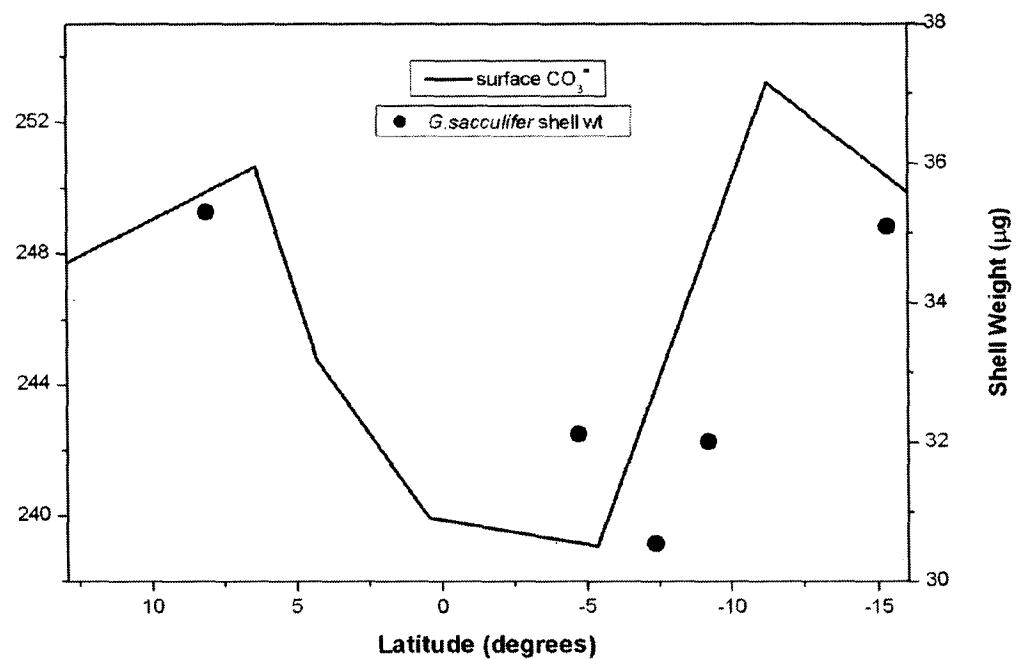


**Fig. 30. Surface ocean  $\text{CO}_3^{=}$  concentrations (calculated from GEOSECS stations 417, 418, 419, 420, 421, 424, and 425) and *Globigerinoides sacculifer* shell weights plotted as a function of latitude. Shell weights correspond well with the surface  $\text{CO}_3^{=}$**

#### 4.2.1 Understanding calcite dissolution mechanisms in the Indian Ocean:

The calcite dissolution mechanism proposed by Lohman (1995) has some drawbacks. It suffers from an inability to distinguish changes in bottom-water carbonate ion concentration from changes in bottom-water to pore-water concentration offset (Broecker, 2003). It becomes seemingly important to understand whether the shell weight change is caused due to bottom water or pore water undersaturation, in order to use it as a reliable paleocarbonate ion proxy. As seen



above, by applying three paleocarbonateion proxies, calcium carbonate size index, planktonic foraminifera shell weights and calcite crystallinity to a set of core top samples it has been documented that calcite dissolution commences from 2250m onwards and intensifies at around 3900m water depth in the Western Tropical Indian Ocean. Two processes involve dissolution of calcite on the seafloor; 1) Interface dissolution and 2) pore-water dissolution. The former occurs only at water depths greater than that of saturation horizon, but the later occurs above calcite saturation horizon. It is driven by respiration CO<sub>2</sub> released to pore waters (Emerson and Bender, 1981). It is required to understand whether the dissolution occurring at the 3900m water depth in the western Tropical Indian Ocean is due to saturation state of the overlying bottom waters or due to acidification of pore waters during organic matter remineralization. In this quest, the shell weights have been used following a method by de Villiers, (2005).

As mentioned earlier, calcite dissolution in sediments above lysocline depths could take place in acidified pore waters. The core top foraminifera are also initially exposed to the benthic fluff layer at the sediment-water interface (de Villiers, 2005). Therefore, this interface is perhaps a better description of the initial exposure environment of coretop foraminifera. Therefore the term  $\Delta\text{CO}_3^{\text{interface}}$  is used instead of  $\Delta\text{CO}_3^{\text{pore-waters}}$ .

To understand whether dissolution taking place at site SK199C/7 is due to this corrosive benthic fluff layer the  $\Delta\text{CO}_3^{\text{interface}} - \Delta\text{CO}_3^{\text{bottom water}}$  gradient was calculated. For doing this the relationship from the core top data of Broecker and Clark, (2001a) for *P.obliquiloculata* shell weight and bottom water  $\Delta\text{CO}_3^{\text{interface}}$  from the Indian Ocean given below was used:

$$\Delta\text{CO}_3^{\text{interface}} = [P.obliquiloculata \text{ shell weight } (\mu\text{g}) - 24.53] / 0.2759.$$

Using the above relation and shell weights of *P.obliquiloculata*,  $\Delta\text{CO}_3^{=}$  interface was calculated. The gradient ( $\Delta\text{CO}_3^{=}$  interface -  $\Delta\text{CO}_3^{=}$  bottom water) was then calculated using  $\Delta\text{CO}_3^{=}$  bottom water values. Thus, a value of +5 $\mu\text{M}$  is obtained at 3900m water depth. de Villiers (2005) has determined the  $\Delta\text{CO}_3^{=}$  interface to be within  $\pm 10\mu\text{M}$  of bottom water. The value of +5 $\mu\text{M}$  falls within the range of  $\pm 10\mu\text{M}$  suggesting that dissolution at 3900m water depth is due to undersaturation in  $\text{CO}_3^{=}$  concentration of bottom waters.

In an attempt to understand the factors which control calcite dissolution along a transect of tropical Indian Ocean, for the first time, the shell weights were employed as a paleocarbonate ion proxy to a set of core tops from depth ranges 2250 to 3900 m in the tropical Indian Ocean. Using the relationship between *P.obliquiloculata* shell weight and bottom water  $\Delta\text{CO}_3^{=}$  from the core top data of Broecker and Clark, (2001d) from the Indian Ocean and the data from the present study,  $\Delta\text{CO}_3^{=}$  interface -  $\Delta\text{CO}_3^{=}$  bottom water is calculated to be +5 $\mu\text{M}$ . Shell weight measurements of planktonic foraminifera species *G. sacculifer* and *N. dutertrei* also reveal the gradient;  $\Delta\text{CO}_3^{=}$  interface to be within  $\pm 10\mu\text{M}$  of bottom water values. This suggest that there is no gradient in  $\Delta\text{CO}_3^{=}$  across the sediment-bottom water interface below a depth of 1000m. The planktonic foraminifera shell weights in this sector of the tropical Indian Ocean clearly display that the dissolution of foraminifera shells is not due to corrosiveness of bottom waters caused due to pore water acidification. Rather, the corrosive effect of the bottom waters is due to the  $\text{CO}_3^{=}$  undersaturation of the bottom water. This is an important findings in terms of understanding the paleocarbonate ion concentration in this sector of the Indian Ocean and eliminates an important drawback of the shell weight as a carbonate ion proxy as stated earlier.

#### **4.2.2 Constraints in using size index and shell weights to determine carbonate ion concentrations:**

As seen above, the size index, planktonic foraminifera shell weights and calcite crystallinity have proven to be valid paleocarbonate ion proxies at least when applied to spatially distributed core top samples. In order to apply the size index and planktonic foraminifera shell weights as paleocarbonate ion proxies so as to reconstruct the past changes in carbonate ion and hence understand the carbon dioxide sequestration in the northern Indian Ocean both these proxies need to be validated for temporal sediments. Therefore both these proxies have been applied to the cores from ODP Site 752 and ODP Site 715.

The Site 752 is characterized by very high values of  $\text{CaCO}_3$  throughout the core. This is due to the location of this core on a topographic high where winnowing of sediments is an important factor and this enriches the sediments in larger entities. As stated earlier, the core from Site 752 has been recovered from a very shallow depth of 1086m it was felt that it could be very useful in understanding supralysoclinal carbonate behavior. The high values and minor range in  $\text{CaCO}_3$  variation rules out two important factors controlling the  $\text{CaCO}_3$  content, dilution and dissolution at this site. Therefore the minor variations observed in the carbonate content at site 752 may be due to changes in productivity of the overlying waters. The much lower  $\text{CaCO}_3$  values from Site 715 are due to terrigenous dilution probably from the Indus River discharge due to its proximity to the Indian sub-continent. The  $\text{CaCO}_3$  records from the eastern Arabian Sea are mostly influenced by terrigenous dilution caused by variations in the terrigenous lithogenic flux derived from the Indus River (Naidu, 1991). The  $\text{CaCO}_3$  fluctuations in Site 715 could be caused due to dilution or dissolution, but the major controlling factor is productivity.

Both the Sites 752 and 715 are situated above lysocline depths. It has been estimated that about 25% of  $\text{CaCO}_3$  produced above the lysocline undergoes dissolution (Milliman, 1993). Consequently, dissolution could possibly play an important role here. Therefore the size index has been employed to possibly figure out the role of dissolution at both the sites. Size index values for both the cores show a large disparity. The size index values for ODP Site 752 are high and can be attributed again to winnowing which enriches the sediment in the  $>63\mu\text{m}$  fraction. On the contrary the size index values from the ODP Site 715 are much lower though the core is from above the lysocline. Broecker and Clark (1999), showed that in the pressure-normalized  $\text{CO}_3^{=}$  ion concentration range of 105-70 $\mu\text{mol/kg}$ , a linear decline in the ratio of  $\text{CaCO}_3$  in the  $>63\mu\text{m}$  fraction to the total  $\text{CaCO}_3$  in the bulk sample occurs. This size index change was observed to be from a value of 55% to 0. These results suggested that the size index could be used as a paleocarbonate ion proxy. The results implied that the initial size composition of the  $\text{CaCO}_3$  deposited throughout the tropical region of the Atlantic, Pacific and the Indian Ocean is quite uniform and that influence of variations in the flux ratio of organic carbon to that of  $\text{CaCO}_3$  must be small. Depth transect of shallower cores on the Ceara Rise suggest that for  $\text{CO}_3^{=*}$  values higher than 105 $\mu\text{mol kg}^{-1}$  the index values stand no longer valid. For water depths above 4000 m the index is nearly constant at a value of  $52 \pm 2\%$ . Broecker *et al.*, (1999), suggested that the size index validated for the water depths below 4000 m does not continue for water depths above. It has been observed that higher values of the index are to be found in tropical Indian Ocean cores from between 2000m and 3000m depth (Peterson, 1984). By contrast, results from Sites 752 and 715 in the present study are at odds with the findings by Broecker *et al.* (1999) and Peterson (1984). Also the size fraction index at the core top for the ODP site 715 of 34% is not

consistent with the values obtained by Peterson (1984), for the Indian Ocean cores from depths ranging from 2000 to 3000m. Therefore there is a need to verify the reasons for the observed values in size index.

The size index and total CaCO<sub>3</sub> percentage versus age for Site 752 and 715 show contrasting results (Fig. 21 a and b). At Site 752 the variations in size index and total CaCO<sub>3</sub> percentage show a similar trend and hence it can be inferred that the observed high values in both size index and CaCO<sub>3</sub> content are a result of supersaturation with respect to CO<sub>3</sub><sup>=</sup> ion concentrations of waters bathing the sediment. But, the values are substantially higher as compared to values reported by Broecker and Clark (1999), in pressure-normalized CO<sub>3</sub><sup>=</sup> ion concentration range of 105-70µmol/kg, ruling out any dissolution at this Site. This endorses the fact that the minor variations observed in the carbonate content at site 752 could be only due to changes in productivity of the overlying waters. As stated earlier both the cores lies above the lysocline. At shallow depths the CO<sub>3</sub><sup>=</sup> is nearly constant through time. The coretop variations observed between the cores used in the present study and other cores from the Indian Ocean may be attributed to rain rates of non-calcareous material and/or calcite and organic carbon to the sediments, which depend on the surface-water productivity.

The Site 715 shows an exactly opposite variation pattern for CaCO<sub>3</sub>% and size index (Fig. 21b). The size index in this case may not reflect the dissolution pattern. Two possible explanations are offered for the observed variations. i) Breakup in foraminifer's shells can continue for thousands of years after burial. This Organic matter respiration is a likely driving mechanism for dissolution in sediments overlain by supersaturated bottom waters (Adler *et al.*, 1989; Cai *et al.*, 1995; Hales and Emerson, 1997). Significant dissolution occurs as a result of metabolic CO<sub>2</sub> release

from decaying organic matter into sediment pore waters (Emerson and Bender, 1981; Jahnke *et al.*, 1997). It has been proposed that an ocean-wide change in the ratio of organic to inorganic carbon in the sinking biological material could decouple the preservation history of  $\text{CaCO}_3$  from seawater  $\text{CO}_3^{=}$  (Archer and Maier-Reimer, 1994). The  $>63\mu\text{m}$  size fraction is related to the percentage of whole foraminifera. During dissolution whole foraminifera break into fragments, coarse fragments break into finer fragments, and fine fragments then become completely dissolved (Le and Shackleton, 1992). In this case the size index will underestimate the  $\text{CO}_3^{=}$  concentration of the waters bathing the sea floor.

de Villiers, (2005) suggests that in addition the respiratory dissolution flux in shallower sediments is not necessarily the pore waters but rather the benthic fluff layer. This layer can be centimeters thick in shallower sediments (Beaulieu, 2002). It has been reported that sedimentary organic carbon respiration is most rapid when a fluff layer is present (Martin and Sayles, 1999). The  $\text{CaCO}_3$  must pass through this layer before burial. The exposure time of foraminifera to under saturation in the fluff layer will be a function of sedimentation rate as well as the frequency of phytodetrital input (de Villiers., 2005). ii) As stated earlier, there is a striking resemblance of  $<63\mu\text{m}$  fraction  $\text{CaCO}_3$  with the total  $\text{CaCO}_3$  content (Fig. 22 b). Hence it can be interpreted as  $<63\mu\text{m}$  fraction controls the total  $\text{CaCO}_3$  content of sediment at this site. McCave *et al.*, (1995) using a more sophisticated method of sediment characterization has shown that the sediment ( $<10\mu\text{m}$ ) is dominantly coccoliths and the 10-63 $\mu\text{m}$  fraction contains mainly foraminiferal fragments. In the present scenario the size index expresses predominantly the ratio of whole adult foraminifera to coccoliths and foraminiferal fragments and juveniles, respectively. If one considers

that no breakup takes place after deposition, this index directly reflects the variations in calcareous nannofossils productivity.

*G. ruber* is a dissolution sensitive species and smaller size fractions of *G. ruber* are better preserved than the larger ones (de Villiers, 2005). *G. ruber* shell weights from the core ODP Site 715 show an anomalous trend throughout the core (Fig. 23). Such difference has been attributed to different morphological differences in *G. ruber* shells from the glacial and Holocene (Broecker *et al.*, 2003 and reference therein). Overall trend of shell weights show a resemblance to the size index and total CaCO<sub>3</sub> only during the last 10kyr. This actually means that as predicted by Broecker and Clark (2001a), the influence of coccoliths is seen throughout the glacial period which is a major drawback in applying the size index to glacial as a paleocarbonate ion proxy. Secondly, the shell weights of *G. ruber* are also not very robust in determining the glacial-interglacial carbonate ion content.

Broecker and Clark (1999) envisioned their size index to be a measure of the extent of fragmentation of foraminifera shells. However, in support of findings in the present study, a recent study conclusively shows similar results (Chiu and Broecker, 2008). Rather, the size index is a measure of the ratio of foraminifera CaCO<sub>3</sub> to coccoliths CaCO<sub>3</sub>. This ratio decreases with the extent of dissolution because foraminifera dissolve far more rapidly than coccolithophores.

### **4.3 Reconstruction of paleocarbonate ion in the northern Indian Ocean:**

Cores AAS9/21 and SK218/A from Arabian Sea and Bay of Bengal respectively recovered from two different oceanic regimes. Both show a gradient in CaCO<sub>3</sub> content from LGM to Holocene and then within the Holocene (Fig. 24 a and

b). Core AAS9/21 shows a smooth transition from high  $\text{CaCO}_3$  content from LGM to recent. Whereas, Core SK218/A shows a decrease in  $\text{CaCO}_3$  content from LGM to around 12kyr and then an increase. The  $\text{CaCO}_3$  values from Core SK218/A located in the Bay of Bengal are a result of terrigenous dilution. This core is fed by sediments from the Ganges-Bhramaputra river system. Terrigenous dilution also affects cores from the Arabian Sea through sediment supply from the Indus River. From the  $\text{CaCO}_3$  content it is evident that dilution must be effecting both the core locations to different levels.

It is hereby aimed to understand the  $\text{CO}_3^{=}$  concentration changes during the glacial-interglacial which in turn gives an idea of the extent of dissolution. The simplest method of understanding dissolution of carbonates is to determine the  $\text{CaCO}_3$  content of sediment. But the  $\text{CaCO}_3$  content as a function of water depth in today's ocean or at any specific time in the past is highly non-linear (Broecker, 2003). Therefore, it is sought to obtain aid from specific proxies targeting at dissolution effects.

In the present study, the paleocarbonate ion reconstruction task is taken up through the application of two important proxies, namely the size index and planktonic foraminifera shell weights. The size index in particular has been applied extensively and has some important drawbacks. Size index when applied to glacial age sediments, the core top calibration relationship did not apply (Broecker and Clark, 2001a). This was attributed to ratio of fine to coarse  $\text{CaCO}_3$  grains in initial material which was higher during glacial than during Holocene. Despite its drawback this method has led to some important findings. First is that during glacial times the mean depth of transition zone did not differ greatly from today's. This finding eliminates the hypothesis, which has been put forward to explain the lower glacial atmospheric



CO<sub>2</sub> content, namely the 'coral reef hypothesis' (Berger, 1982). According to this idea, shallow-water carbonates (corals and coralline algae) formed during high-sea stands of period of interglaciation would be eroded and subsequently dissolved during the low-sea stands of periods of glaciations, alternately reducing and increasing the seas CO<sub>3</sub><sup>=</sup> concentration. For this hypothesis to be viable the transition zone would have to have been displaced downwards by several kilometers during glacial times. It was suggested that this displacement was not more than a few hundred meters (Broecker and Clark, 2001). Two other findings stand out, first as shown by Farrell and Prell (1989), at water depths in 4km range in the eastern equatorial Pacific, the impact of dissolution was greater during interglacials than during glacial (i.e. the transition zone was deeper during glacial time). Secondly, it was demonstrated that there was better preservation during the glacial than in the interglacials (Imbrie, 1992). These findings gave rise to the conclusion that the difference between the depths of the transition zone in the Atlantic from that in the Pacific was somewhat smaller than now during glacial time. In addition, the existence of a pronounced dissolution event in the Atlantic Ocean at the onset of the last glacial cycle has also been documented (Curry and Lohmann, 1986).

Such major findings provide credibility to the size index proxy and hence it has been used further on the cores AAS9/21 and SK218/A. To comprehend these results, the planktonic foraminifera shell weights are also used. Both the proxies applied collectively ought to give a better picture of dissolution process in this region. This justifies the idea of having a multiproxy approach to the problem. As seen earlier from the application of three proxies to the coretop samples distributed throughout the tropical Indian Ocean, it was concluded that more than one proxy is required to elucidate the carbonate ion concentration history. Such an idea is also supported by

recent studies emphasizing the use of a multiproxy approach (Mekik and Raterink, 2008; Ni *et al.*, 2007).

For the application of size index proxy one important assumption need to be tested, that whether the initial size distribution of the carbonates remained constant with time. As a test of this assumption measurements have been made on a core, AAS9/21 collected from shallow water depths in the Arabian Sea, much above the lysocline. The planktonic foraminifera shell weights also need to be tested for similar reasons.

Size index values in AAS9/21 range from 10 to 40% which are marginally lower compared to the core SK218/A which range from 10 to 46% (Fig. 25a and b). Moreover, size index results show a change from the LGM to Holocene. These results imply that the initial size distribution of the  $\text{CaCO}_3$  deposited throughout the tropics is not uniform during the Holocene and LGM. The size index change in AAS9/21 which is clearly lying much above the lysocline could be due to a change in size distribution during glacial-interglacial or due to abundance of coccoliths as encountered in Site 715. Size index values from SK218/A show a decreasing trend possibly because of manifestation of dissolution due to change in saturation state of bottom water  $\text{CO}_3^{=}$  during the Holocene. The second important proxy namely, the foraminifera shell weights from AAS9/21 show an increase from 31 to 41  $\mu\text{g}$  and those from SK218/A range from 29 to 35  $\mu\text{g}$  (Fig. 26a and b). It has been shown in the present study that the initial shell weights depend on surface water carbonate ion in the tropics. This relation needs to be evaluated for the glacial-interglacial period.

#### **4.3.1 Role of temperature and/or carbonate ion in determining initial shell weights:**

High concentrations of carbon dioxide in the atmosphere cause surface seawater to become more acidic and lower the calcium carbonate saturation state through the consequent decrease in  $[\text{CO}_3^{=}]$  (Broecker and Peng, 1982). If marine calcification is sensitive to the concentration of atmospheric carbon dioxide, its effect should be reflected in the paleoceanographic record as a response to glacial-interglacial fluctuations in  $p\text{CO}_2$  (Barker and Elderfield, 2002).

Earlier it was pointed out that thickness and weight of foraminifera shells vary with growth conditions which is caused due to carbonate ion concentrations (Barker and Elderfield, 2002). The unanswered question is whether or not the dependence of shell weight on surface water carbonate ion concentration established for the temperate species apply to tropical species (Broecker, 2003). The present study demonstrates that this dependence does apply to the tropical species as well.

Broecker and Clark, (2002b), point out that in today's ocean a very tight correlation exists between surface water  $\text{CO}_3^{=}$  and temperature, and therefore coretop shell weights cannot be used to distinguish between a temperature or a  $\text{CO}_3^{=}$  dependence. Shell weights of several planktonic foraminiferal species from narrow size fractions from the North Atlantic were found to vary systematically as a function of latitude (Barker and Elderfield, 2002). They combined these findings with a record of shell weight across glacial-interglacial Termination-I to demonstrate that the changes are a result of ambient  $[\text{CO}_3^{=}]$  changes rather than calcification temperature and are consistent with known changes in atmospheric  $p\text{CO}_2$ . However  $\text{CO}_3^{=}$

concentration and temperature relationship are not constant from basin to basin (Broecker, 2003).

Atmospheric  $p\text{CO}_2$  at the LGM was  $\sim 90$ ppmv lower than preindustrial (Holocene) (surface  $[\text{CO}_3^{=}]$  was higher) and temperature was lower as well. Therefore temperature control would be indicated by lower shell weights before Termination I whereas a carbonate ion control would be indicated by higher shell weights (Barker and Elderfield, 2002).

It is important at present to see whether the dependence of shell weights on surface water  $\text{CO}_3^{=}$  concentrations applies for temporal samples or not. Results in the present study were combined with Mg/Ca thermometry, a proxy for paleotemperature. The Mg/Ca data was not available for all the sections where the shell weights have been determined. Only sections where this data was available have been plotted. There seems to be a linear relationship between *G. sacculifer* shell weights and Mg/Ca ratios, with higher shell weights corresponding to lower Mg/Ca ratios; indicative of lower temperatures ( $R^2=0.6$ ) (Fig. 31). Due to strong temperature dependence of  $\text{CO}_2$  solubility in seawater and the subsequent dissolution of  $\text{CO}_2(\text{aq})$  into  $\text{HCO}_3^-$  and  $\text{CO}_3^{=}$ , modern open ocean surface water  $[\text{CO}_3^{=}]$  varies as a function of temperature. Thus, the observed trend in shell weight would fit with a  $[\text{CO}_3^{=}]$  control as well as a temperature control. In the present study shell weights are highest during the LGM and show a large decrease in the early Holocene. Due to the fact that shell weights are heavier during glacial time suggests that the control on shell weight is carbonate ion and not calcification temperature. This places new constraints on the coral reef hypothesis and could possibly explain the survival of reef corals on Bermuda. Therefore, this study suggest that, glacial-interglacial changes in foraminifera shell

weight are related to changes in ambient carbonate ion concentration through time in response to changing atmospheric CO<sub>2</sub>.

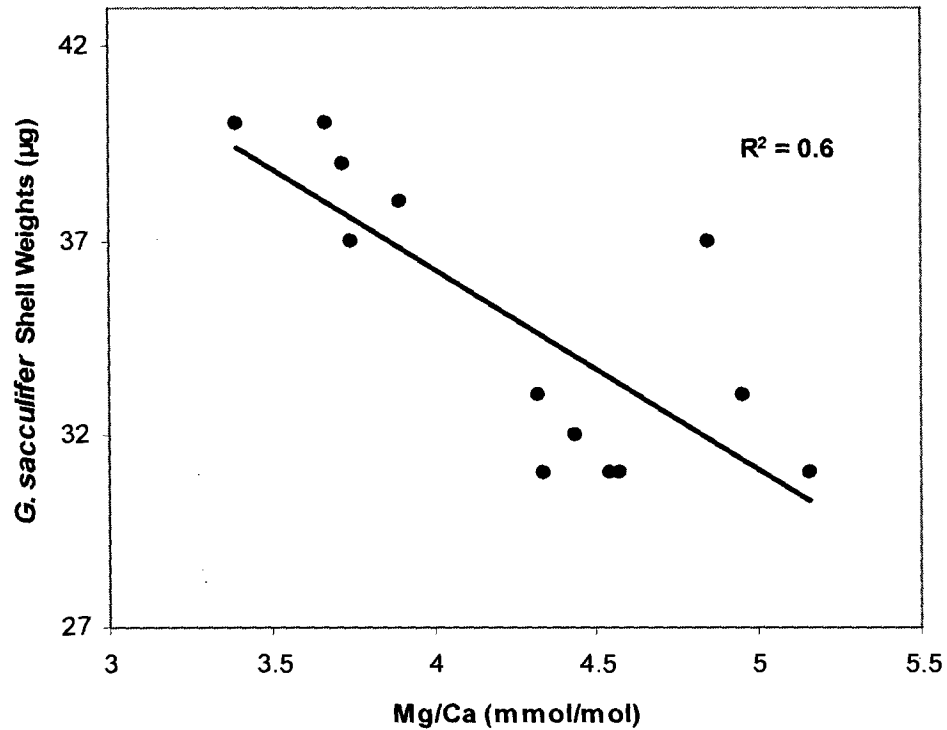


**Fig. 31.** *G. sacculifer* shell weights from both the cores AAS9/21 and SK218/A at selective sections show a linear relation to Mg/Ca ratio at corresponding depths ( $R^2=0.6$ ).

Attempts to reconstruct past CO<sub>3</sub><sup>=</sup> distributions suffer from the common drawback that much of the dissolution occurs in sediment pore waters rather than on the seafloor. This dissolution is driven by respiration CO<sub>2</sub> which lowers the pore-water CO<sub>3</sub><sup>=</sup> concentration below that in bottom water. It has already been shown using the shell weight technique that in today's waters of the western tropical Indian Ocean, there is no offset between bottom water and pore-waters. Therefore the statement that the dissolution occurring at the depths in the western tropical Indian Ocean is due to bottom water undersaturation can be confidently put forward. But, in order to convert shell weights to bottom-water carbonate ion concentrations there is one important postulate which need to be satisfied (Broecker *et al.*, 2003); whether the magnitude of

pore water dissolution was same or different during Holocene and glacial period. This is dealt with in subsequent discussions.

#### 4.3.2 Carbonate ion change from Last Glacial Maximum to Holocene:

Size index application to the cores AAS9/21 and SK218/A shows a change of 25% between LGM and Holocene. This amount when translated using the best fit line between size index and pressure-normalized carbonate ion concentration, as determined by Broecker and Clark, (1999), yields a value of  $16\mu\text{mol/kg}$  in terms of  $\text{CO}_3^{=}$  concentration which is an underestimation. Overall the size index values during the Holocene are quite low (10 to 25%) for these shallow depth cores as compared to the coretop studies discussed earlier (Broecker and Clark, 1999). This could be probably due to the terrigenous material affecting these cores. Since the size index gives an underestimation of the  $\text{CO}_3^{=}$  concentration it proves inefficient here in predicting the  $\text{CO}_3^{=}$  change, the second alternative, i.e. shell weight is used.

The core AAS9/21 lays much above the lysocline and therefore it is very interesting to notice the change in *G. sacculifer* shell weights from the LGM to present. Barker and Elderfield (2002) established the initial shell weight dependency on carbonate ion concentration in surface water for temperate planktonic foraminifera species. The application to tropical species was hitherto unknown before the present study. Since during the peak glacial time the atmospheres  $\text{pCO}_2$  was 90ppmv lower than until the pre-industrial era, the carbonate ion concentration in tropical surface waters must have been  $40\text{-}50\mu\text{mol/kg}$  higher at that time. Based on the Barker and Elderfield (2002) trend of  $\sim 1\mu\text{g}$  increase in shell weight per  $9\mu\text{mol/kg}$  increase in carbonate ion concentration, this translates to an  $8\mu\text{g}$  heavier initial shell weights during glacial times. While this correction does not change the depth dependence or

interocean concentration difference, it does greatly alter the magnitude of the change. The indistinctness of the shell weight variations in the glacial-interglacials need to be made explicable for getting a comprehensive design of the glacial-age deep-sea carbonate ion concentrations (Broecker, 2003).

To convert shell weights into  $\text{CO}_3^{=}$  this study has adopted a  $0.3\mu\text{g}$  drop in shell weight per  $\mu\text{mol/kg}$  drop in pressure-normalized  $\text{CO}_3^{=}$  concentrations (Broecker and Clark, 2001d). Carbonate ion concentrations were calculated from shell weights of both the cores AAS9/21 and SK218/A. The  $\text{CO}_3^{=}$  concentrations calculated from core AAS9/21 do not give an estimation of the bottom water concentrations but is a manifestation of  $\text{CO}_2$  dissolution in the surface seawaters and gives a carbonate ion change in surface waters during the glacial-interglacial.

During the Holocene the atmospheric partial pressure of  $\text{CO}_2$  ( $\text{pCO}_2$ ) is typically close to 280 parts per million by volume (p.p.m.v.). During peak glacial times, such as the LGM about 18kyr ago, atmospheric  $\text{pCO}_2$  is 180 to 200 ppmv or roughly 80 to 100 ppmv lower (Petit *et al.*, 1999). The core AAS9/21 exhibits a shell weight variation which when translated to glacial-interglacial carbonate ion concentration translates to a  $45\mu\text{mol/kg}$  change. In terms of shell weight this change is from  $41\mu\text{g}$  to  $31\mu\text{g}$  i.e. a change of  $10 \pm 2\mu\text{g}$  during the glacial-interglacial transition against the change of  $8\mu\text{g}$  suggested by Barker and Elderfield (2002) (Fig. 32). This glacial-interglacial carbonate ion concentration when overlaid on the  $\text{CO}_2$  record of an ice core from Taylor Dome, Antarctica (Smith *et al.*, 1999) shows that corresponding to a 90ppmv change in atmospheric  $\text{CO}_2$  a change of  $45\mu\text{mol/kg}$  in  $\text{CO}_3^{=}$  occurred (Fig. 32). The record from the present study is in excellent agreement with the ice core records and is suggestive of the extent of  $\text{CO}_2$  sequestration occurring in the Arabian Sea. The 180 to 280ppmv glacial-interglacial  $\text{CO}_2$  change

has occurred constantly for at least eight 100kyr cycles known at present (EPICA community members, 2004).

Several mechanisms have been put forth which elucidate the glacial-interglacial carbonate ion and hence CO<sub>2</sub> changes. Shackleton (1977) suggested mass of carbon stored in the terrestrial biomass was smaller during glacial than during the interglacial periods which was later confirmed by Curry *et al.*, (1988) based on benthic foraminifera <sup>13</sup>C records. Broecker (1982) suggested a glacial increase in the strength of the biological pump as the driver of lower glacial CO<sub>2</sub> levels. McElroy (1983) described possible mechanisms by which the reservoirs of phosphate and nitrate might increase during glacial times, which would allow enhanced low-latitude biological production to lower atmospheric CO<sub>2</sub>. Later several workers have suggested increased nutrient utilization in the high-latitude surface ocean to cause lower atmospheric pCO<sub>2</sub> of glacial times (Sarmiento and Toggweiler, 1984; Broecker and Peng, 1989; Martin, 1990). Toggweiler (1999) hypothesizes reduced deep-water ventilation of the glacial Southern Ocean to cause lowering of glacial atmospheric CO<sub>2</sub> whereas, that increased nutrient utilization and reduced deep-water ventilation of the glacial Southern Ocean caused lowering of glacial atmospheric CO<sub>2</sub> is demonstrated by Sigman and Boyle (2000).

Another possible mechanism was put forth by Archer and Maier-Reimer (1994) who explained the lower CO<sub>2</sub> content of the glacial atmosphere. An increase in the organic carbon/calcite ratio of material reaching the sediments was postulated for the last glacial (rain ratio). In a scenario with the effects of porewater chemistry on carbonate preservation, a higher relative rate of organic carbon rain decreases the porewater saturation with respect to calcite and would lead to a proportionally greater dissolution in the sediment driven by respiratory carbon dioxide (Emerson and



Bender, 1981; Berelson *et al.*, 1990; Archer, 1991; Jahnke *et al.*, 1997). This would lead to an increase of the carbonate ion in the bottom water and, through the mechanism of  $\text{CaCO}_3$  compensation would decrease the atmospheric carbon dioxide content. While Jahnke *et al.*, (1994) found no evidence for dissolution driven by metabolic carbon dioxide above the saturation horizon, Hales *et al.*, (1994) observed dissolution. Another proposed explanation for a higher carbonate ion concentration in the ocean, and hence, lower atmospheric  $\text{CO}_2$  content during glacials, is the “coral reef hypothesis” (Berger, 1982; Opdyke and Walker, 1992). According to this hypothesis, the coral growth rates were lower during glacials when the sea level had dropped and the continental shelves were exposed. This would imply a shift of  $\text{CaCO}_3$  deposition to the deep sea and therefore would have led to a deepening of the oceans saturation horizon and better carbonate preservation. However, this hypothesis calls for a global ocean increase in the saturation state (Opdyke and Walker, 1992; Archer and Maier-Reimer, 1994), and cannot be invoked to explain the observed preservation difference between the Atlantic and the Indo-Pacific, respectively.

The observed late Pleistocene preservation cycles are also consistent with estimated glacial–interglacial pH changes in the Atlantic and Pacific (Sanyal *et al.*, 1995) wherein the deep water of both oceans had a higher pH during the last glacial period. Accordingly, both the Atlantic and Pacific Oceans had a higher glacial deep-sea carbonate ion concentration. However, it is very likely that the boron isotope-based carbonate ion change will not be equivalent to the amount of change in preservation, as the boron-based paleo-pH estimates need to be coupled with dissolution driven by metabolic  $\text{CO}_2$  so as not to have an unrealistic change in lysocline depth of several kilometers. Better deep-sea carbonate preservation implies a high deep-sea carbonate-ion concentration, which in turn would lead to lowered

glacial atmospheric carbon dioxide content. Yet another recent mechanism is the ‘glacial burial hypothesis’ (Zeng, 2003) in which vegetation and soil carbon is buried and preserved under ice sheets during glaciations, and released back into the atmosphere during deglaciation.

#### 4.3.3 Carbonate ion change during the Holocene:

As stated in earlier discussions, the size index from both the cores does not give a good estimation of the in-situ carbonate ion concentration for the glacial-interglacial. This is probably due to the effect of terrigenous dilution at both the core sites. The situation for the Holocene seems to be even more complicated. Therefore the size index has been avoided in discussing the carbonate ion change.

In the Holocene period the change in carbonate ion calculated from the shell weight data from core AAS9/21 (change of  $2\mu\text{g}$ ) is  $9\mu\text{mol/kg}$  (Fig. 32). In terms of

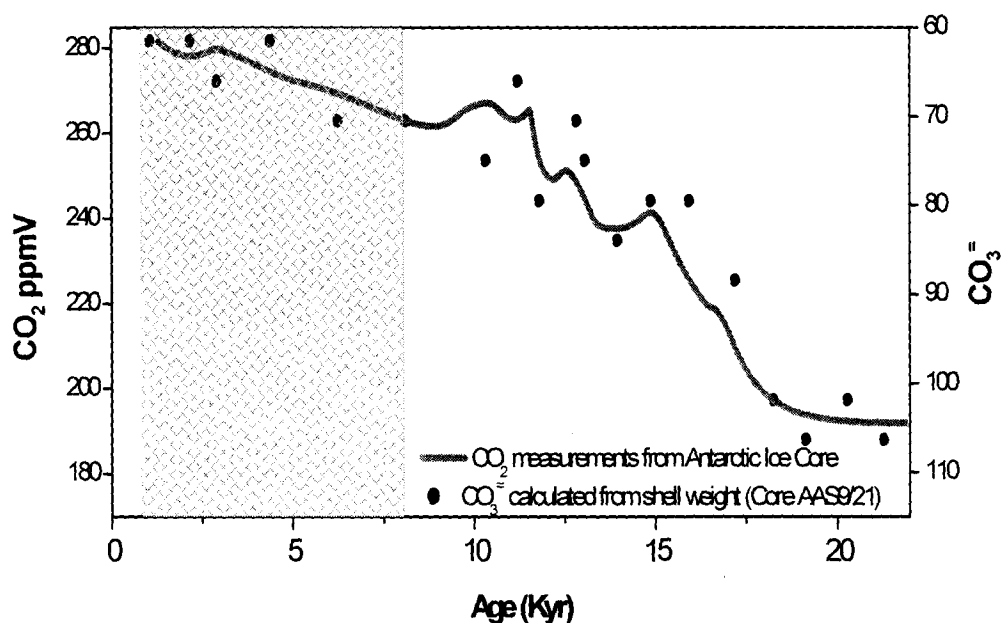


Fig. 32.  $\text{CO}_3^-$  concentrations calculated from *G. sacculifer* shell weights from the core AAS9/21 show a close relation to  $\text{CO}_2$  measurements from an ice core (Taylor Dome, Antarctica. \* see text) Shaded portion shows the Holocene period.

CO<sub>2</sub> rise this change is of 20ppmv (Indermülhe, 1999). Indermülhe (1999) presented a high-resolution record of CO<sub>2</sub> concentrations as measured in air bubbles trapped in an ice core from Taylor Dome, Antarctica, covering the entire Holocene. The record shows a decrease of the CO<sub>2</sub> concentration from 268 ppmv at 10.5 kyr BP (the end of the transition from the last glacial to the Holocene) to 260 ppmv at 8.2 kyr BP. During the recent 7kyr, the CO<sub>2</sub> concentration increased almost linearly to 285 ppmv (Indermülhe, 1999). The results from core AAS9/21 are in agreement with the changes discussed from ice cores as well as the results from Broecker and Clark, (2007), who suggest that this change during the Holocene is from 6 to 13 $\mu$ mol/kg.

In the Bay of Bengal core SK218/A, size fraction of 355 to 420 $\mu$ m, most of the *G. sacculifer* shells are broken for the last 10kyr. This signifies the corrosiveness of this region at 3307m depth during the Holocene period. This could also mean that the transition zone of carbonate ion is situated quite shallow compared to the rest of this region, which needs further studies before confirmation. Shell weights of *G. sacculifer* do not show a gradual decrease from the LGM to Holocene as expected. The situation seems to be that the organic matter respiration or pore water dissolution was pronounced in this region during the LGM with the effect increasing in magnitude during the Holocene period. In practice, since the planktonic foraminifera shells trace the surface water carbonate ion concentrations a correction of around 8 $\mu$ g would be required to be applied to the glacial shells. However, as in the present core SK218/A the shell weight trend seems to be indicating pore water dissolution. Since the extent of this pore water dissolution is not known hence correction is not applied here. Rather this pore water dissolution could be contributing to lighter shells during the glacials.

Broecker *et al.*, (1999) proposed that the rise in the atmosphere's CO<sub>2</sub> content during the last 8 kyr was driven by the compensation for the 500 gigatons of carbon withdrawn from the ocean-atmosphere system to regenerate the forest wood and soil humus destroyed during the last glacial period. Ridgwell *et al.*, (2003) reasoned this on the growth of coral reefs, whereas Ruddiman (2005) calls on deforestation conducted by humans. The results presented here suggest that the drop in abyssal ocean carbonate ion concentration over the past 8 kyr may have been larger than that required matching the 20 ppmv increase in atmospheric CO<sub>2</sub> content. If so, it would require that the carbonate ion decrease in the abyssal ocean was larger than that in the surface ocean. To generate such a difference would require either a change in the pattern of large-scale thermohaline circulation or a change in the power of the biologic pump, or both (Broecker and Stocker, 2006). Another possibility is that a shift in either circulation pattern or biological pumping has been taking place over the last 8 kyr. One possible explanation is that the production of deep water in the northern Atlantic has weakened relative to that in the Southern Ocean (Broecker and Clark, 2007)

Ruddiman, (2003) claims that the rise in atmospheric carbon dioxide (CO<sub>2</sub>) over the last 8000 years is anthropogenic rather than natural in origin. His case was based on the fact that following each of the three preceding glacial terminations; the CO<sub>2</sub> content of the atmosphere peaked early on and then underwent a steady decline. Without interaction with sedimentary CaCO<sub>3</sub>, Ruddiman's scenario requires a release of about 570 gigatons of terrestrial carbon (GtC). Model simulations that include interaction with sedimentary CaCO<sub>3</sub> increase this requirement to 700 GtC (Joos *et al.*, 2004). The release of 700 GtC from the terrestrial biosphere would lower the <sup>13</sup>C to <sup>12</sup>C ratio in the entire inventory of ocean-atmosphere carbon by about 0.45 per mil.

Indermühle *et al.*, (1999) interpreted carbon isotope measurements made on eight samples of CO<sub>2</sub> recovered from Antarctic ice to suggest a 0.2 per mil <sup>13</sup>C decline over the last 8000 years.

However, Broecker *et al.*, (2001b) challenged the validity of this <sup>13</sup>C decline. They pointed to a Holocene record of <sup>13</sup>C to <sup>12</sup>C ratio in planktonic foraminifera from the equatorial Pacific that showed no downward trend over the last 8000 years. Broecker *et al.*, (1993) proposed that the post-8000-year CO<sub>2</sub> rise was the result of CaCO<sub>3</sub> compensation triggered by the extraction of CO<sub>2</sub> from the ocean to create the early Holocene increase in forest biomass. With the onset of warm conditions, the forests and bogs destroyed during glacial time reformed. On the basis of the <sup>13</sup>C record kept by the benthic foraminifera, this re-growth sequestered about 500 GtC (Curry *et al.*, 1988). The removal of this amount of CO<sub>2</sub> from the ocean-atmosphere reservoir lowered the atmosphere's CO<sub>2</sub> content and increased the carbonate ion content of ocean water. Thus, the drop in atmospheric CO<sub>2</sub> caused by the re-growth of forests would have been followed by a recovery related to a readjustment of the ocean carbonate chemistry. As CaCO<sub>3</sub> has nearly the same carbon isotope composition as seawater, compensation would not produce any <sup>13</sup>C change. Such a rise in atmospheric CO<sub>2</sub> content as a result of calcium carbonate compensation was not seen during the last interglacials. The explanation likely lies in the current smaller eccentricity with associated decline in Northern Hemisphere summer insolation associated with the 20,000- year cycle (Broecker, 2006). The explanation for the absence of a CO<sub>2</sub> plunge during the present interglacial is that the 20,000-year cycle is too weak to initiate a rapid decline toward glacial conditions and thus to produce a 'short' interglacial period. Hence, while in three previous interglacials the CO<sub>2</sub> decrease driven by the 20,000-year precession cycle overwhelmed the upward trend

due to calcium carbonate compensation, during the present one this has not happened. A test of the orbital explanation was provided recently by the stage 11 CO<sub>2</sub> record from the Dome Concordia (Antarctica) (EPICA Community Members, 2004) with that from Vostok (Siegenthaler *et al.*, 2005). New CO<sub>2</sub> measurements on the EPICA ice core now cover all of stage 11. This spliced record shows that atmospheric CO<sub>2</sub> stayed above 270 ppm for about 28,000 years, from about 420 thousand years before present (kyr B.P.) to 392 kyr B.P. The early part of MIS 11 is similar to that for the Holocene. Hence, the cause for the CO<sub>2</sub> rise during the last 8000 years was 'natural' and not 'anthropogenic' (Broecker, 2006).

Though several mechanisms are now available which inform us regarding the mechanisms of glacial/interglacial CO<sub>2</sub> changes, much work remains to be done before an agreement can materialize on the specific driver. The results from the present study suggest that the carbonate ion change brought about by a change in atmospheric CO<sub>2</sub> in the northern Indian Ocean is at par with that of the rest of the world oceans in general. Yet, this study is not aimed at unraveling the exact mechanism to bring about the said change. More intense studies will be required in pinning down a specific driver of glacial/interglacial CO<sub>2</sub> change. The mystery of glacial/interglacial CO<sub>2</sub> change has certainly provided a focus for study of the interaction among the diverse processes operating in the natural environment, resulting in real progress toward a science of the Earth (Sigman and Boyle, 2000).

#### **4.4 The Indian Ocean CCD change:**

Various workers have attempted to estimate the depths of the lysocline and the CCD in the Indian Ocean. Present day CCD in the 10°N-0° region is estimated to be at 4500 m in the Bengal Fan region, at 4800 m in the Arabian Sea and in excess of

5100m in the Somali Basin and at the equatorial zone where it is the deepest (Kolla *et al.*, 1976). Cullen and Prell, (1984), based on variations in abundance of dissolution resistant foraminifera with water depth reveal that the foraminiferal lysocline (FL) to be at 3800m in the equatorial Indian Ocean, 3300m in the Arabian Sea and 2600 to 2000m in the Bay of Bengal. The Foraminiferal Compensation Depth, which is similar to the CCD is below 4600m in eastern equatorial region, below 5000m in western equatorial region and below 3307m in the Bay of Bengal (Cullen and Prell, 1984). Sabine *et al.*, (2002) suggest that the calcite saturation depths in the Indian Ocean range from 2900–3900 m with the deepest saturation depth in the central Indian Ocean. This is necessarily the lysocline and as shown in earlier discussions of the present study, intense dissolution has been encountered at a depth of 3900m water depth. Banakar *et al.*, (1998), place the lysocline at 4400m and the CCD at 4700m water depth at the equator in the central Indian Ocean.

In the present study  $\text{CO}_3^{=}$  concentration has been calculated for the glacial Indian Ocean using *G. sacculifer* shell weights from cores AAS9/21 and SK218/A. The LGM value has been determined averaging the shell weights from 18 to 20kyr for both the cores. At a depth of 1807m the glacial  $\text{CO}_3^{=}$  calculated from *G. sacculifer* shell weights is  $103\mu\text{mol/kg}$ . The present  $\text{CO}_3^{=}$  at the water depth of 1807m calculated from GEOSECS station 417 is  $70\mu\text{mol/kg}$ . This means there is a large difference of  $\sim 33\mu\text{mol/kg}$  between present and glacial  $\text{CO}_3^{=}$  concentrations (Fig. 33). As stated earlier, shell weights from core AAS9/21 are a manifestation of  $\text{CO}_2$  dissolution in the surface seawaters and give a carbonate ion change in surface waters during the glacial in the present case. Since the core is from a very shallow depth, there are no noticeable effects of dissolution. Therefore the carbonate ion concentrations calculated from shell weights do not give the actual picture of bottom water  $\text{CO}_3^{=}$

concentrations at this depth. If the shell weight correction of  $8\mu\text{g}$  as stated earlier be applied to the shell weights from core AAS9/21 and based on the Barker and Elderfield (2002) trend of  $\sim 1\mu\text{g}$  increase in shell weight per  $9\mu\text{mol/kg}$  increase in  $\text{CO}_3^{=}$  concentration and taking into consideration the uncertainty in shell weight measurements of  $\pm 2\mu\text{g}$ , the  $\text{CO}_3^{=}$  concentration during the glacial will work out to be equivalent to the present. Such a lack of difference in the  $\text{CO}_3^{=}$  concentrations during the glacial and today has been observed for the Pacific Ocean also, at depth of 2.3km (Broecker and Clark, 2001c).

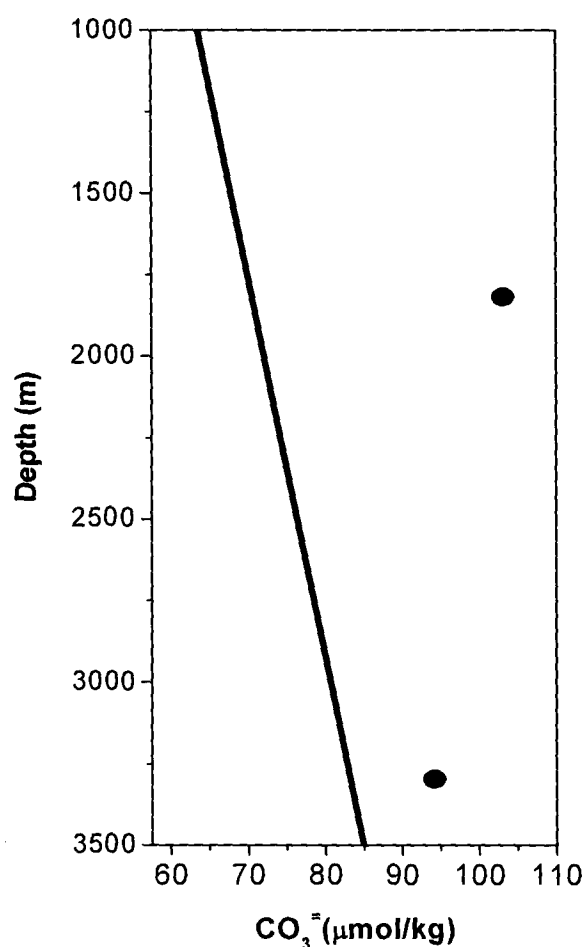


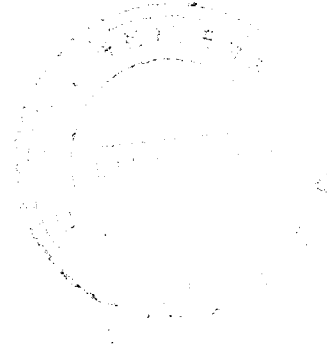
**Fig. 33.**  $\text{CO}_3^{=}$  versus water depth (m) for today's Indian Ocean (shown by smooth line). The black dots are the glacial  $\text{CO}_3^{=}$  concentrations calculated from *G. sacculifer* shell weights from the cores AAS9/21 and SK218/A.



Using the extent of calcium carbonate dissolution observed in foraminifer faunal assemblages from the CLIMAP data set, a decrease in carbonate ion concentration was observed in glacial Atlantic Ocean, by roughly 20  $\mu\text{mol/kg}$ , while a little change of 5  $\mu\text{mol/kg}$  occurred in the Indian and Pacific relative to today (Anderson and Archer, 2002). Today's in-situ carbonate ion concentration at the depth of 3307m is  $\sim 83 \mu\text{mol/kg}$  as calculated from GEOSECS stations (Fig. 9). At 3307m water depth, the LGM calculated  $\text{CO}_3^{=}$  is 93  $\mu\text{mol/kg}$ . So a difference of 10  $\mu\text{mol/kg}$  is observed from LGM to present. Therefore it is seen that the  $\text{CO}_3^{=}$  gradient was steeper during the glacial, increasing from almost no difference between glacial and today at 1807m to 10  $\mu\text{mol/kg}$  at 3307m and should be even more at greater water depths. Broecker and Clark, (2001c) also point out to increasing gradients in  $\text{CO}_3^{=}$  concentrations with water depth during glacials. Considering the change in  $\text{CO}_3^{=}$  of 15  $\mu\text{mol/kg}$  per km increase in water depth (Broecker, 2008), the difference of 10  $\mu\text{mol/kg}$  in the present case for the Indian Ocean implies at least a  $\sim 600\text{m}$  difference in the saturation horizon. From the fact that the *G. sacculifer* shells are absent and/or broken during the Holocene at a depth of 3307m (Core SK218/A) it is evident that the present day CCD is very shallow and lies at  $\sim 3300\text{m}$  or shallower in the Bay of Bengal. This estimation is also supported by the study of Cullen and Prell (1984). The difference of  $\sim 600\text{m}$  stated above would mean that during glacial the CCD was at around 3900m water depth.

Since the pore water dissolution during the glacial is unknown the exact variation in the CCD from glacial to present cannot be exactly estimated. Also, this result is fraught with potential biases as it is averaged from shell weights from a single core i.e., SK218/A. Broecker, (2008), propose that the CCD must have been 0.4 km deeper in the tropical Indian Ocean during glacial. The results in the present study,

stating a difference of ~600m (0.6km) are somewhat in agreement with this. More significantly the  $\text{CO}_3^{=}$  gradient observed during the LGM is greater relative to present. Such large gradients in  $\text{CO}_3^{=}$  concentration in the glacial ocean have important implications because such gradients are absent in today's ocean (Broecker et al., 2001c). The implications of such a gradient are that the waters supplying the deep sea had a greater range in density, thereby permitting stratification to persist.



## CHAPTER V

### SUMMARY AND CONCLUSIONS

To understand the fate of Carbon dioxide in the northern Indian Ocean for the Last Quaternary period, two entities were assessed; the calcium carbonate content and the paleocarbonate ion content from ocean sediments. The  $\text{CaCO}_3$  content data from ten deep-sea cores congregated from the equatorial region of the Atlantic, Pacific and Indian Ocean covering a time span of 0.6Ma was reviewed. As observed by a large number of studies, the  $\text{CaCO}_3$  content fluctuates in a cyclic pattern through the glacial-interglacial. Largely, there are two typical patterns observed; the 'Atlantic pattern', exhibiting better preservation during the interglacials and poor preservation during glacials and the 'Pacific pattern' which exhibits poor preservation during interglacial and better preservation during the glacials. There are studies exemplifying either/both types of patterns for the Indian Ocean. The Indian Ocean carbonate fluctuations are not conclusive as to which pattern they exhibit, due to few studies. The overall patterns observed over the equatorial regions of the world oceans are attributed to changing bottom water circulation and hence changing saturation state with respect  $\text{CO}_3^{=}$  concentration. Therefore, the bottom water  $\text{CO}_3^{=}$  concentration is considered to be the most important factor in understanding the glacial-interglacial ocean operation.

To understand the  $\text{CO}_2$  variations in the past it is necessary to know how the  $\text{CO}_3^{=}$  concentration varied in response to the atmospheric  $\text{CO}_2$  change. Studies with respect to paleocarbonate ion reconstruction have been extensively carried out in the Atlantic and Pacific oceans. Major thrust has been laid on using many of the available

paleocarbonate ion proxies. In this study three paleocarbonate ion proxies have been applied; 1) size index 2) planktonic foraminifera shell weights and 3) calcite crystallinity. These proxies have been applied several times in the Atlantic and Pacific oceans and therefore the shortcomings and existing gaps in knowledge are well known. In this context a few studies were carried out from the Indian Ocean to understand the paleocarbonate ion variations. In this study, before the application of any of these proxies, their validation and suitability of application to the northern Indian Ocean is evaluated. For doing this, several core top samples have been employed providing a good spatial coverage. In this endeavor the shortcomings of these major proxies have come forth. Only after clearing the major drawbacks the proxies have been applied to the northern Indian Ocean in order to understand the glacial-interglacial carbonate ion fluctuations.

This study provides a systematic basis to resolve some important aspects of the calcium carbonate fluctuations during the Late Quaternary Period. The prominent findings of this study are summarized as under:

- 1) Previous studies suggest that the  $\text{CaCO}_3$  content in the ocean sediments fluctuated systematically in the Atlantic, Pacific and the Indian Oceans. Though these variations are influenced by three factors namely, productivity, dilution and dissolution. Out of these three factors, dissolution plays an important role in the deep seas, primarily due to bottom water  $\text{CO}_3^{=}$  undersaturation. This claim is made based on the linear relation between coretops of the ten sediments cores from the Atlantic, Pacific and Indian Oceans and the carbonate ion concentration of the water bathing these coretops. The  $\text{CO}_3^{=}$  concentration of bottom-waters in the major world

oceans have changed depending on the bottom-water circulation which created two distinct carbonate fluctuation patterns. These are typically christened the 'Atlantic pattern' and the 'Pacific pattern'. It is believed here that the Indian Ocean displays a Pacific type of pattern due to the similar kind of bottom-water circulation prevailing in both these oceans. This highlights the importance of  $\text{CO}_3^{=}$  alone in shaping the carbonate fluctuations.

- 2) To determine the carbonate ion concentrations in the past it is necessary to use certain proxies which could give a fair calculation of this entity. Three paleocarbonate ion proxies, size index, planktonic foraminifera shell weight, and calcite crystallinity, have been employed in this study. These proxies are primarily validated. In support of this the proxies have been applied to a set of core top samples from the western tropical Indian Ocean in the water depth ranges from 1086 to 4730m. All three proxies show a linear relation to one another and hence complement each other well. The significant finding here from the application of these proxies is that calcite dissolution starts to affect planktonic foraminifera from 2250 m depth onward and intense calcite dissolution begins around 3900 m depth in this sector of the tropical Indian Ocean.

To substantiate the effect of dissolution on foraminifera shells, SEM micrographs of *Globigerinoides sacculifer* from a water depth of 2250 and 3944m were compared. Apparently, shells from deeper depth show dissolution features whereas shallow depth shells show well-preserved tests. A perplexing result is that the three planktonic foraminifera species,

*Globigerinoides sacculifer*, *Pulleniatina obliquiloculata*, and *Neogloboquadrina dutertrei*, show wide variability in shell weights from core top sediments in the depth range of 3300 to 3400 m bathed by similar bottom water  $\text{CO}_3^{=}$  concentrations. This anonymity is determined and attributed to shell calcification in surface waters which have different  $\text{CO}_3^{=}$  concentrations. This study makes it apparent for the first time that initial shell weights in the tropics depend on the surface water  $\text{CO}_3^{=}$  concentrations as seen for the temperate species, shown in other studies. Further, surface water  $\text{CO}_3^{=}$  concentrations override milder dissolution effects experienced by samples from shallower water depths bathed by similar bottom water  $\text{CO}_3^{=}$  concentrations. An important conclusion of this study is that the calcite dissolution effects are best resolved using a multiproxy approach, such that there is no indistinctness in the results.

- 3) To be certain whether the application of the proxies yields a correct estimation of the bottom water  $\text{CO}_3^{=}$  concentration, it is important to understand the possible dissolution mechanisms. Two processes drive dissolution of calcite after it reaches the seafloor. First is the degree of saturation state of  $\text{CO}_3^{=}$  concentration of the overlying bottom waters and the second, due to sedimentary organic matter respiration and resulting acidification of pore waters. Therefore it is necessary to examine whether the intense dissolution occurring at 3900m in the Indian Ocean is a result of undersaturation of overlying bottom waters with respect to  $\text{CO}_3^{=}$  concentration. In actual conditions, the core top foraminifera are initially exposed to the benthic fluff layer at the sediment-water interface. Therefore,

this interface is perhaps a better description of the initial exposure environment in foraminifera from core tops. To understand whether dissolution taking place at 3900m water depth is due to this corrosive benthic fluff layer the  $\Delta\text{CO}_3^{=}$  interface -  $\Delta\text{CO}_3^{=}$  bottom water gradient was calculated and found to be + 4.2 $\mu\text{M}$  which is within  $\pm 10\mu\text{M}$  of bottom water, the value derived by de Villiers(2005). This suggest that there is no significant gradient in  $\Delta\text{CO}_3^{=}$  across the sediment-bottom water interface at a depth of 3900m. Therefore, it is concluded that the intense dissolution along this transect in the western Tropical Indian Ocean is due to bottom water  $\text{CO}_3^{=}$  undersaturation. This finding provides a boost to the application of the shell weight proxy for the northern Indian Ocean.

- 4) The suitability of two proxies, size index and planktonic foraminifera shell weights was verified with respect to understanding the temporal variations in  $\text{CO}_3^{=}$  concentrations. For this purpose, size index proxy was applied to two ODP Sites 715 and 752 which were drilled above the regional lysocline depth in the Indian Ocean. The size index as measured in Site 752 and Site 715 showed significant variations, though both the sites are from shallow depths. High values of size index at ODP Site 752 and its distal location from any landmass suggest that the observed variations are due to changes in productivity of the overlying waters. Low values of size index at ODP Site 715 suggest significant dissolution has occurred throughout the core. The reasonably synchronized mismatch between size index and  $\text{CaCO}_3$  occurring at ODP Site 715 is a unique result. Such an outcome is not noticed at ODP Site 752. The size index alone is not adequate to reason out the

observed mismatch. Therefore, the  $\text{CaCO}_3$  content from the  $<63\mu\text{m}$  fraction was studied. The  $\text{CaCO}_3$  content from the  $<63\mu\text{m}$  fraction from ODP Site 715 shows a match with the total  $\text{CaCO}_3$  content. From the  $<63\mu\text{m}$  variations it is evident that the finer fraction which is composed of juvenile forams, foraminiferal fragments and coccoliths dominates the carbonate content and holds the key to the observed variations. It is concluded here that the size index may not give a correct estimation of the carbonate ion content of bottom waters in regions dominated by coccolithophores, as encountered in the present study. *G. ruber* shells from the ODP Site 715 show an anomalous trend throughout the core which has been attributed to different morphological changes in *G. ruber* during glacial and interglacial. This study signifies that the influence of coccoliths is seen throughout the glacial period which is a major drawback in applying the size index to the glacial as a paleocarbonate ion proxy, as also confirmed by some previous studies.

- 5) Two cores are AAS9/21 from the Arabian Sea and SK218/A from the Bay of Bengal are employed to reconstruct the history of carbonate ion in these two basins for the past 25kyr. The  $\text{CaCO}_3$  content variations from both the cores do not provide a clear picture of the fluctuations occurring during the past 25 kyr. The possible reason is the large amount of terrigenous dilution due to influx of major rivers in both these regions. In the present circumstances two important proxies are used to understand temporal variations in  $\text{CO}_3^{=}$  concentrations; the size index and *G. sacculifer* shell weights. Size index application for both the cores gives an underestimation



of  $\text{CO}_3^{=}$  concentration and are not consistent with the  $\text{CaCO}_3$  content changes. Size index values in AAS9/21 which lies at shallow depth are lower as compared to the size index values in Core SK218/A. Moreover, size index results for Core AAS9/21 which lie much above the lysocline, show an increasing trend from recent to the Last Glacial Period. These results imply that the initial size distribution of the  $\text{CaCO}_3$  deposited throughout the tropics is not uniform during present and glacial time. But, in general the high values of  $\text{CaCO}_3$  and size index during the Last Glacial Period and lower during the Holocene reveals a Pacific type of pattern for the northern Indian Ocean.

The second proxy, planktonic foraminifera shell weights, was applied to both the cores. Shell weights from both the cores were combined with Mg/Ca thermometry, a proxy for paleotemperature. There seems to be an inverse linear close fit relation between *G. sacculifer* shell weights and Mg/Ca ratios, with higher shell weights corresponding to lower Mg/Ca ratios; indicative of lower temperatures ( $R^2=0.6$ ). Shell weights are seen to be highest during the LGM and show a large decrease into the early Holocene. Due to the fact that shell weights are heavier during glacial time and the inverse relationship between temperature (Mg/Ca) and shell weights, suggests that the control on shell weight is carbonate ion and not calcification temperature. Such a change in shell weights during the glacial-interglacial based on the surface water  $\text{CO}_3^{=}$  changes is a novel result for the tropics. This places new constraints on the coral reef hypothesis and could possibly explain the survival of reef corals on Bermuda.

- 6) The carbonate ion concentration calculated from shell weights from the Core AAS9/21 shows a good match with CO<sub>2</sub> measured from Antarctic ice cores for the last 25kyr. The glacial-interglacial change in CO<sub>2</sub> of 100ppmv registers a 45μmol/kg change in CO<sub>3</sub><sup>=</sup> concentration as calculated from *G. sacculifer* shell weight change of 10 ± 2μg. Again, through the Holocene a shell weight change of 2μg is noticed. This 2μg change in shell weights during the course of the Holocene calculates to a CO<sub>3</sub><sup>=</sup> concentration of 9μmol/kg and in agreement with previous work. In terms of CO<sub>2</sub> rise this change is of 20ppmv as measured from air bubbles trapped in an ice core from Taylor Dome, Antarctica, covering the entire Holocene. This indicates the amount of CO<sub>2</sub> sequestered by the Arabian Sea during the 25kyr period.

The absence of well preserved *G. sacculifer* shells in core SK218/A for the Holocene period suggests dissolution at 3307m depth in the Bay of Bengal. The minor dissolution observed at SK218/A site is attributed to pore water dissolution in this region during the glacial with the dissolution effect increasing during the Holocene period. In practice, since the planktonic foraminifera shells trace the surface water carbonate ion concentrations a correction of around 8μg need to be applied to the glacial shells (Broecker, 2003). Since there was an effect of pore water dissolution on the foraminifera shells this probably compensates for the surface water carbonate ion effect. Therefore this correction has not been applied at 3307m water depth. The CO<sub>3</sub><sup>=</sup> concentration has been calculated for the glacial Indian Ocean using *G. sacculifer* shell weights from cores AAS9/21 and SK218/A. It is seen that the CO<sub>3</sub><sup>=</sup> gradient was steeper during the glacial. This gradient between glacial and today is 10μmol/kg at 3307m,

whereas no such gradient exist in the water depth of 1807m. This difference of  $10\mu\text{mol/kg}$  in the present case for the Indian Ocean implies at least a  $\sim 600\text{m}$  difference in the CCD which must have been at around 3900m during the glacial. The results presented here are in agreement with other studies which suggest that the  $\text{CO}_3^{=}$  gradient was steeper during the glacial. The implications of such gradients are that the waters supplying the deep sea had a greater range in density, thereby permitting stratification to persist.

## References:

- Adelseck, C.G., and T.F. Anderson (1978), The late Pleistocene record of productivity fluctuations in the eastern equatorial Pacific Ocean, *Geology*, 6, 388-391.
- Adler, M., C. Hensen, F. Wenzhofer, K. Pfeifer, and H. D. Schulz (2001), Modelling of calcite dissolution by oxic respiration in supralysoclineal deep-sea sediments, *Marine Geology*, 177, 167-189.
- Anderson, D. M., and D. Archer (2002), Glacial-interglacial stability of ocean pH inferred from foraminifer dissolution rates, *Nature*, 416, 70-73.
- Archer, D.E. (1991), Equatorial Pacific calcite preservation cycles: production or dissolution? *Paleoceanography*, 6, 561-571.
- Archer, D., and E. Maier-Reimer (1994), Effect of deep-sea sedimentary calcite preservation on atmospheric CO<sub>2</sub> concentration, *Nature*, 367, 260-263.
- Arrhenius, G. (1952), Sediment cores from the East Pacific. In: H. Petterson (Ed.), *Reports of the Swedish Deep Sea Expedition*, 5, 1947-1948, 201 pp.
- Arrhenius, G. (1988), Rate of production, dissolution and accumulation of biogenic solids in the ocean, *Palaeogeography Palaeoclimatology Palaeoecology*, 67, 119-146.
- Banakar, V K, G. Parthiban, J. N. Pattan and P. Jauhari (1998), Chemistry of surface sediment along a north–south transect across the equator in the Central Indian Basin: an assessment of biogenic and detrital influences on elemental burial on the seafloor; *Chemical Geology*, 147, 217–232.
- Barker, S., and H. Elderfield (2002), Foraminiferal calcification response to glacial-interglacial changes in atmospheric CO<sub>2</sub>, *Science*, 297, 833–836.

- Barker, S., M. Greaves and H. Elderfield (2003), A study of cleaning procedures used for foraminiferal Mg/Ca paleothermometry, *Geochemistry Geophysics Geosystems*, 4(9), 8407, doi:10.1029/2003GC000559.
- Barnola, J.-M., D. Raynaud, Y.S. Korotkevich, and C. Lorius (1987), Vostok ice core provides 160,000-year record of atmospheric CO<sub>2</sub>, *Nature*, 329:408-14.
- Barthelemy-Bonneau, M. -C. (1978), Dissolution expérimentale et naturelle de foraminifères planctoniques—Approches morphologique, isotopique et cristallographique, Ph.D. thesis, 231 pp., Univ. Pierre et Marie Curie, Paris.
- Bassinot, F.C., L. Beaufort, E. Vincent, D. Labeyrie, F. Rostek, P. J. Muller, X. Quidelleur, and Y. Lancelat (1994), Coarse fraction in pelagic carbonate sediments from the tropical Indian Ocean: a 150 ka record of carbonate dissolution, *Paleoceanography*, 9, 579-600.
- Bassinot, F.C., F. Mélières, M. Gehlen, C. Levi, and L. Labeyrie (2004), Crystallinity of foraminifera shells: A proxy to reconstruct past bottom water CO<sub>3</sub><sup>=</sup> changes?, *Geochemistry Geophysics Geosystems*, 5(8), 10.1029/2003GC000668.
- Bé, A.W.H. (1967), Foraminifera families: Globigerinidae and Globorotalliidae, Fiche no.108, In: J.H.Frasier (Ed.). Fiches d'identification du zooplancton, Charlottenlund, Denmark: Conseil International pour l'Exploration de la Mer.
- Beaulieu, S.E. (2002), Accumulation and fate of phytodetritus on the seafloor. *Oceanography and Marine Biology: an Annual Review*, 40, 171-232.
- Berelson, W. M., D. E. Hammond, G.A. Cutter (1990), In situ measurements of calcium carbonate dissolution rates in deep-sea sediments, *Geochimica et Cosmochimica Acta*, 54, 3013-3020.

- Berger, W.H. (1973), Deep-sea carbonates: Pleistocene dissolution cycles, *Journal of Foraminiferal Research*, 3(4): 187-195.
- Berger, W.H. (1977), Deep-sea carbonate and the deglaciation preservation spike in pteropods and Foraminifera, *Nature*, 269, 301-304.
- Berger, W.H. (1978), Sedimentation of deep-sea carbonate: maps and models of variations and fluctuations, *Journal of Foraminiferal Research*, 8 (4) 286-302.
- Berger, W.H. (1982), Increase of carbon dioxide in the atmosphere during deglaciation: the coral reef hypothesis, *Naturwissenschaften*, 69, 87-88.
- Berger, W.H. (1992), Pacific carbonate cycles revisited: arguments for and against productivity control. In: K. Ishizak, T. Saito, (Eds), *Centenary of Japanese Micropaleontology*, Terra Scientific Publishing, Tokyo, 15-25.
- Berner, R.A. and K. Caldeira (1997), The need for mass balance and feedback in the geochemical carbon cycle, *Geology*, 25, 955– 956.
- Boyle, E.A., and L.D.Keigwin (1982), Deep circulation of the North Atlantic over the last 200,000 years: geochemical evidence, *Science*, 218, 784-786.
- Broecker, W.S., and T.Takahashi (1978), The relationship between lysocline depth and in situ carbonate ion concentration, *Deep-Sea Research I*, 25: 65-95.
- Broecker, W. S. (1982), Ocean chemistry during glacial time, *Geochimica et Cosmochimica Acta*, 46, 1689-1706.
- Broecker, W.S., and T.H. Peng (1982), *Tracers in the Sea*, Eldigio, New York, 690pp.
- Broecker, W.S. and T.-H. Peng (1989), The cause of the glacial to interglacial atmospheric CO<sub>2</sub> change: A polar alkalinity hypothesis, *Global Biogeochemical Cycles*, 3, 215-239.

- Broecker, W. S., G. Bonani, C. Chen, E. Clark, S. Ivy, M. Klas, and T.-H. Peng (1993), A search for an Early Holocene CaCO<sub>3</sub> preservation event, *Paleoceanography*, 8, 333–339.
- Broecker, W.S., and E. Clark (1999), CaCO<sub>3</sub> size distribution: A paleocarbonate ion proxy, *Paleoceanography*, 14, 596-604.
- Broecker, W. S., E. Clark, D. C. McCorkle, T.-H. Peng, I. Hajdas, and G. Bonani (1999), Evidence for a reduction in the carbonate ion content of the deep sea during the course of the Holocene, *Paleoceanography*, 14, 744–752.
- Broecker, W. S., and S. Sutherland (2000), Distribution of carbonate ion in the deep ocean: Support for a post-Little Ice Age change in Southern Ocean ventilation?, *Geochemistry Geophysics Geosystems*, 1 (7), doi:10.1029/2000GC000039.
- Broecker, W. S., and E. Clark (2001a), Reevaluation of the CaCO<sub>3</sub> size index paleocarbonate ion proxy, *Paleoceanography*, 16(6), 669–671.
- Broecker, W. S., and E. Clark (2001b), A dramatic Atlantic dissolution event at the onset of the last glaciation, *Geochemistry Geophysics Geosystems*, 2, 11, 2001GC000185.
- Broecker, W. S., and E. Clark (2001c), Glacial-to-Holocene redistribution of carbonate ion in the deep sea, *Science*, 294, 2152–2155.
- Broecker, W. S., and E. Clark (2001d), An evaluation of Lohmann's foraminifera weight dissolution index, *Paleoceanography*, 16(5), 531–534.
- Broecker, W. S., R. Anderson, E. Clark and M. Fleisher (2001a), Records of seafloor CaCO<sub>3</sub> dissolution in the central equatorial Pacific, *Geochemistry Geophysics Geosystems*, 2(6), 2000GC000151.

- Broecker, W. S., J. Lynch-Stieglitz, E. Clark, I. Hajdas, and G. Bonani (2001b), What caused the atmosphere's CO<sub>2</sub> content to rise during the last 8000 years?, *Geochemistry Geophysics Geosystems*, 2(10), doi:10.1029/2001GC000177.
- Broecker, W. S., and E. Clark (2002a), A major dissolution event at the close of MIS 5e in the western equatorial Atlantic, *Geochemistry Geophysics Geosystems*, 3(2), doi: 10.1029/2001GC000210.
- Broecker, W. S., and E. Clark (2002b), Carbonate ion concentration in glacial-age deep waters of the Caribbean Sea, *Geochemistry Geophysics Geosystems*, 3(3), 1021, doi:10.1029/ 2001GC000231.
- Broecker, W. S., and E. Clark (2003a), CaCO<sub>3</sub> dissolution in the deep sea: Paced by insolation cycles, *Geochemistry Geophysics Geosystems*, 4(7), 1059, doi:10.1029/2002GC000450.
- Broecker, W. S., and E. Clark (2003b), Holocene atmospheric CO<sub>2</sub> increase as viewed from the seafloor, *Global Biogeochemical Cycles*, 17(2), 1052, doi: 10.1029/2002GB001985.
- Broecker, W. S., and E. Clark (2003c), Glacial-age deep sea carbonate ion concentrations, *Geochemistry Geophysics Geosystems*, 4(6), 1047, doi: 10.1029/2003GC000506.
- Broecker, W. S., and E. Clark (2003d), Pseudo dissolution of marine calcite, *Earth Planetary Science Letters*, 208(3–4), 291–296.
- Broecker, W. S., E. Clark, and A. W. Droxler (2003), Shell weights from intermediate depths in the Caribbean Sea, *Geochemistry Geophysics Geosystems*, 4(7), 1060, doi: 10.1029/2002GC000491.
- Broecker, W.S. (2003), The oceanic CaCO<sub>3</sub> cycle, in: H.D. Holland, K.K. Turekian (Eds.), *Treatise on Geochemistry*, Elsevier, 529–549.



- Broecker, W.S. (2006), Abrupt climate change revisited, *Global and Planetary Change*, 54, 211–215.
- Broecker, W. S., and T. Stocker (2006), The Holocene CO<sub>2</sub> rise: Anthropogenic or natural?, *Eos Transaction, AGU*, 87(3), 27.
- Broecker, W. S., and E. Clark (2007), Is the magnitude of the carbonate ion decrease in the abyssal ocean over the last 8 kyr consistent with the 20 ppm rise in atmospheric CO<sub>2</sub> content?, *Paleoceanography*, 22, PA1202, doi:10.1029/2006PA001311.
- Broecker, W. S. (2008), A need to improve reconstructions of the fluctuations in the calcite compensation depth over the course of the Cenozoic, *Paleoceanography*, 23, PA1204, doi:10.1029/2007PA001456.
- Bruce, J.G.(1974), Some details of upwelling off Somalia and Arabian coasts, *Journal of Marine Research*,32:419-423.
- Cai, W.-J., C. E. Reimers, T. Shaw, (1995), Microelectrode studies of organic carbon degradation and calcite dissolution at a California Continental rise site, *Geochimica Cosmochimica Acta*, 59, 497-511.
- Chiu, T-C. and W. S. Broecker, (2008), Towards better paleo-carbonate ion reconstructions –New insights regarding the CaCO<sub>3</sub> size index, (in Press, *Paleoceanography*).
- Crowley, T. J. (1983), Calcium-carbonate preservation patterns in the central North Atlantic during the last 150,000 years, *Marine Geology*, 51, 1–14.
- Cullen, J.L. and W.L. Prell (1984), Planktonic foraminifera of the northern Indian Ocean: distribution and preservation in surface sediments, *Marine Micropaleontology*, 9, 1–52.

- Curry, W. B., and G. P.Lohman, (1983), Reduced advection into Atlantic Ocean deep eastern basins during last glaciation maximum, *Nature*, 306, 577-580
- Curry, W.B. and G.P.Lohman (1986), Late Quaternary carbonate sedimentation at the Sierra Leone Rise (eastern equatorial Atlantic Ocean) *Marine Geology*, 70: 223-250.
- Curry, W. B., J. C.Duplessy, L. D. Labeyrie, and N. J.Shackleton (1988), Changes in the distribution of d13C of deep water TCO<sub>2</sub> between the last glaciation and the Holocene, *Paleoceanography*, 3, 317-341.
- Damuth, J.E. (1973), *The Western Equatorial Atlantic: Morphology, Quaternary Sediments, and Climatic Cycles: Ph.D. Dissertation, Columbia University, 602 p.*
- Damuth, J.E. (1975), Quaternary climate change as revealed by calcium carbonate fluctuations in Western Equatorial Atlantic sediments, *Deep-Sea Research*, 22: 725-743.
- de Menocal, P., D. Archer, P. Leth (1997), Pleistocene variations in Deep Atlantic circulation and calcite burial between 1.2 and 0.6 Ma: A combined data model approach, *Proceedings of the Ocean Drilling Programme, Scientific Results*, 154, 285-298.
- de Villiers, S. (2005), Foraminiferal shell-weight evidence for sedimentary calcite dissolution above the lysocline, *Deep-Sea Research I*, 52, 671-680.
- Duncan, R.A., J.Backman, L.C. Peterson, et al., (1990), *Proceedings ODP, Scientific Results*, 115:College Station, TX (Ocean Drilling Program), 1-887.
- Emerson, S., and M. Bender (1981), Carbon fluxes at the sediment-water interface of the deep-sea: calcium carbonate preservation. *Journal of Marine Research*, 39, 139-162.

- Engleman, E. E., L.L. Jackson and D. R. Norton (1985), Determination of carbonate carbon in geological materials by coulometric titration, *Chemical Geology*, 53, 125-128.
- EPICA Community Members (2004), Eight glacial cycles from an Antarctic ice core. *Nature*, 429, 623-628.
- Fairbanks, R.G., M. Sverdrlove, R. Free, P.H. Wiebe, and A.H.W. Bé (1982), Vertical distribution and isotopic fractionation of living planktonic foraminifera from the Panama Basin, *Nature*, 298, 841-844.
- Farell, J.W., and W.L. Prell (1989), Climatic change and CaCO<sub>3</sub> preservation: An 800,000- year bathymetric reconstruction from the central equatorial Pacific Ocean, *Paleoceanography*, 4, 447-466.
- Gardner, J.V. (1975), Late Pleistocene carbonate dissolution cycles in the eastern Equatorial Atlantic, In: *Dissolution of deep-sea carbonates*, W.V.Sliter, A.W.H.Bé, and W.H. Berger (Eds), Cushman Foundation for Foraminiferal Research, Special Publication, 14:129-141.
- Gehlen, M., F.C. Bassinot, L. Chou and D. McCorkle (2005), Reassessing the dissolution of marine carbonates: I. Solubility, *Deep-Sea Research I*, 52, 1445–1460.
- George, M. D., M. D.Kumar, S. W. A. Naqvi, et al.,(1994), A study of the carbon dioxide system in the northern Indian Ocean during premonsoon, *Marine Chemistry*, 47, 243–254.
- Gröstch, J., G. Wu, and W.H.Berger (1991), Carbonate cycles in the Pacific: Reconstruction of saturation fluctuations, In: G. Einsele, W. Ricken, A. Seilacher (Editors), *Cycles and Events in Stratigraphy*, Springer, Berlin, 110-125.

- Hales, B., S.Emerson and D.Archer (1994), Respiration and dissolution in the sediments of the western North Atlantic: estimates from models of in situ microelectrode measurements of porewater oxygen and pH, *Deep-Sea Research I*, 41, 695–719.
- Hales, B., and S.Emerson (1997), Calcite dissolution in sediments of the Ceara Rise: in situ measurements of porewater O<sub>2</sub>, pH and CO<sub>2</sub> (aq), *Geochimica et Cosmochimica Acta*, 61, 501-514.
- Hemleben, C. and M. Spindler (1983), Recent advances in research on living planktonic foraminifera, *Utrecht Micropaleontological Bulletins*, 30, 141-170.
- Houghton J.T., L.G.Meiro Filho, and B.A. Callander et al., (1996), *Climate Change 1995, The Science of Climate Change*, Cambridge University Press, ISBN 0 521 56436 0.
- Imbrie, J., J.D.Hayes, D.G.Martinson et al., (1984), The orbital theory of Pleistocene climate: support from a revised chronology of the marine 18O record, In: Berger,A., Imbrie, J., Hays, J., Kukla, G., saltzman, B. (Eds), *Milankovitch and climate, Part I*, Hingham, D. Reidel, 269-305.
- Imbrie, J. (1992), Editorial: A good year for Milankovitch, *Paleoceanography*, 7, 687-690.
- Indermühle, A., T. F. Stocker, F. Joos, et al., (1999), Holocene carbon-cycle dynamics based on CO<sub>2</sub> trapped in ice at Taylor Dome, Antarctica, *Nature*, 398, 121–126.
- Jahnke, R. A., D. B. Craven and J.-F. Gaillard (1994), The influence of organic matter diagenesis on CaCO<sub>3</sub> dissolution at the deep-sea floor, *Geochimica et Cosmochimica Acta*, 58, 2799-2809.

- Jahnke, R.A., D.B. Craven, D.B. Mc Corkle et al., (1997), CaCO<sub>3</sub> dissolution in California continental margin sediments: the influence of organic matter remineralization, *Geochimica Cosmochimica Acta*, 61, 2587-3604.
- Joos, F., S. Gerber, I. Prentice, B. Otto-Bliesner and P. Valdes (2004), Transient simulations of Holocene atmospheric carbon dioxide and terrestrial carbon since the Last Glacial Maximum, *Global Biogeochemical Cycles*, 18, doi:10.1029/2003GB002156.
- Kellogg, T.B. (1975), Late Quaternary climatic changes in the Norwegian-Greenland Sea. In Bowling, S.A., and Weller, G. (Eds.), *Climate of the Arctic: Univ. Alaska, Fairbanks*, 3-36.
- Kellogg, T.B. (1976), Paleoclimatology and paleoceanography of the Norwegian and Greenland Seas: the last 450,000 years, *Marine Micropaleontology*, 2, 235-249.
- Keigwin, L.D. (1987), Pliocene stable-isotope record of Deep Sea Drilling Project Site 606: sequential events of 18O enrichment beginning at 3.1 Ma, In W.F. Ruddiman, , R.B.Kidd, E.Thomas et al., *Initial Reports, DSDP, 94 (Pt. 2): Washington (U.S. Govt. Printing Office)*, 911-920.
- Kolla, V., A.W.H.Bé. and P.E.Biscaye (1976), Calcium carbonate distribution in the surface sediments of the Indian Ocean, *Journal of Geophysical Research*, 81: 2605-2616.
- Kuenen, P. H. (1950), *Marine Geology: New York, John Wiley and Sons, Inc.* 376-385.
- Le, J., and N. J. Shackleton (1992), Carbonate dissolution fluctuations in the western equatorial Pacific during the late Quaternary, *Paleoceanography*, 7, 21-42.

- Lipson, H., and H. Steeple (1970), Interpretation of X-Ray Powder Diffraction Patterns, MacMillan, Old Tappan, N. J. 335 pp.
- Lohmann, G.P. (1995), A model for variation in the chemistry of planktonic foraminifera due to secondary calcification and selective dissolution, *Paleoceanography*, 10, 445-447.
- Martin, J. H. (1990), Glacial-interglacial CO<sub>2</sub> change: The iron hypothesis, *Paleoceanography*, 5, 1-13.
- Martin, W., and F. Sayles (1999), Benthic cycling of biogenic components of the particulate flux to the seafloor in the Southern Ocean in March and April, 1998, *EOS Transactions*, 80(49), 241.
- Mc Cave, I.N., B. Manigetti and S.G. Robinson (1995), Sortable silt and fine sediment/composition slicing: parameters for paleocurrent speed and paleoceanography, *Paleoceanography*, 10, 593-610.
- Mekik, F. and L. Raterink (2008), Effects of surface ocean conditions on deep-sea calcite dissolution proxies in the tropical Pacific, *Paleoceanography*, 23, PA1216, doi:10.1029/2007PA001433.
- Milliman, J.D., P.J. Troy, W.M. Balch, et al., (1999), Biologically mediated dissolution of calcium carbonate above the chemical lysocline? *Deep-Sea Research I*, 46, 1653–1669.
- Mix, A. C., and R. G. Fairbanks (1985), North Atlantic surface control of Pleistocene deep-ocean circulation, *Earth Planetary Science Letters*, 73, 231-243.
- Moore, T. C., T. H. van Andel, C. Sancetta, N. Pias (1978), Cenozoic hiatuses in pelagic sediments, *Micropaleontology*, 24, 113–138.
- Murray, D.W., and W.L. Prell (1992), Late Pliocene and Pleistocene climatic oscillations and monsoon upwelling recorded in sediments from the Owen

- Ridge, northwestern Arabian sea, In: C. P. Summerhayes, W. L. Prell, K. C. Emeis (Eds), *Upwelling Systems: Evolution Since the Early Miocene*, Geological Society, London, 301-309.
- Naidu, P.D. (1991), Glacial to interglacial contrasts in the calcium carbonate and influence of Indus discharge in two eastern Arabian Sea cores, *Palaeogeography Palaeoclimatology Palaeoecology*, 86,255-263.
- Naidu, P.D., B.A.Malmgren, and L.Bornmalm (1993), Quaternary history of calcium carbonate fluctuations in the western equatorial Indian Ocean (Somali Basin), *Palaeogeography Palaeoclimatology Palaeoecology*, 103, 21-30.
- Naidu, P.D., B.A.Malmgren, and L.Bornmalm (1994), What controls the calcium carbonate content in Quaternary sediment cores raised from below the carbonate lysocline depth in the equatorial Indian Ocean? *Proceedings of the 29th International Geological Congress, Part B*, 201-209, VSP Zeist, The Netherlands.
- Naidu, P.D., and B. A. Malmgren (1999), Quaternary carbonate record from the equatorial Indian Ocean and its relationship with productivity changes, *Marine Geology*, 161, 49-62.
- Naqvi, S.W.A., H.W. Bange, S.W. Gibb, C. Goyet, A.D. Hatton and R.C. Upstill-Goddard (2005), Biogeochemical ocean-atmosphere transfers in the Arabian Sea, *Progress in Oceanography*, 65, 2-4, 116-144.
- Ni, Y., G. L. Foster, T. Bailey, et al., (2007), A core top assessment of proxies for the ocean carbonate system in surface dwelling foraminifers, *Paleoceanography*, 22, PA3212, doi:10.1029/2006PA001337.

- Nürnberg, D., J. Bijma, and C. Hemleben (1996), Assessing the reliability of magnesium in foraminiferal calcite as a proxy for water mass temperatures, *Geochimica Cosmochimica Acta*, 60, 803 – 814.
- Oba, T. (1969), Biostratigraphy and isotope paleotemperatures of some deep sea cores from the Indian Ocean, *Tohoku University Science Report*, 11 Series (Geology), 1-195.
- Olausson, E. (1965), Evidence of climatic changes in North Atlantic deep-sea cores, with remarks on isotopic paleotemperatures analysis. In: M. Sears (Ed.), *Progress in Oceanography*, Pergamon, Norwich, 3, 221-251.
- Olausson, E. (1967), Climatological, geoeconomical and paleoceanographical aspects on carbonate deposition, In: *Progress in Oceanography*, 4, M. Sears (Ed.) Pergamon, Norwich, pp. 221-252.
- Olausson, E. (1969), On the Würm-Flandrian boundary in deep-sea cores, *Geologie en Mijnbouw*, 48, 349-361.
- Olausson, E. (1971), Quaternary correlations and the geochemistry of oozes, In: Funnel, B.M. (Ed.), *The Micropaleontology of Oceans*, Cambridge University Press, 375-398.
- Olausson, E. (1985), The Glacial Oceans, *Palaeogeography Palaeoclimatology Palaeoecology*, 50, 291-301.
- Opdyke, B. N. and Walker, J. C. G. (1992), Return to the coral reef hypothesis: basin to shelf partitioning of CaCO<sub>3</sub> and its effects on atmospheric CO<sub>2</sub>, and Walker, *Geology*, 20, 733-736.
- Petit, J.R., J. Jouzel, D. Raynaud et al., (1999), Climate and atmospheric history of the past 420,000 years from the Vostok ice core, Antarctica, *Nature*, 399, 429-436.



- Peterson, L.C. (1984), Late Quaternary deep-water paleoceanography of the eastern equatorial Indian Ocean: Evidence from benthic foraminifera, carbonate dissolution and stable isotopes, Ph.D. thesis, 429 pp., Brown Univ, Providence, R.I.
- Peterson, L.C. and W. L. Prell (1985a), Carbonate dissolution in recent sediments of the eastern equatorial Indian Ocean: preservation patterns and carbonate loss above the lysocline, *Marine Geology*, 64, 259-290.
- Peterson, L.C. and W. L. Prell (1985b), Carbonate preservation and rates of climatic change: an 800 kyr record from the Indian Ocean, In: E.Sundquist, W.S Broecker (Eds), *The Carbon Cycle and Atmospheric CO<sub>2</sub>: Natural variations Archean to Present*, Geophysical Monograph Series, 32, AGU, Washington, D.C, 251-270.
- Peterson, L. C., and J. Backman (1990), Late Cenozoic carbonate accumulation and the history of the carbonate compensation depth in the western equatorial Indian Ocean, *Proceedings of the Ocean Drilling Program, Scientific Results*, 115, 467– 471.
- Peterson, L.C. (2001), 'Calcium carbonates', In: *Encyclopedia of Ocean science*, Ed by: Steele, J.H., Turekian, K.K., Thorpe, S.A. Academic Press,U.K., 1(A-C), 359-368.
- Rea, D.K. (1990), Paleooceanography of the eastern Indian Ocean from ODP Leg 121 drilling on Broken Ridge, *Geological Society of America Bulletin*, 102, 679-690.
- Ridgwell, A. J., M. J. Kennedy, K. Caldeira, (2003), Carbonate deposition, climate stability, and Neoproterozoic Ice ages, *Science*, 302, 859–862.

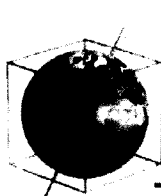
- Ridgwell, A. and R. E. Zeebe (2005), The role of the global carbonate cycle in the regulation and evolution of the Earth system, *Earth and Planetary Science Letters*, 234, 299-315.
- Ruddiman, W. F., and A. McIntyre (1976), Northeast Atlantic paleoclimatic changes over the past 600,000 years, In: *Investigation of Late Quaternary Paleoceanography and Paleoclimatology*: Eds. R.M. Cline and J.D. Hays, GSA Memoir, 145, 111-146.
- Ruddiman, W. F. (2003), The anthropogenic greenhouse era began thousands of years ago, *Climatic Change*, 61, 261–293.
- Ruddiman, W. F. (2005), How did humans first alter global climate? *Scientific American*, 292, 46–53.
- Sabine, C. L., R. Wanninkhof, R. M. Key et al., (2000), Seasonal CO<sub>2</sub> fluxes in the tropical and subtropical Indian Ocean, *Marine Chemistry*, 72, 33–53.
- Sanyal, A., N. G. Hemming, G. N. Hanson, and W. S. Broecker, (1995), Evidence for a higher pH in the glacial ocean from boron isotopes in foraminifera, *Nature*, 373, 234–236.
- Sarmiento, J. L. and J. R. Toggweiler (1984), A new model for the role of the oceans in determining atmospheric PCO<sub>2</sub>, *Nature*, 308, 621-624.
- Schott, W. (1983), Monsoon response of the Somalia Current and associated upwelling, *Progress in Oceanography*, 12, 357-381.
- Schulte, S. and E. Bard (2003), Past changes in biologically mediated dissolution of calcite above the chemical lysocline recorded in Indian Ocean sediments, *Quaternary Science Reviews*, 22, 1757–1770.

- Shackleton, N. J. (1977), The oxygen isotope stratigraphic record of the Late Pleistocene, *Philosophical Transactions, Royal Society of London*, B280, 169-179.
- Shackleton, N.J., M. A. Hall, J. Line and C, Shuxi (1983), Carbon isotope data in core V19-30 confirm reduced carbon dioxide concentration in the ice age atmosphere, *Nature (London)*, 306, 319-322.
- Shallow, J.C. (1984), Some aspects of the physical oceanography of the Indian Ocean, *Deep-Sea Research*, 31, 639-650.
- Siegenthaler, U., T. F. Stocker, E. Monnin, D. Lüthi, J. Schwander, B. Stauffer, D. Raynaud, J.-M. Barnola, H. Fischer, V. Masson-Delmotte, and J. Jouzel (2005), Stable carbon cycle-climate relationship during the Late Pleistocene, *Science*, 310, 1313–1317.
- Sigman, D. M., and E. A. Boyle (2000), Glacial/interglacial variations in atmospheric carbon dioxide, *Nature*, 407, 859-869.
- Sigman, D. M., and G. H. Haug (2003), Biological Pump in the Past, In: *Treatise on Geochemistry*, H.D. Holland and K.K. Turekian (Eds), Elsevier Science, Oxford.
- Smith, H. J., H. Fischer, M. Wahlen, D. Mastroianni, and B. Deck (1999), Dual modes of the carbon cycle since the Last Glacial Maximum, *Nature*, 400, 248-250.
- Snoeckx, H., and D. K. Rea (1994), Late Quaternary CaCO<sub>3</sub> stratigraphy of the eastern equatorial pacific, *Paleoceanography*, 9, 341-351.
- Takahashi, T. (1989), The carbon dioxide puzzle, *Oceanus*, 32, 22–29.

- Takahashi, T., R.A. Feely, R.F. Weiss et al., (1997), "Global air-sea flux of CO<sub>2</sub>: An estimate based on measurements of sea-air PCO<sub>2</sub> difference", 94, Proceedings of the National Academy of Sciences, USA, 8929-8299.
- Takahashi, T. (2001), 'Carbon Dioxide (CO<sub>2</sub>) Cycle', In: Encyclopedia of Ocean sciences, J. H. Steele, K. K. Turekian, S. A. Thorpe (Eds), Academic Press, U. K., 1(A-C), 400-407.
- Toggweiler, J. R. (1999), Variations in atmospheric CO<sub>2</sub> driven by ventilation of the ocean's deepest water, *Paleoceanography*, 14, 571-588.
- Van Andel, T. H. (1975), Mesozoic/Cenozoic calcite compensation depth and the global distribution of calcareous sediments, *Earth Planetary Science Letters*, 26, 187– 194.
- Volat, J.L., L. Pastouret, and L. Vergnaud-Grazzini (1980), Dissolution and carbonate fluctuations in Pleistocene deep-sea cores: a review, *Marine Geology*, 34, 1-28.
- Walter, L. M. and J.W. Morse (1985), The dissolution kinetics of shallow marine carbonates in seawater: a laboratory study, *Geochimica et Cosmochimica Acta*, 49, 1503–1513.
- Weninger, B., O. Jöris, U. Danzeglocke (2006), Calpal-Cologne Radiocarbon Calibration and Paleoclimate Research Package, Universität zu Köln, Institut für Ur-und Frühgeschichte Radiocarbon Laboratory.
- Wiseman, J.D.H. (1956), The rates of accumulation of nitrogen and calcium carbonate on the equatorial Atlantic floor, *Advances in Science*, 12, 579.
- Wiseman, J.D.H. (1965), The changing rate of calcium carbonate sedimentation on the equatorial Atlantic floor and its relation to continental late Quaternary

- stratigraphy, Reports of the Swedish Deep-Sea Expedition, 7(7), sediment cores from the North Atlantic Ocean, 288-354.
- Wu, G., and Berger, W. H. (1989), Planktonic foraminifera: differential dissolution and the quaternary stable isotope record in the west equatorial Pacific, *Paleoceanography*, 4, 181-198.
- Wyrki, K. (1973), Physical oceanography of the Indian Ocean, In B. Zeitzschel (Ed.), *The biology of the Indian Ocean*, (18–36), Berlin: Springer.
- Zeebe, R.E., and D. Wolf-Gladrow (2001), *CO<sub>2</sub> in seawater: equilibrium, kinetics, isotopes*, Elsevier Oceanographic Series, 65, Elsevier, New York.
- Zeng, N. (2003), Glacial-Interglacial Atmospheric CO<sub>2</sub> Changes – The Glacial Burial Hypothesis, *Advances in Atmospheric Sciences*, 20, 677–693.
- Zhong, S .J. and A. Mucci, (1993), Calcite precipitation in seawater using a constant addition technique—a new overall reaction kinetic expression, *Geochimica et Cosmochimica Acta*, 57, 1409–1417.

# PUBLICATIONS



Click  
Here  
for  
Full  
Article

## Calcite dissolution along a transect in the western tropical Indian Ocean: A multiproxy approach

Sushant S. Naik

National Centre for Antarctic and Ocean Research, Goa, India 403804 (sushant@ncaor.org)

P. Divakar Naidu

National Institute of Oceanography, Goa, India 403004

[1] Three paleocarbonate ion proxies, size index, planktonic foraminifera shell weight, and calcite crystallinity, have been employed here to a set of core top samples from the western tropical Indian Ocean in the water depth ranges from 1086 to 4730 m. All three proxies complement each other well and reveal that calcite dissolution starts to affect planktonic foraminifera from 2250 m depth onward and intense calcite dissolution begins around 3900 m depth in this sector of the tropical Indian Ocean. Three planktonic foraminifera species, *Globigerinoides sacculifer*, *Pulleniatina obliquiloculata*, and *Neogloboquadrina dutertrei*, show wide variability in shell weights from core top sediments in the depth range of 3300 to 3400 m bathed by similar bottom water  $\text{CO}_3^{2-}$  concentrations. This variability is attributed to shell calcification, and shell weights are controlled by  $\text{CO}_3^{2-}$  concentration in the surface waters. Further, surface water  $\text{CO}_3^{2-}$  concentrations override milder dissolution effects experienced by samples from shallower water depths bathed by similar bottom water  $\text{CO}_3^{2-}$  concentrations.

**Components:** 3374 words, 10 figures, 2 tables.

**Keywords:** calcite dissolution; carbonate ion; shell weights; size index; crystallinity.

**Index Terms:** 4825 Oceanography: Biological and Chemical: Geochemistry.

**Received** 20 February 2007; **Revised** 18 May 2007; **Accepted** 5 June 2007; **Published** 17 August 2007.

Naik, S. S., and P. D. Naidu (2007), Calcite dissolution along a transect in the western tropical Indian Ocean: A multiproxy approach, *Geochem. Geophys. Geosyst.*, 8, Q08009, doi:10.1029/2007GC001615.

### 1. Introduction

[2] Attempts to reconstruct the carbonate ion history from sediments of the world oceans have yielded two important proxies; the size index [Broecker and Clark, 1999] and the shell weight method [Lohmann, 1995]. Both these proxies have been applied largely to the Atlantic Ocean [Broecker and Clark, 1999, 2001a, 2001b, 2001c, 2003a, 2003b, 2003c, 2003d; Broecker et al., 1999, 2001], the Pacific Ocean [Broecker and Clark,

1999, 2001a, 2001b, 2003a, 2003b, 2003c, 2003d; Broecker et al., 2001] the Indian Ocean [Broecker and Clark, 1999, 2001a] and the Caribbean Sea [Broecker and Clark, 2002; Broecker et al., 2003]. Largely, in the above studies the shell weights of selected planktonic foraminifer species has been successfully utilized in understanding the carbonate ion variations during the Holocene and the Last Glacial Maxima (LGM).

[3] More recently size index and planktonic foraminifera shell weight have been employed to

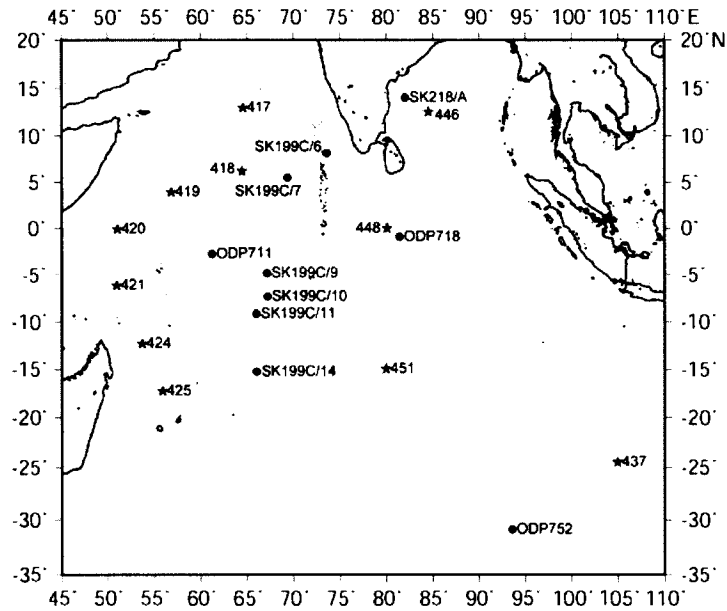


**Figure 1.** Map showing core top locations in the tropical Indian Ocean along with GEOSECS stations. Solid round dots indicate core top locations, and stars indicate GEOSECS station locations.

discuss calcite dissolution above the lysocline in the Atlantic, Pacific and Indian oceans [de Villiers, 2005; Schulte and Bard, 2003]. Though these studies could quantify the  $\text{CO}_3^{2-}$  concentrations to some extent, they could certainly identify the calcite dissolution and preservation events [Broecker et al., 2003]. Recently calcite crystallinity was also used as a proxy of carbonate ion in the Atlantic and Pacific Oceans [Bassinot et al., 2004; Gehlen et al., 2005]. However, the paleo-carbonate ion studies in the Indian Ocean are quite sparse compared to more rigorously studied Atlantic and Pacific oceans. This communication is aimed to address (1) dissolution of carbonates along a transect from the western tropical Indian Ocean by employing the size index, planktonic foraminifera shell weight and calcite crystallinity and (2) whether the shell weight of foraminifera are related to  $\text{CO}_3^{2-}$  concentrations in surface waters or not.

## 2. Methods

[4] Core top sediments used in this study were obtained during the cruises of *ORV Sagar Kanya* (SK 199C; SK 218) and Ocean Drilling Program Sites 711, 718 and 752 (Figure 1). All the samples were oven dried at 50°C; a portion of the sample was weighed and disaggregated by soaking in

distilled water and then wet sieved through a  $>63 \mu\text{m}$  sieve. The residue was collected carefully and dried, and both the size fractions,  $>63 \mu\text{m}$  and  $<63 \mu\text{m}$  were weighed separately. The content of  $\text{CaCO}_3$  in the sediment sample as a whole and in the  $>63 \mu\text{m}$  fractions were determined using coulometric titration method ( $1\sigma$  precision:  $\pm 0.7\%$ ,  $n = 10$ ). The size index was calculated as the percentage of  $\text{CaCO}_3$  content in the  $>63 \mu\text{m}$  fraction compared to the  $\text{CaCO}_3$  content in the bulk sediment [Broecker and Clark, 1999].

[5] A portion of the coarse fraction ( $>63 \mu\text{m}$ ) was cleaned and sonicated. The material was then dried and passed through sieves in order to isolate 350–420  $\mu\text{m}$  size fractions. Fifty shells of each *Globigerinoides sacculifer*, *Pulleniatina obliquiloculata* and *Neogloboquadrina dutertrei* were picked and weighed on a microbalance ( $1\sigma$  precision:  $\pm 2 \mu\text{g}$ ,  $n = 10$ ).

[6] *Globigerinoides sacculifer* shells were crushed gently and calcite crystallinity was measured on a XRD system following the procedure adopted by Bassinot et al. [2004]. We used the “Full Width at Half Maximum” (FWHM) of the (104) calcite X-ray diffraction peak (given in degree  $2\theta$ ) as an indication of the degree of crystallinity of foraminifera shells. The system utilized is a Philips PW1840-XRD instrument (Cu-K $\alpha$ , 40 KV,



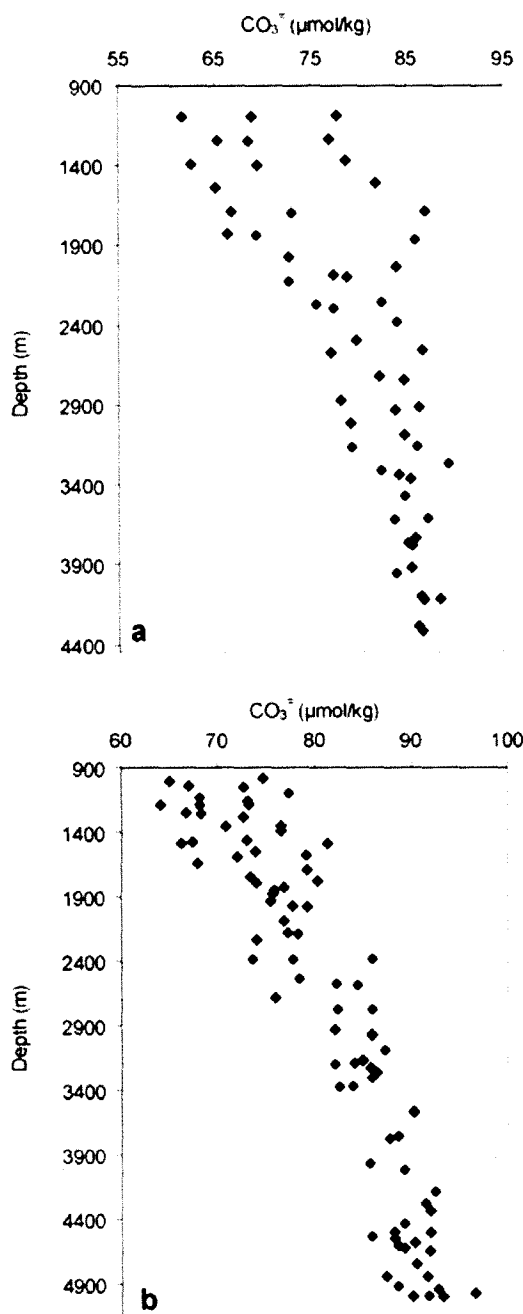


**Figure 2.** In situ  $\text{CO}_3^{2-}$  concentrations ( $\mu\text{mol/kg}$ ) calculated from GEOSECS stations versus depth (m) at (a) stations 417, 420, and 425 for the western tropical Indian Ocean and (b) station 446, 448, 451, and 437 for the eastern tropical Indian Ocean.

20 mA). Counting aperture of 0.2 mm and goniometer rotation speed of  $1.2^\circ 2\theta/\text{min}$  were manually adjusted within the instrument. Reproducibility of measurements is  $\pm 0.003^\circ 2\theta$ . SEM images of indi-

vidual planktonic foraminifera shells were obtained using a 6360 LV, JEOL instrument.

### 3. Results and Discussions

[7] Carbonate ion concentrations,  $[\text{CO}_3^{2-}]$ , of water bathing the core tops were computed from GEOSECS stations in the western Indian Ocean (417, 420, and 425) and eastern Indian Ocean (446, 448, 451, and 437) following procedure adopted by T. Takahashi (personal communication, 2006). The  $\text{CO}_3^{2-}$  concentration changes in the water column are quite similar in the western and eastern Indian Ocean (Figures 2a and 2b). Therefore these concentrations can be confidently extrapolated to our core top locations. The size index shows high values for core tops from above 3000 m water depth (Table 1 and Figure 3). In the Indian Ocean, the size index shows values higher than  $52 \pm 2$  (the value determined by Broecker and Clark [1999]), for core top samples from above the lysocline which is quite contrary to those in the Atlantic Ocean. From 2250 m onward, there is a gradual decrease in size index values. In the pressure-normalized  $\text{CO}_3^{2-}$  concentration ( $\text{CO}_3^{2-} = \text{CO}_3^{2-} + 20(4-h)$ ; where  $h$  is the depth in km) range of 126–70  $\mu\text{mol/kg}$ , a linear decline in the ratio of  $\text{CaCO}_3$  in the >63 micron fraction to the total  $\text{CaCO}_3$  in bulk sample occurs (Table 2 and Figure 4). The linear decline suggests that dissolution could be affecting shallowest samples in the present study. The slope of this reference line for the three tropical regions of Atlantic, Pacific and Indian Oceans is  $0.66 \mu\text{mol/kg}$  [Broecker and Clark, 1999]. Our size index values superimposed on this reference line show a considerable close fit with an average offset of  $-0.33$  from the reference line (Figure 3). This translates to a very negligible shift in saturation horizon of  $\text{CO}_3^{2-}$  in the Indian Ocean.

[8] Large variation of size index value (14%) within a change of  $1 \mu\text{mol/kg}$  in  $\text{CO}_3^{2-}$  concentration (from 96 to 97  $\mu\text{mol/kg}$ ) in a water depth range of 100 m (from 3300 to 3400 m) is noticed, which is significant in the Indian Ocean (Figure 4). In order to better document the dissolution process at these depths we have resorted to the shell weight method of Lohmann [1995] on selected core tops. The shell weight method gives a better picture of the dissolution intensity as it specifically targets at cleaned shells that are from a narrow size range nullifying the ill effects caused by finer entities [Broecker and Clark, 2001c]. *G. sacculifer* is a species sensitive to dissolution and hence we

**Table 1.**  $\text{CO}_3^{=}$  Calculated From Program by T. Takahashi (Personal Communication, 2006)<sup>a</sup>

Station	Depth, m	Latitude	Longitude	$\text{CO}_3^{=}$	$\text{CO}_3^{*}$	Size Index
ODP 752	1086	30.89°S	93.57°E	67.06	126.86	77.76
SK199C/6	2250	8.13°N	73.56°E	77.59	112.59	94.74
SK 218/A	3000	14.03°N	82.00°E	81.87	101.87	68.97
SK199C/10	3305	7.36°S	67.17°E	83.61	97.51	39.36
SK199C/9	3320	4.86°S	67.09°E	83.70	97.29	44.9
SK199C/14	3368	15.27°S	66.01°E	83.97	96.61	48.4
SK199C/11	3373	9.17°S	65.95°E	83.99	96.54	53.8
SK199C/7	3944	5.51°N	69.34°E	87.25	88.37	12.95
ODP 711	4430	2.74°S	61.16°E	90.02	81.42	8
ODP 718	4730	0.92°S	81.39°E	89.38	74.78	11.7

<sup>a</sup> Pressure-normalized carbonate ion concentration,  $[\text{CO}_3^{*}]$ , calculated from Broecker and Clark [1999].  $\text{CO}_3^{*} = \text{CO}_3^{=} + 20(4 - h)$ , where h is the depth in km.

perform shell weight measurements initially on this species. It is observed that the scatter in size index values at similar  $\text{CO}_3^{*}$  concentrations manifests in the shell weights (Table 2). To substantiate this observation we also performed shell weight measurements on two other species *N. dutertrei* and *P. obliquiloculata*. Both species exhibit similar shell weight trend at these depths (Figure 5). A good correlation between *G. sacculifer* shell weights and *P. obliquiloculata* and *N. dutertrei* shell weights confirms that the scatter is not a result of sieving method, measurement error or shell fill.

[9] A linear decrease in shell weight is observed in the pressure-normalized carbonate ion ( $\text{CO}_3^{*}$ ) range from 90 to 125  $\mu\text{mole kg}^{-1}$  in the tropical region of the world oceans with a weight loss of  $0.30 \pm 0.05 \mu\text{g } \mu\text{mol}^{-1} \text{kg}^{-1}$  [Broecker and Clark, 2001a]. Bottom water  $\text{CO}_3^{*}$  concentration bathing the core tops in the present study are in the range of 88 to 113  $\mu\text{mol kg}^{-1}$ , lying in the shell weight decrease zone documented by Broecker and Clark [2001a]. We find that in the present study foraminifera shell weights show marginally higher values than those in the eastern Indian Ocean [Broecker and Clark, 2001a]. Though *G. sacculifer* shows the larger shell weights among the three species, all of them follow the same trend. We find a large variability in shell weights corresponding to  $\text{CO}_3^{*}$  concentration of around 97  $\mu\text{mole kg}^{-1}$  which lie at a depth of 3300 to 3400 m (Figure 6 and Tables 1 and 2). In order to better document the process at these depth we employed another proxy discussed below.

[10] Shells that show a narrow (104) calcite peak on XRD powder diagrams are interpreted as being better crystallized than those showing a broader diffraction peak and dissolution improves shell

crystallinity [Bassinot et al., 2004]. Therefore the calcite crystallinity could be used as a dissolution index that could be tied to a carbonate ion change in the deep sea [Bassinot et al., 2004]. We have carried out the crystallinity measurements on *G. sacculifer* which is a dissolution sensitive spe-

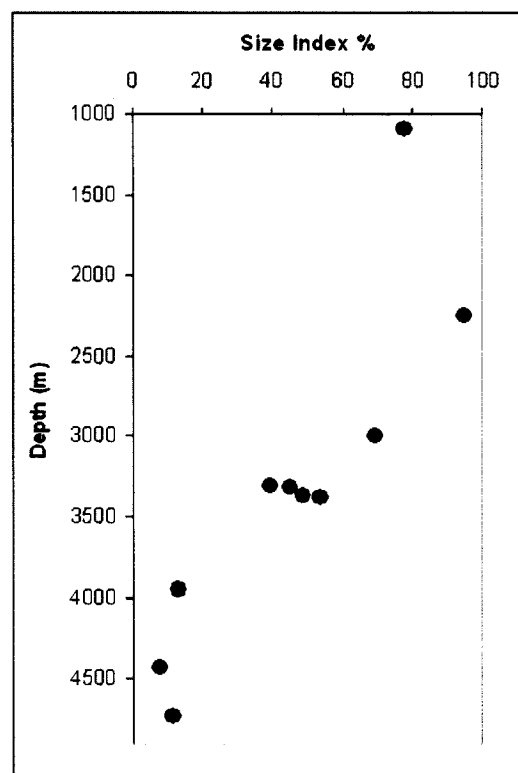


**Figure 3.** Size index values plotted as a function of depth in the tropical Indian Ocean. A gradual decrease in the size index values from 2250 m onward and a drastic decrease from 3900 m water depth are noticed.

**Table 2.** Selected Core Top Samples With Shell Weights in Micrograms of Three Different Species at Calcite Saturation Concentration of Overlying Bottom Waters<sup>a</sup>

Station	<i>G. Sacculifer</i>	<i>P. Obliquiloculata</i>	<i>N. Dutertrei</i>	Calcite (104) FWHM (°2θ)
SK199C/6	35.3	33.17	33.33	0.275
SK199C/10	30.54	29.11	27	0.27
SK199C/9	32.12	32.05	29	0.265
SK199C/14	35.1	35.1	34.5	0.27
SK199C/11	32	31.63	29.3	0.27
SK199C/7	26.77 <sup>b</sup>	26	25.4	0.25

<sup>a</sup> Also are shown the calcite (104) FWHM values in °2θ.

<sup>b</sup> Insufficient number of shells.

cies. Sites SK199C/6, 9, 10, 11 and 14 show similar crystallinity values over a range of bottom water [CO<sub>3</sub><sup>=\*</sup>] (Figure 7) which indicate that dissolution affects more or less evenly in the water depths ranging from 3300 to 3400 m. Comparatively, site SK199C/7 shows lower calcite (104) FWHM (Full Width at Half Maximum) value suggesting intense dissolution at this water depth (3900 m).

[11] All the three proxies, size index, shell weights and calcite crystallinity, applied to a set of core top samples in the western Indian Ocean show a linear regression varies from 0.7 to 0.75 between them (Figure 8). All three proxies reveal that dissolution affects planktonic foraminifera from 2250 m and that intense dissolution occurs from 3900 m onward. However, a large variations in size index (14%) is noticed within a range of 100 m (3300 to 3400 m) water depths, whereas shell weight and crystallinity do not show similar changes.

[12] In addition, we have compared the SEM micrographs of *G. sacculifer* from deeper depth (3944 m) Site SK199C/7 and shallower depth (2250 m) Site SK199C/6. Apparently, *G. sacculifer*

from deeper depth site show dissolution features (Figures 9a and 9b), whereas shallow depth site show well-preserved *G. sacculifer* shells (Figures 9c and 9d). This observation as well as less abundance of *G. sacculifer* and *G. ruber* (P. D. Naidu, unpublished data, 2007) from the sediments beyond 3900 m water depth endorses that intense calcite dissolution occurs from 3900 m depth in the Indian Ocean.

[13] Foraminiferal shell weights from surface sediments not only depend on bottom water CO<sub>3</sub><sup>=\*</sup> concentrations but also by the carbonate ion concentrations in the waters wherein they calcify [Barker and Elderfield, 2002]. Thus shell weight of several species of planktonic foraminifera from core top sediments vary systematically as function of latitude in the North Atlantic Ocean [Barker and Elderfield, 2002]. *G. sacculifer* is a surface dwelling species and calcifies at shallower depths as compared to *N. dutertrei* and *P. obliquiloculata* [Fairbanks et al., 1982] and therefore *G. sacculifer* shell weight should be affected by the carbonate ion concentrations of the surface waters. To under-

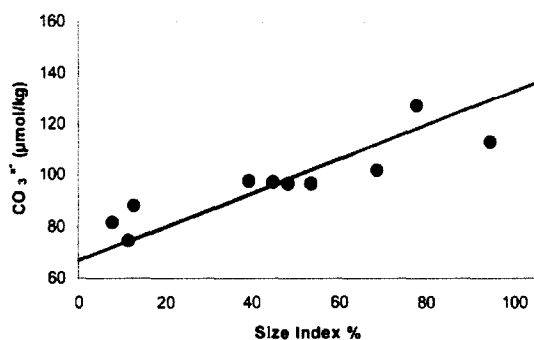


**Figure 4.** Size index versus CO<sub>3</sub><sup>=\*</sup> concentration (µmol/kg) plotted on a reference line [Broecker and Clark, 1999] for the three major world oceans.

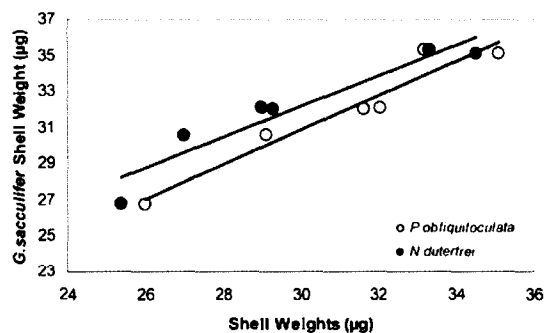


**Figure 5.** *Globigerinoides sacculifer* shell weights versus *Pulleniatina obliquiloculata* and *Neogloboquadrina dutertrei* shell weights show a linear trend, suggesting no measurement error or shell fill.

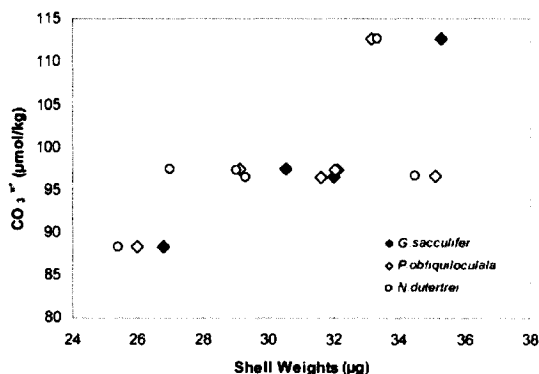


**Figure 6.** Shell weights of *Globigerinoides sacculifer*, *Pulleniatina obliquiloculata*, and *Neogloboquadrina dutertrei* versus bottom water CO<sub>3</sub><sup>=</sup> concentrations. A large variability is seen at pressure-normalized carbonate ion concentrations of 97 μmol/kg.

stand relationship between shell weights and surface water carbonate ion concentration, we have compared shell weights variability of *G. sacculifer* from sites SK199C/6, 7, 9, 10, 11 and 14 and surface water carbonate ion concentrations for these sites in the western Indian Ocean (Figure 10). Though there could possibly be marginal difference in the present surface carbonate ion concentrations and those at which the shells must have calcified, shell weights at sites SK199C/6, 9, 10, 11 and 14 shows a reasonably good correspondence with surface water CO<sub>3</sub><sup>=</sup> concentrations. Surface waters are supersaturated with respect to CO<sub>3</sub><sup>=</sup> concentrations, therefore, higher calcification rates in surface waters produce thicker shells without any change in shell size which is reflected in the shell weights of planktonic foraminifera

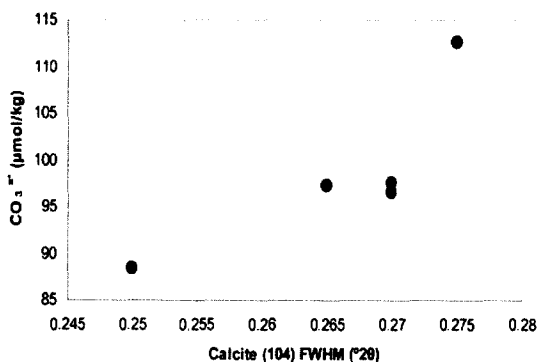


**Figure 7.** Calcite (104) FWHM (°2θ) values plotted against pressure-normalized CO<sub>3</sub><sup>=</sup> concentrations (μmol/kg). The lowest value of calcite (104) FWHM is seen at a CO<sub>3</sub><sup>=</sup> concentration of 88 μmol kg<sup>-1</sup>.

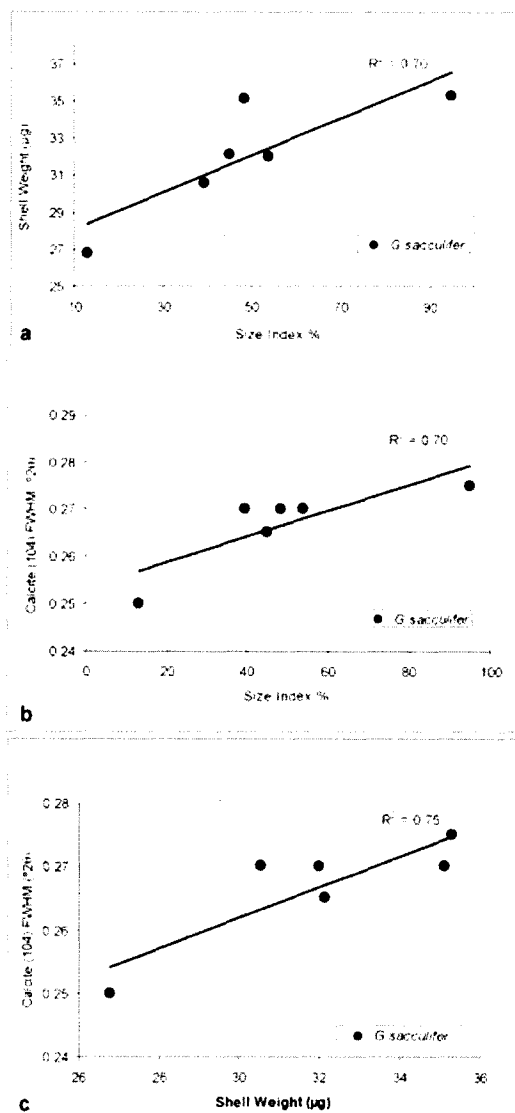


**Figure 8.** Comparison between the three proxies shows good linear regression. (a) Shell weight (μg) versus size index % (R<sup>2</sup> = 0.7), (b) calcite (104) FWHM (°2θ) versus size index % (R<sup>2</sup> = 0.7), and (c) calcite (104) FWHM (°2θ) versus shell weight (μg) (R<sup>2</sup> = 0.75).

[Barker and Elderfield, 2002]. We observe here that foraminiferal calcite from sediment bathed by similar CO<sub>3</sub><sup>=</sup> concentration from depths shallower than 3900, trace the surface ocean CO<sub>3</sub><sup>=</sup> concentrations.

#### 4. Summary and Conclusions

[14] In an attempt to understand the status of calcite dissolution along a transect of tropical

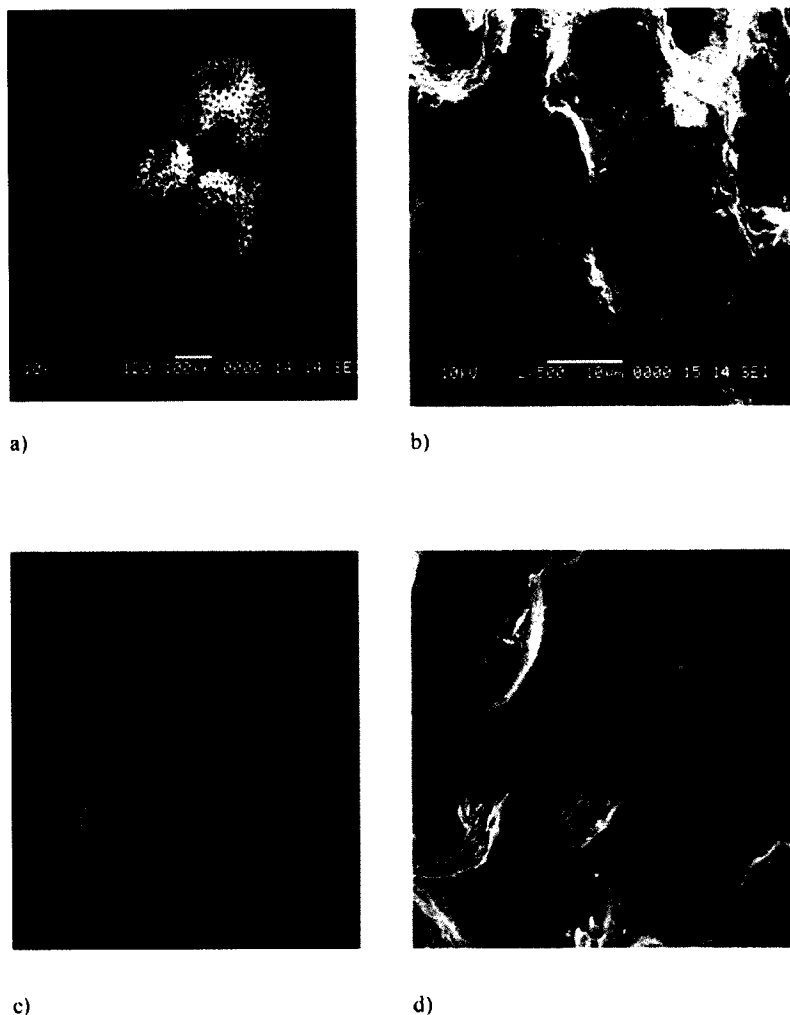


**Figure 9.** (a and b) SEM micrographs of *Globigerinoides sacculifer* from 3944 m water depth (SK199C/7) showing dissolution features. (c and d) Well-preserved tests of *Globigerinoides sacculifer* from 2250 m water depth (SK199C/6).

Indian Ocean, for the first time, we employed the three paleocarbonate ion proxies; size index, shell weights and calcite crystallinity to a set of core tops from depth ranges 1086 to 4370 m. Size index values show a global trend of decrease of  $\text{CO}_3^{=}$  concentration with increasing water depth and decreasing bottom water  $\text{CO}_3^{=*}$  concentration. Size index and planktonic foraminifera shell weights suggest that calcite dissolution starts from 2250 m onward. All the three proxies complement each other and reveal that most intense calcite dissolution undergoes from 3900 m depth. The intense calcite dissolution from 3900 m could be due to under saturation of  $\text{CO}_3^{=}$  concentration in the bottom waters. The size index also reveals a decreasing trend with decreasing bottom water saturation with respect to  $\text{CO}_3^{=*}$  concentration.

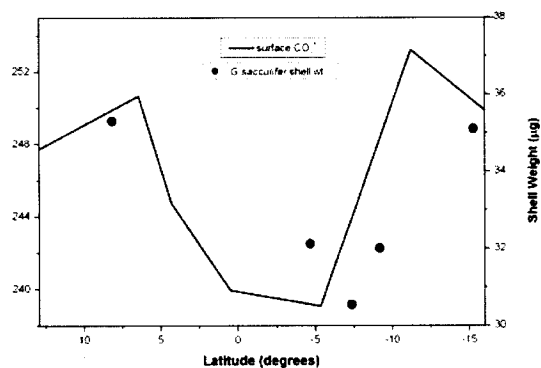


**Figure 10.** Surface ocean  $\text{CO}_3^{=}$  concentrations (calculated from GEOSECS stations 417, 418, 419, 420, 421, 424, and 425) and *Globigerinoides sacculifer* shell weights plotted as a function of latitude. Shell weights correspond well with the surface  $\text{CO}_3^{=}$  concentrations.

[15] *G. sacculifer*, *P. obliquiloculata* and *N. duterrei* show different shell weights in spite of similar  $\text{CO}_3^{2-}$  concentration in the bottom water within 3300 to 3400 m depth in the tropical Indian Ocean. This trend in shell weights is due to shell calcification which is related to surface waters  $\text{CO}_3^{2-}$  concentrations. We, therefore conclude that the planktonic foraminiferal shell weights for depths above the carbonate ion saturation horizon depends on the surface water carbonate ion concentrations in the tropical Indian Ocean.

### Acknowledgments

[16] We thank both the anonymous reviewers and Laurent Labeyrie, Editor, for their constructive comments, which improved the interpretation. A set of samples was provided by the Ocean Drilling Program, which is sponsored by the U.S. National Science Foundation and participating countries under the management of the Joint Oceanographic Institutions. We thank S. Chaturvedi for sharing SK samples. This is National Institute of Oceanography contribution 4262.

### References

- Barker, S., and H. Elderfield (2002), Foraminiferal calcification response to glacial-interglacial changes in atmospheric  $\text{CO}_2$ , *Science*, *297*, 833–836.
- Bassinot, F. C., F. Mélières, M. Gehlen, C. Levi, and L. Labeyrie (2004), Crystallinity of foraminifera shells: A proxy to reconstruct past bottom water  $\text{CO}_3^{2-}$  changes?, *Geochem. Geophys. Geosyst.*, *5*, Q08D10, doi:10.1029/2003GC000668.
- Broecker, W. S., and E. Clark (1999),  $\text{CaCO}_3$  size distribution: A paleocarbonate ion proxy, *Paleoceanography*, *14*, 596–604.
- Broecker, W. S., and E. Clark (2001a), An evaluation of Lohmann's foraminifera weight dissolution index, *Paleoceanography*, *16*(5), 531–534.
- Broecker, W. S., and E. Clark (2001b), Glacial-to-Holocene redistribution of carbonate ion in the deep sea, *Science*, *294*, 2152–2155.
- Broecker, W. S., and E. Clark (2001c), Reevaluation of the  $\text{CaCO}_3$  size index paleocarbonate ion proxy, *Paleoceanography*, *16*(6), 669–671.
- Broecker, W. S., and E. Clark (2002), Carbonate ion concentration in glacial-age deep waters of the Caribbean Sea, *Geochem. Geophys. Geosyst.*, *3*(3), 1021, doi:10.1029/2001GC000231.
- Broecker, W. S., and E. Clark (2003a),  $\text{CaCO}_3$  dissolution in the deep sea: Paced by insolation cycles, *Geochem. Geophys. Geosyst.*, *4*(7), 1059, doi:10.1029/2002GC000450.
- Broecker, W. S., and E. Clark (2003b), Holocene atmospheric  $\text{CO}_2$  increase as viewed from the seafloor, *Global Biogeochem. Cycles*, *17*(2), 1052, doi:10.1029/2002GB001985.
- Broecker, W. S., and E. Clark (2003c), Glacial-age deep sea carbonate ion concentrations, *Geochem. Geophys. Geosyst.*, *4*(6), 1047, doi:10.1029/2003GC000506.
- Broecker, W. S., and E. Clark (2003d), Pseudo dissolution of marine calcite, *Earth Planet. Sci. Lett.*, *208*(3–4), 291–296.
- Broecker, W. S., E. Clark, D. C. McCorkle, T.-H. Peng, I. Hajdas, and G. Bonani (1999), Evidence for a reduction in the carbonate ion content of the deep sea during the course of the Holocene, *Paleoceanography*, *14*, 744–752.
- Broecker, W. S., J. Lynch-Stieglitz, E. Clark, I. Hajdas, and G. Bonani (2001), What caused the atmosphere's  $\text{CO}_2$  content to rise during the last 8000 years?, *Geochem. Geophys. Geosyst.*, *2*(10), doi:10.1029/2001GC000177.
- Broecker, W. S., E. Clark, and A. W. Droxler (2003), Shell weights from intermediate depths in the Caribbean Sea, *Geochem. Geophys. Geosyst.*, *4*(7), 1060, doi:10.1029/2002GC000491.
- de Villiers, S. (2005), Foraminiferal shell-weight evidence for sedimentary calcite dissolution above the lysocline, *Deep Sea Res., Part 1*, *52*, 671–680.
- Fairbanks, R. G., M. Sverdrlove, R. Free, P. H. Wiebe, and A. H. W. Be (1982), Vertical distribution and isotopic fractionation of living planktonic foraminifera from the Panama Basin, *Nature*, *298*, 841–844.
- Gehlen, M., F. C. Bassinot, L. Chou, and D. McCorkle (2005), Reassessing the dissolution of marine carbonates: I. Solubility, *Deep Sea Res., Part 1*, *52*, 1445–1460.
- Lohmann, G. P. (1995), A model for variation in the chemistry of planktonic foraminifera due to secondary calcification and selective dissolution, *Paleoceanography*, *10*, 445–447.
- Schulte, S., and E. Bard (2003), Past changes in biologically mediated dissolution of calcite above the chemical lysocline recorded in Indian Ocean sediments, *Quat. Sci. Rev.*, *22*, 1757–1770.



## Possible factors that control calcite dissolution in the western tropical Indian Ocean

The oceans act as a major controlling device of atmospheric  $\text{CO}_2$  through the chemistry of the oceans and preservation of calcium carbonate in deep-sea sediments<sup>1</sup>. Carbon dioxide dissolved in sea water is present as  $\text{CO}_2$  gas,  $\text{H}_2\text{CO}_3$ ,  $\text{HCO}_3^-$  and  $\text{CO}_3^{2-}$ . All these species together constitute the Dissolved Inorganic Carbon (DIC)<sup>2</sup> which controls the sea water pH, which in turn controls preservation/dissolution of  $\text{CaCO}_3$ . Precipitation of carbonate carbon results in an increase in ocean  $\text{pCO}_2$ , and with it an increase in atmospheric  $\text{CO}_2$  concentration. Conversely, dissolution of  $\text{CaCO}_3$  results in a decrease in  $\text{pCO}_2$  (and atmospheric  $\text{CO}_2$ ) decrease<sup>3</sup>.

Therefore, in order to understand the past atmospheric  $\text{CO}_2$  fluctuations, it is necessary to know the dissolution and preservation patterns of calcium carbonate in the world oceans<sup>4</sup>. Two processes result in the dissolution of calcite after it reaches the seafloor. First, the degree of saturation state of  $\text{CO}_3^{2-}$  concentration of the overlying bottom waters<sup>5</sup>, and second, due to sedimentary organic matter respiration and resulting acidification of pore waters<sup>6,7</sup>.

Applying three palaeocarbonate ion proxies – planktonic foraminifera size index, shell weight and calcite crystallinity – to a set of core top samples, it has been documented that calcite dissolution commences from 2250 m onwards and intensifies at around 3900 m water depth in the western tropical Indian Ocean<sup>8</sup>. The present communication is aimed to address whether the dissolution of carbonate in the western tropical Indian Ocean is caused due to saturation state of the overlying bottom waters or due to acidification of pore waters driven by organic matter remineralization.

Six core top sediment samples used in this study were obtained during the cruises of *ORV Sagar Kanya* (SK 199C; Figure 1). All samples were oven-dried at 50°C; a portion of the sample was weighed and disaggregated by soaking in distilled water and then wet-sieved through a  $>63 \mu\text{m}$  sieve. A portion of the coarse fraction ( $>63 \mu\text{m}$ ) was cleaned and sonicated. We have resorted here to the shell weight method<sup>9</sup>. The  $>63 \mu\text{m}$  material was then dried and passed

through sieves in order to isolate 350–420  $\mu\text{m}$  size fractions. Fifty shells of *Pulleniatina obliquiloculata* were picked and weighed on a microbalance (1 $\sigma$  precision:  $\pm 2 \mu\text{g}$ ,  $n = 10$ ). Carbonate ion concentrations,  $[\text{CO}_3^{2-}]$  of water bathing the core tops were computed from GEOchemical SECTION Studies (GEOSECS) stations in the western Indian Ocean (nos 417, 420 and 425) and eastern Indian Ocean (nos 446, 448, 451 and 437) following the procedure adopted by Taro Takahashi (pers. commun.). The pressure-normalized  $\text{CO}_3^{2-}$  concentration was calculated as follows:  $\text{CO}_3^{2-*} = \text{CO}_3^{2-} + 20(4 - h)$ ; where  $h$  is the depth (in km)<sup>10</sup>.

A linear decrease in shell weight was observed in the pressure-normalized carbonate ion ( $\text{CO}_3^{2-*}$ ) range from 90 to 125  $\mu\text{mol kg}^{-1}$  in the tropical region of the world oceans<sup>11</sup>, with a weight loss of  $0.30 \pm 0.05 \mu\text{g } \mu\text{mol}^{-1} \text{ kg}^{-1}$ . Bottom water  $\text{CO}_3^{2-*}$  concentration bathing the core tops in the present study is in the range 88–113  $\mu\text{mol kg}^{-1}$ , lying in the shell weight decrease zone documented by Broecker

and Clark<sup>11</sup> (Table 1). At a  $\text{CO}_3^{2-*}$  concentration of 97  $\mu\text{mol kg}^{-1}$ , a large variability in shell weight was noticed, which has been attributed to surface water  $\text{CO}_3^{2-}$  ion concentrations<sup>8</sup>. We find that in the present study, foraminifera shell weights show marginally higher values than those in the eastern Indian Ocean<sup>11</sup>.

As mentioned earlier, calcite dissolution in sediments above lysocline depths could take place in acidified pore waters. The core top foraminifera are also initially exposed to the benthic fluff layer at the sediment–water interface<sup>12</sup>. Therefore, this interface is perhaps a better description of the initial exposure environment in foraminifera from the core tops. Therefore, we use the term  $\Delta\text{CO}_3^{2-}$  interface instead of  $\Delta\text{CO}_3^{2-}$  pore-water.

To understand whether the dissolution taking place at Site SK199C/7 is due to this corrosive benthic fluff layer, we calculated the  $\Delta\text{CO}_3^{2-}$  interface –  $\Delta\text{CO}_3^{2-}$  bottom water gradient. We used the relationship from the core-top data of Broecker and Clark<sup>11</sup> for *P. obliquiloculata* shell weight and

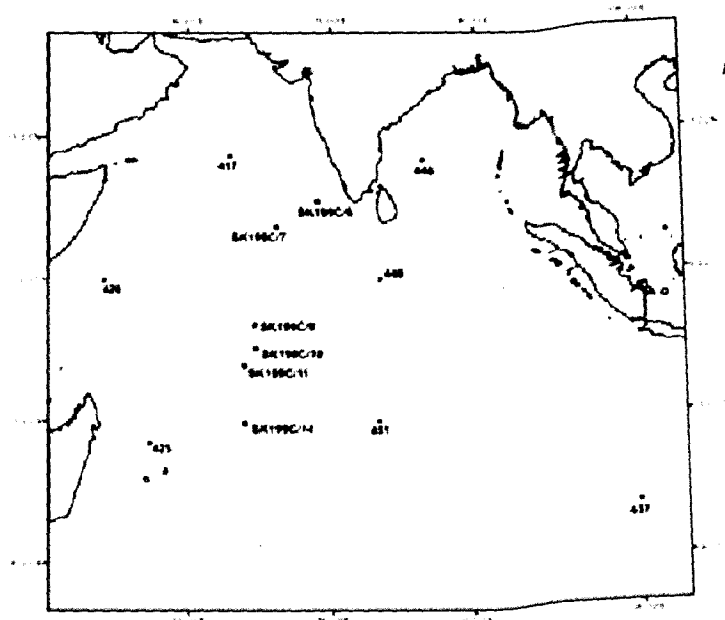


Figure 1. Map showing core top locations in the tropical Indian Ocean along with GEOSECS stations used in the calculation of  $\text{CO}_3^{2-}$  concentrations. Solid circles indicate core top locations and stars indicate GEOSECS stations with numbers.

**Table 1.** Shell weights ( $\mu\text{g}$ ) of foraminifera species *Pulleniatina obliquiloculata*.  $\text{CO}_3^-$  ( $\mu\text{mol/kg}$ ) calculated using the program developed by Takahashi; pressure-normalized carbonate ion concentration,  $[\text{CO}_3^{*}]$  calculated from Broecker and Clark<sup>10</sup>,  $\text{CO}_3^{*} = \text{CO}_3 + 20(4 - h)$ ; where  $h$  is the depth (in km);  $\Delta\text{CO}_3^-$  values calculated as  $\text{CO}_3^{*} - \text{CO}_3^-$

Station	Depth (m)	Latitude	Longitude	Shell weight			
				<i>P. obliquiloculata</i>	$\text{CO}_3^-$	$\text{CO}_3^{*}$	$\Delta\text{CO}_3^-$
SK199C/6	2250	8.13°N	73.56°E	33.17	77.59	112.59	35
SK199C/10	3305	7.36°S	67.17°E	29.11	83.61	97.51	13.9
SK199C/9	3320	4.86°S	67.09°E	32.05	83.70	97.29	13.6
SK199C/14	3368	15.27°S	66.01°E	35.1	83.97	96.61	12.64
SK199C/11	3373	9.17°S	65.95°E	31.63	83.99	96.54	12.54
SK199C/7	3944	5.51°N	69.34°E	26	87.25	88.37	1.12

bottom water  $\Delta\text{CO}_3^-$ , from the Indian Ocean as given below.

$\Delta\text{CO}_3^- = [P. obliquiloculata \text{ shell weight } (\mu\text{g}) - 24.53]/0.2759$ .

Using the above relation and shell weights of *P. obliquiloculata*, we calculated  $\Delta\text{CO}_3^-$  interface. The gradient ( $\Delta\text{CO}_3^-$  interface -  $\Delta\text{CO}_3^-$  bottom water) was then calculated using  $\Delta\text{CO}_3^-$  bottom water values (Table 1).

Thus, we obtain a value of  $+4.2 \mu\text{M}$  at 3900 m water depth. de Villiers<sup>12</sup> determined the  $\Delta\text{CO}_3^-$  interface to be within  $\pm 10 \mu\text{M}$  of bottom water. Shell weight measurements from both *Globigerinoides sacculifer* and *Globigerinoides ruber* suggest that there exists no significant gradient in  $\Delta\text{CO}_3^-$  across the sediment-bottom water interface below a depth of 1000 m in the Indian Ocean. Our value of  $+4.2 \mu\text{M}$  falls within the range of  $\pm 10 \mu\text{M}$ , suggesting that dissolution of carbonate around 3900 m water depth is due to undersaturation in  $\text{CO}_3^-$  concentration of bottom waters.

Calcium carbonate dissolution starts around 2250 m and intensifies at 3900 m in the tropical Indian Ocean<sup>8</sup>. We needed to study whether this intense dissolution occurring at 3900 m is a result of undersaturation of overlying bottom waters with respect to carbonate ion. This is important in order to know the calcite satu-

ration depth in the western tropical Indian Ocean, which is necessary to understand the oceanic response to the currently increasing  $\text{CO}_2$  levels. We used the relationship between *P. obliquiloculata* shell weight and bottom water  $\Delta\text{CO}_3^-$  from the core top data of Broecker and Clark<sup>11</sup> and data from the present study. We calculated  $\Delta\text{CO}_3^-$  interface -  $\Delta\text{CO}_3^-$  bottom water to be  $+4.2 \mu\text{M}$ , which is within  $\pm 10 \mu\text{M}$  of bottom water, the value derived by de Villiers<sup>12</sup>. This suggests that there is no gradient in  $\Delta\text{CO}_3^-$  across the sediment-bottom water interface at a depth of 3900 m. Therefore, we conclude that the intense dissolution along this transect in the western tropical Indian Ocean is due to bottom water  $\text{CO}_3^-$  undersaturation.

- Archer, D. and Maier-Reimer, E., *Nature*, 1994, **367**, 260–263.
- Naik, S. S. and Naidu, P. D., *Geochem. Geophys. Geosyst.*, 2007, **8**, Q08009.
- Lohmann, G. P., *Paleoceanography*, 1995, **10**, 445–447.
- Broecker, W. S. and Clark, E., *Paleoceanography*, 1999, **14**, 596–604.
- Broecker, W. S. and Clark, E., *Paleoceanography*, 2001, **16**, 531–534.
- de Villiers, S., *Deep-Sea Res. I*, 2005, **52**, 671–680.

ACKNOWLEDGEMENTS. We thank Dr S. Chaturvedi for sharing SK samples. This is National Institute of Oceanography contribution no. 4366.

Received 5 November 2007; revised accepted 2 April 2008

S. S. NAIK<sup>1</sup>  
P. DIVAKAR NAIDU<sup>2,\*</sup>

- Berger, W. H., *Geol. Soc. Am. Bull.*, 1974, **18**, 1385–1402.
- Riley, J. P. and Chester, R., *Introduction to Marine Chemistry*, Academic Press, London, 1971, p. 465.
- Broecker, W. S. and Peng, T.-H., *Global Biogeochem. Cycles*, 1987, **1**, 15–29.
- Naidu, P. D. and Malmgren, B. A., *Mar. Geol.*, 1999, **161**, 49–62.
- Berger, W. H., *J. Foraminiferal Res.*, 1973, **3**, 187–195.
- Emerson, S. and Bender, M., *J. Mar. Res.*, 1981, **39**, 139–162.

<sup>1</sup>National Centre for Antarctic and Ocean Research,

Goa 403 804 India

<sup>2</sup>National Institute of Oceanography,

Goa 403 004, India

\*For correspondence.

e-mail: divakar@nio.org

## *Corallodiscus Batalin* (Gesneriaceae): A new generic record for Eastern Ghats, Orissa

The floristics of southern Orissa, often considered incomplete, was sporadically approached by Mooney, Gamble, Haines and subsequent workers. Hence, it provides an ideal background for further exploration and discovery of taxonomic novelties. We collected an interesting specimen belonging to family Gesneriaceae

from Similipadar Hills (19°41'12.53"N, 83°4'28.97"E) in the Karlapat range, Kalahandi District, part of the Eastern Ghats, Orissa. Critical analysis and scrutiny of the floristic work done by several researchers<sup>1–8</sup> helped us to identify this specimen as *Corallodiscus lanuginosus* (Wallich ex R.Br.) B. L. Burtt. *C. lanugi-*

*nosus* is a highly variable taxon and has been reported to grow in moist rock crevices at 600–3600 m amsl from northeast India to China. Recent discovery of this species from the Western Ghats<sup>8</sup> and the Eastern Ghats (Prasad, RRL (B), col. no. 10217), extends its distribution to peninsular India. However, contrary to the